THEORETICAL ANALYSIS OF THE TYPE I $F_A(Na)$ AND TYPE II $F_A(Li)$ CENTERS IN KCl

A Thesis

submitted in partial fulfilment of

the requirements for the degree of

Doctor of Philosophy

at

The University of Manitoba

by

Chong Kim Ong

March, 1973

ACKNOWLEDGEMENTS

The author would like to express his sincere thanks and deep appreciation to his supervisor, Dr. J.M. Vail, for his guidance throughout the course of the work. Dr. R.J. Brown's computer programs have been much appreciated.

ABSTRACT

Details of the electronic and ionic structure of the absorption energy and the ground and excited state reorientation energies of the F_A(Na) and F_A(Li) centers have been studied theoretically. The variational method is used to estimate the energy levels and wave functions, and one-parameter Gaussian-localized trial wave functions are used. The lattice is treated as unpolarizable point ions plus the ion-size correction arising from the approximate pseudopotential method developed by Bartram, Stoneham, and Gash. The lattice energy is the sum of the Coulomb interaction and the Born-Mayer repulsion, with Tosi's single exponential parameters as devised for perfect KCl, NaCl, and LiCl lattices. The lattice distortions and the electronic wave function are calculated self-consistently, using the method of lattice statics as modified for the case of an excess-electron defect with non-harmonic lattice distortion. The Franck-Condon principle is used for absorption and emission. The F_{A1}-absorption energy agrees with the experiment but with F_{A1}-F_{A2} splittings about three times too large. This discrepancy is probably largely due to ion-size correction. Energies of the relaxed excited state (RES) in vacancy and saddle-point configurations

are also estimated. The RES of $F_A(Li)$ is found stabilized in the saddle-point configuration in agreement with experiment, but the $F_A(Na)$ stabilization is wrong, although the error in the energy is less than 0.2 eV. Ground state reorientation energies agree with experiment for both centers. The role of the impurity cation in lowering the activation energies in both states is about equally divided between lattice energy and Coulomb electron-lattice interaction. Tentative results suggest that the saddle-point configurations for F- and F_A - centers may be quite different.

CONTENTS

CHAPTER 1

INTRODUCTION

The main aim of the present work was to theoretically estimate the energy levels of $F_A(I)$ and $F_A(II)$ - centers[1] in KCl crystal, including both electronic transitions and the reorientation process. The type I or type II F_A - center in KCl is basically an F - center adjacent to a Na^+ or Li^+ substitutional impurity ion respectively (Fig. 1). The following physical parameters of these defects have been extensively studied:

(1) Optical absorption energy;

(2) Optical emission energy;

(3) Activation energies for reorientation and dissociation.

When the center has absorbed the photon, the bound excess-electron will be excited from its ground state to an excited state in a potential similar to the square well. The energy of the absorbed photon is called the absorption energy. The final state of the excess-electron in absorption, is called the unrelaxed excited state. The lattice then relaxes, until the excess-electron and the defect lattice are in mechanical equilibrium. This is called the relaxed excited state. The most striking single feature of

Figure 1

The ordinary F - center, $F_A(I)$ - center and $F_A(II)$ - center in KCl.

(a) Ordinary F - center in KCl

(b) $F_A(I)$ - center in KCl : Na

(c) $F_A(II)$ - center in KCl : Li

(a)

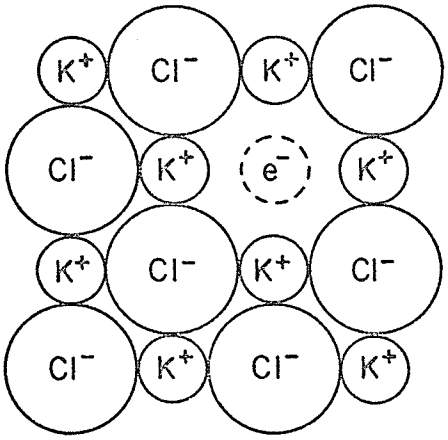
K+
Cl−
K+
Cl−
Cl−
K+
e−
K+
K+
Cl−
K+
Cl−
Cl−
K+
Cl−
K+

(b)

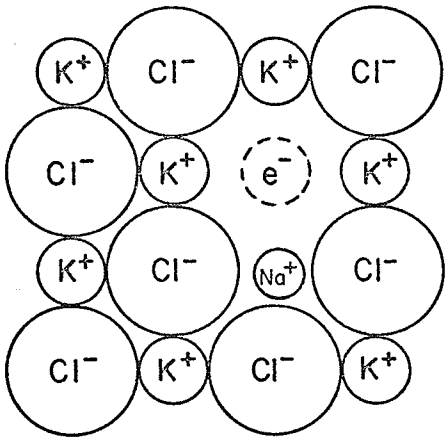
K+
Cl−
K+
Cl−
Cl−
K+
e−
K+
K+
Cl−
Na+
Cl−
Cl−
K+
Cl−
K+

(c)

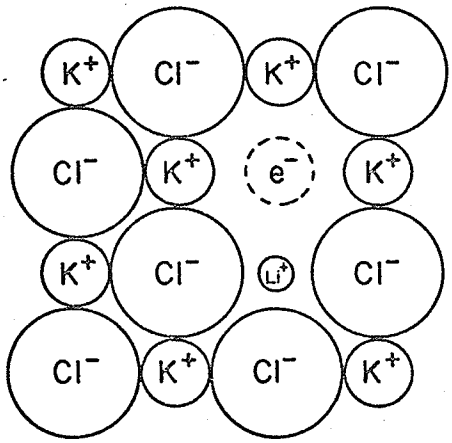
K+
Cl−
K+
Cl−
Cl−
K+
e−
K+
K+
Cl−
Li+
Cl−
Cl−
K+
Cl−
K+

these centers occurs in the $F_A(II)$ - center, where the relaxed excited state is stabilized in the saddle-point configuration (Fig. 2b). In the saddle-point configuration, a negative ion lies half-way between two vacant anion sites. From the relaxed excited state, the emission process occurs and the final state of the optical emission process is the unrelaxed ground state. Again, the lattice relaxes to the equilibrium state, which is the relaxed ground state. In the reorientation process (Fig. 3), the F_A - center moves from one anion site to the nearest one which is adjacent to the impurity by the step-diffusion process, passing through the saddle-point configuration. In the dissociation process the F_A - center moves from one anion site to the nearest one which is not adjacent to the impurity.

1.1 Experimental Situation

Experimentally, the three-fold degenerate F - center absorption transition has been observed to be split into two lines in the F_A - centers. This is due to reduction of the F - center's symmetry by the impurity cation. One of the absorption lines is polarized along the Z (or X) - axis, if the impurity cation is at (010), and is called the F_{A2} level (Fig. 4a), and the other is polarized along the y-axis (Fig. 4b), in the direction of the neighboring impurity cation, and is called the F_{A1} level. The position and shape of the emission band of the $F_A(Na)$ - center is similar to that of the F - center, but for the $F_A(Li)$ - center, it has a larger Stokes shift, a narrower emission band and the absence of thermal and field ionization of the excited state. Lüty[1] concluded that the emission processes occur in the vacancy configuration for the $F_A(Na)$ - center, and in the saddle point configuration for the $F_A(Li)$ - center. The experimental values for

Figure 2

Vacancy and saddle - point configurations of the lattice for F_A - centers in KCl. † denotes the cation, - denotes the anion, and ✱ denotes the impurity substitutional cation.

(a) vacancy configuration

(b) saddle - point configuration

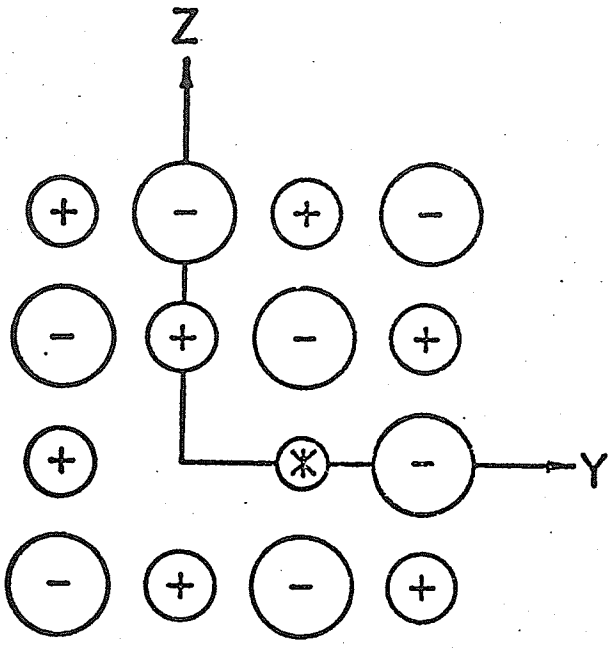

(a)

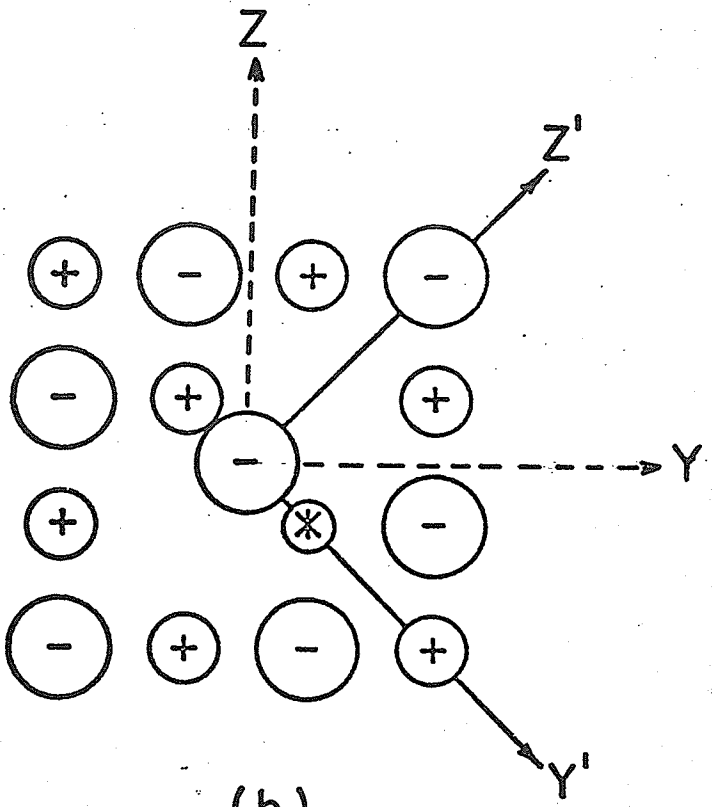

(b)

Figure 3

Model for reorientation of the F_A - center in KCl.
† denotes the K^+ ion, - denotes the Cl^- ion, ✱ denotes the impurity cation and e^- denotes the trapped electron

(a) initial state

(b) intermediate state (saddle point configuration)

(c) final state

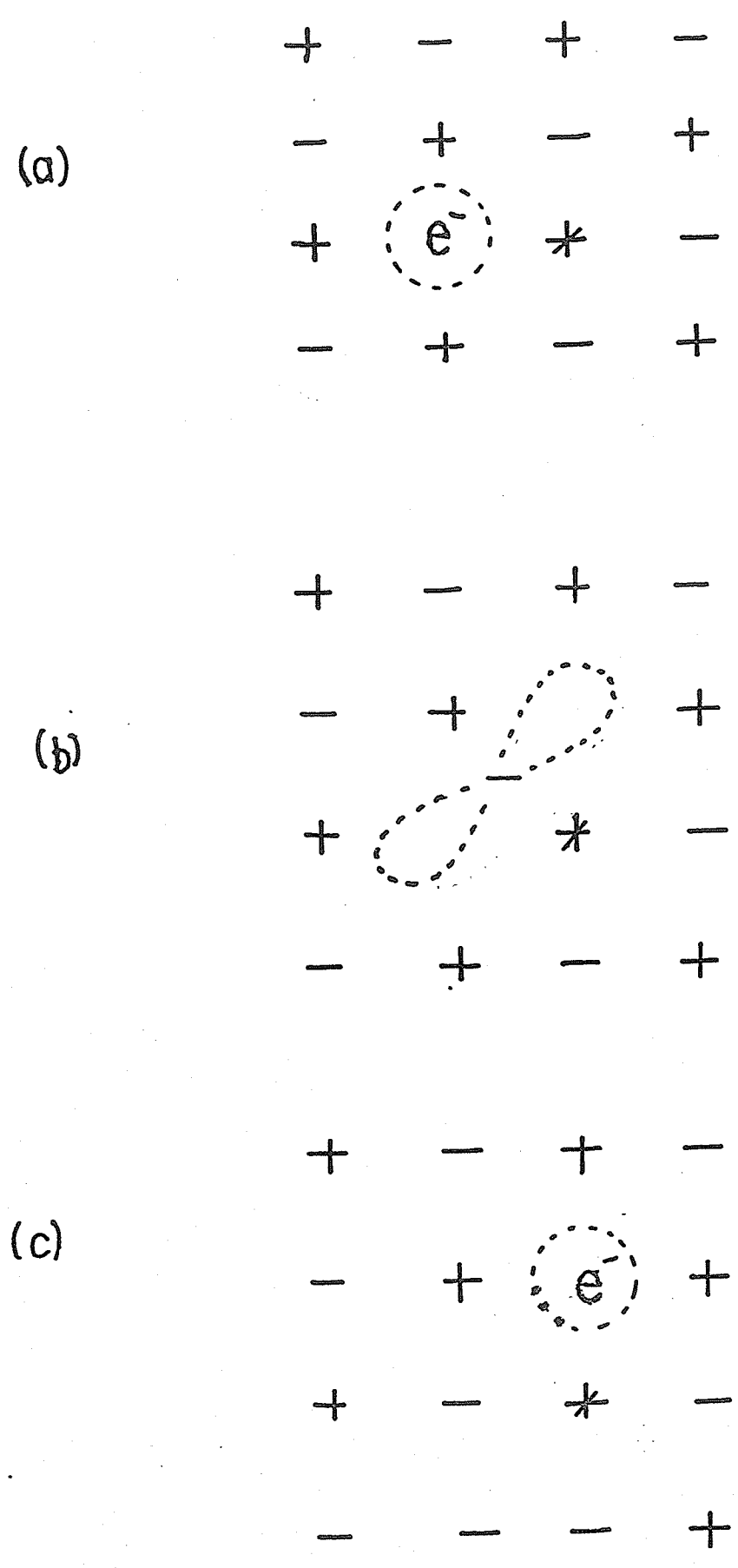
(a)
(b)
(c)

Figure 4

F_{A1} and F_{A2} unrelaxed excited states for F_A - centers in KCl. † denotes K^+ ion, - denotes Cl^- ion, $\ast$ denotes impurity ion, and ---- schematically indicates excess - electron.

(a) F_{A2} unrelaxed excited state

(b) F_{A1} unrelaxed excited state

(a)

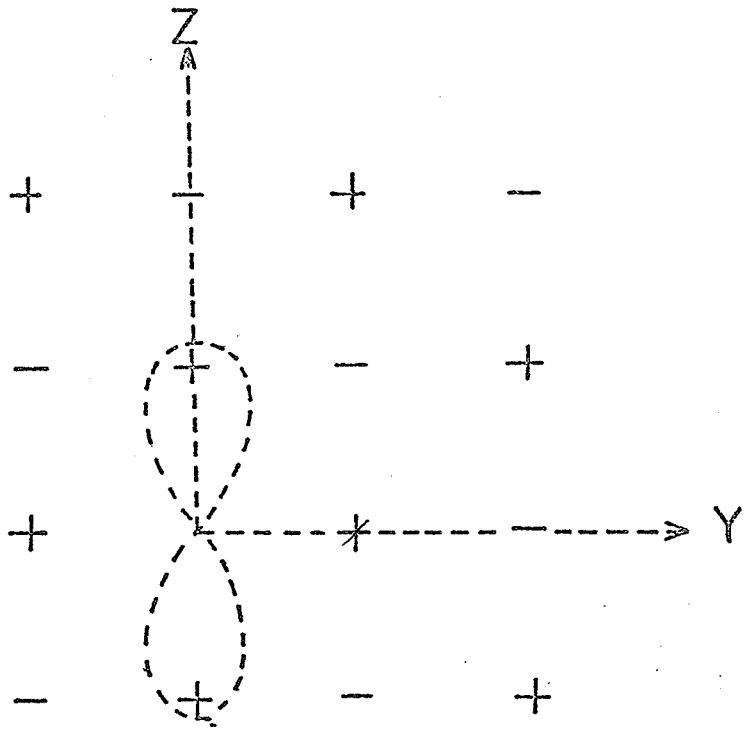

(b)

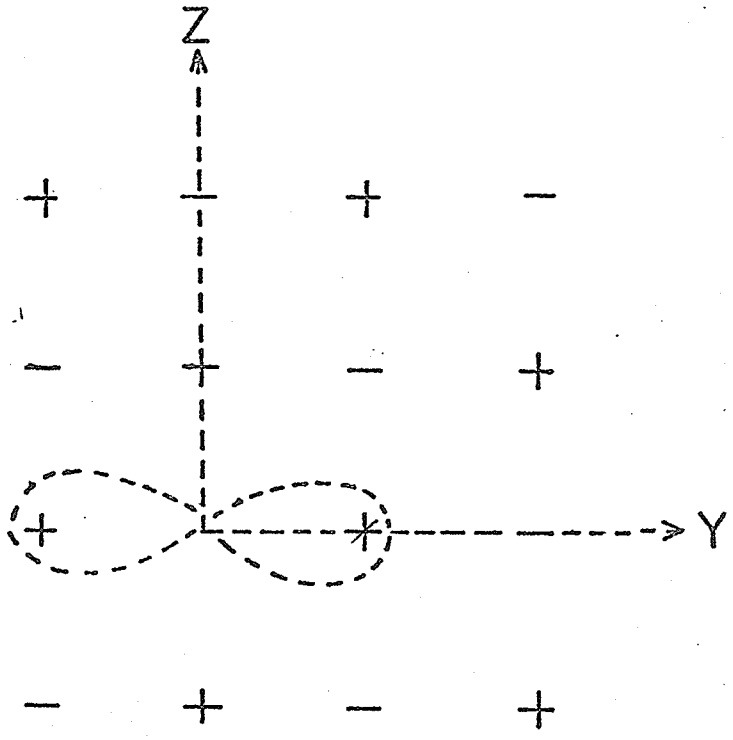

(A) F_{A1} absorption energy;

(B) $F_{A2} - F_{A1}$ absorption splitting;

(C) even parity reorientation activation energy;

(D) even parity relaxation energy in the saddle-point configuration;

(E) emission energy in the saddle-point configuration;

(F) odd parity reorientation activation energy

are shown in Figure 5. All the experimental data are taken from ref. (1). The energy levels relating to both vacancy configuration and saddle-point configuration are shown. The question marks in the figure means that the experimental values are not available.

The F_{A1} and F_{A2} transition measurements have been done by Lüty (ref. (1), p. 188) by optical methods. F_{A1} and F_{A2} absorption spectra can be observed by shining unpolarized light onto the crystal. The overlapping of the F_{A1} and F_{A2} spectra is decreased by using a dichroic crystal with suitable choice of polarization of the incident light. The reorientation process can be observed by the change in its F_{A1} or F_{A2} polarization on heating. Analysis of the temperature dependence of the relative absorption constant (ref. (1), p. 200) yields the reorientation energy.

1.2 Previous Theoretical Investigations

Three theoretical investigations of the absorption processes of both the $F_A(Na)$ and $F_A(Li)$ centers have previously been done [2],[3],[4]. Two other investigations have studied $F_A(Na)$ absorption only[5],[6]. None of the authors attempt to verify the peculiar relaxed excited state of the $F_A(Li)$ centers or the reorientation process for either center.

In order to understand the origin of the splitting, one has to go beyond the point ion approximation. The point ion lattice approximation has been used in an F - center absorption calculation by Gourary and Adrian[7]. Their result is in moderate agreement with experiment. In the point ion lattice approximation, the ions are treated as point charges of appropriate sign. In other words, we neglect the size of the ion core; that is, we neglect the exchange interaction between the excess-electron and the core electron and the interaction of the excess F - electron with the point ion is taken to be purely electrostatic. Thus, the one electron Hamiltonian of the F - electron is the sum of the kinetic energy of the

Figure 5

Experimental energies (eV) for F_A(Li) and F_A(Na) - centers in KCl.

(A) F_{A1} - absorption energy

(B) F_{A2} - F_{A1} absorption splitting

(C) even parity reorientation activation energy

(D) even parity relaxation energy in the saddle-point configuration

(E) emission energy in the saddle point configuration

(F) odd parity reorientation activation energy

The unlabelled energies 1.12 for F_A(Na)-center is the emission energy in the vacancy configuration.

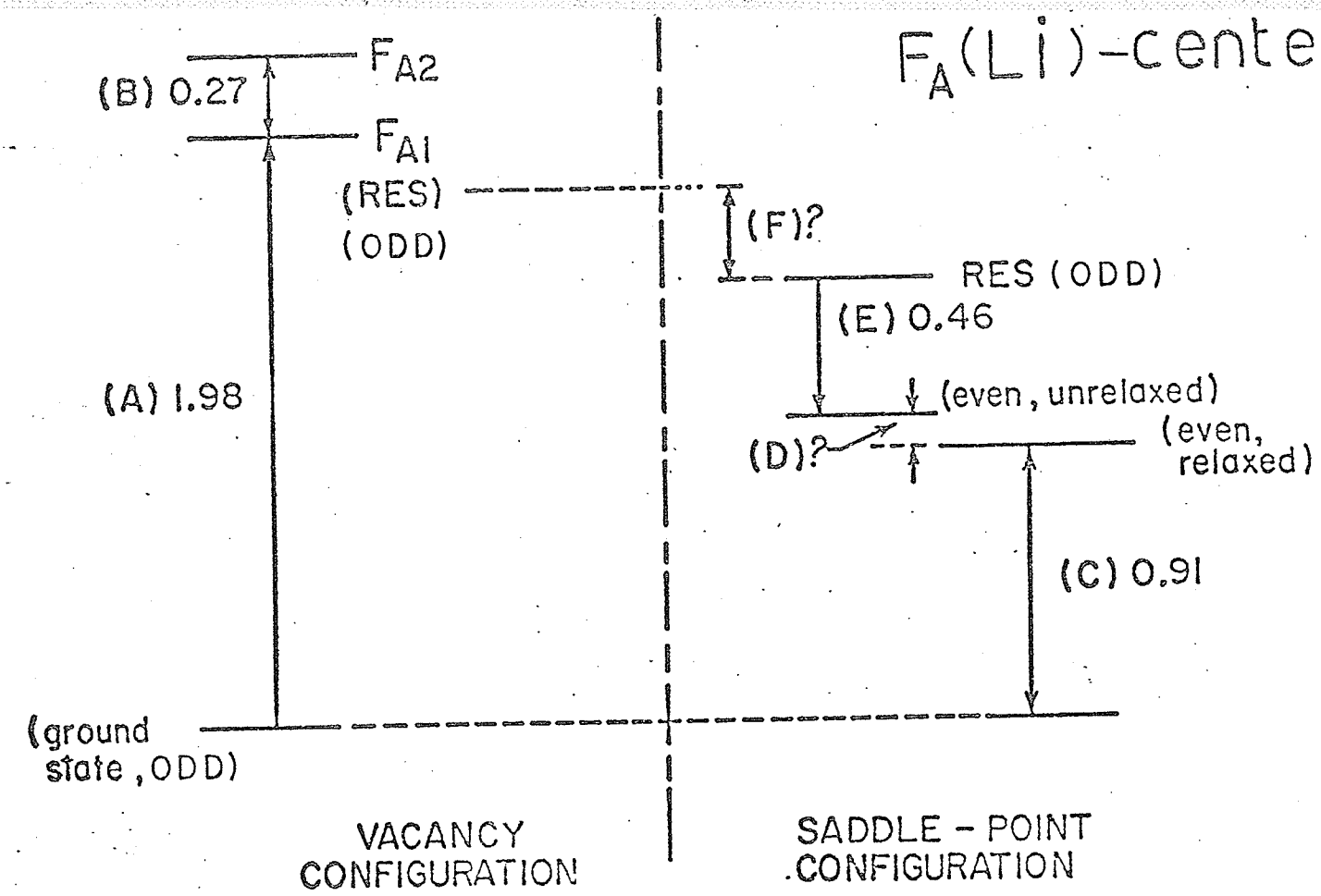
F_A(Li)-center
F_{A2}
(B) 0.27
F_{A1}
(RES)
(ODD)
(F)?
RES (ODD)
(E) 0.46
(A) 1.98
(even, unrelaxed)
(D)?
(even, relaxed)
(C) 0.91
(ground state, ODD)
VACANCY CONFIGURATION
SADDLE - POINT CONFIGURATION

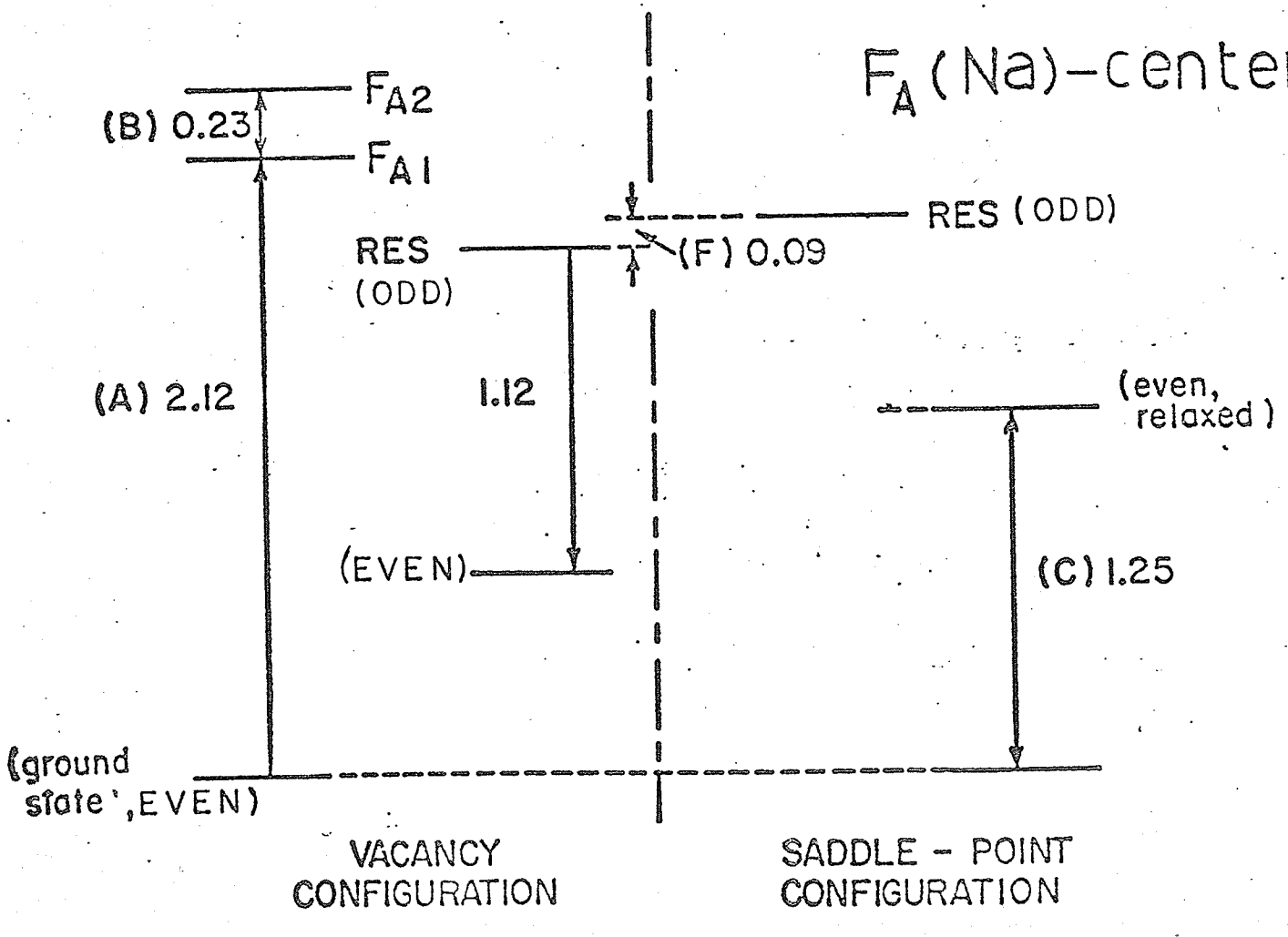
F_A(Na)-center
F_{A2}
(B) 0.23
F_{A1}
RES (ODD)
RES
(ODD)
(F) 0.09
(A) 2.12
1.12
(even, relaxed)
(EVEN)
(C) 1.25
(ground state, EVEN)
VACANCY CONFIGURATION
SADDLE - POINT CONFIGURATION

F - electron and the electrostatic interaction of the F - electron and point ion lattice.

However, the electrostatic and exchange interactions between the excess-electron and the core electrons is important for the F_A - center study. Kojima et al[5] used a linear combination of the atomic orbitals of the six nearest neighbors to the F_A - center as ground and excited state wave functions. They thus included the ion-size effect of the nearest neighbours and neglected the contribution from the other ions. They concluded that the energy differences between the unrelaxed F_{A1} - levels and unrelaxed F - levels are functions of the difference in ionization energy of the host and impurity cation. Smith[2] has calculated the shift in the absorption energy between F and F_A - centers. He treated the difference of pseudopotentials of the nearest neighbour impurity cation and host cation as the perturbation on the point-ion approximation. The pseudopotential is determined from the requirement of the orthogonality of the F_A - center wave function to the core orbitals. Weber and Dick[3] used the approximate pseudopotentials for the ion-size correction, as evaluated by Bartram et al[8] (hereafter referred to as BSG), and which will be discussed further in Chapter 2. In order to get agreement with experiment, they discarded the reduction factor 0.53 which is suggested by BSG. Lattice distortion and ionic polarization are not included in their calculation. Alig[4] has developed an approximate form for ion size correction, similar to BSG, but without the reduction factor 0.53. He also included the lattice distortion and ionic polarization of the six nearest neighbours to the vacancy by the method of Gourary-Adrian[7] (GA). GA - type wave functions have been used for the later three investigations but only Weber and Dick[4] make them self-consistent with the lattice potential.

1.3 Brief Description of our Model and Method

In all previous investigations, and in the present-work, the lattice is considered as static, i.e. no dynamical effects are included. The adiabatic approximation[9] is used to decouple the electronic state from that of the lattice. In the adiabatic approximation, the electron is assumed to move very fast in the potential provided by the lattice, and therefore follows the lattice motion adiabatically. On the other hand, the lattice cannot respond to the electron's instantaneous position, only to its average position. The Franck-Condon principle is also applied, which states that the transition of the electron from one state to another occurs while the lattice remains fixed. In fact, in some states the excess electron may interact with the optical phonon modes to behave like a polaron and such electron lattice interaction is non-adiabatic[10],[11].

Two main problems involved in point-defect calculations are:

(1) to determine the appropriate interionic potential;

(2) for a given potential, to calculate the distortion field about the defect.

For the F_A - center, one further problem has to be solved: the excess-electron wave function.

In the present work, the Born-Mayer potential with Tosi's single exponential parameters[12] was used. That is, we used perfect lattice parameters for the defect lattice. This approximation seems to have been justified in Tosi's calculation[13] of the vacancy migration energy in KCl It remains to be seen how well justified it is in other defects.

The method we used in calculating the excess-electron wave function was variational. The trial wave functions which we used were Gaussian-localized, low-order Legendre polynomials. The ion-size effect has been

included by using BSG approximate pseudopotential with the reduction factor $\alpha = 0.53$. In this approximation, the pseudopotential introduces an extra term into the Hamiltonian. The justification for α has been discussed by Stoneham[42].

The displacements of the ions around the defect from their perfect lattice sites have been calculated and the resulting contribution to the defect system's energy has been included. The method which we used for this is called the lattice statics method[14],[15],[16], in which the whole lattice is treated as discrete and the results can be made exact within the harmonic approximation. The method has been extended by Vail[17] to include non-harmonic lattice distortion near the defect. The criterion that we used for identifying the ions with non-harmonic displacements is that convergency of the solution of $\underline{\xi}$ failed if they were included in region II. (see equation (2.83) and appendix (c)). The further merit of this method is that the distortion field of the lattice is made self-consistent within the excess-electron wave function. There is no doubt that the wave function of the excess-electron will alter as the lattice distorts.

In short, our estimates of electronic defect energies are based on a variational procedure in which parameters in a trial electronic wave function and the ionic displacements are determined self-consistently to minimize the total energy of the system.

1.4 Brief Summary of our Results

Comparison of our calculated results with experiments show the following:

(1) the even-parity reorientation energies of both $F_A(Li)$ and $F_A(Na)$ centers are in good agreement with experiment;

(2) the F_{Al} absorption energy for both $F_A(Li)$ and $F_A(Na)$ centers, agrees with the experiment;

(3) the relaxed excited state of $F_A(Li)$ is stabilized in the saddle point configuration;

(4) the splitting of F_{A1} - F_{A2} absorption is about three times too large, compared with experiment.

Our results fail to describe:

(1) the emission process of the F_A(Li) in the saddle-point configuration;

(2) the relaxed excited state of F_A(Na) stabilized in the vacancy configuration.

Throughout the project, we refused to make any empirical correction to improve our agreement with the experiment, because this would hide the weakness of the model and method, which is one of our objectives to assess.

1.5. Relevance of this Investigation

There are three areas of relevance for this investigation:

(1) qualitative features

In the present investigation, the system's energy can be conveniently expressed in five parts: the electron's kinetic energy, the point ion potential, the ion-size correction, the lattice defect energy, and the harmonic lattice distortion energy. Thus, the role which the excess-electron plays in the step-diffusion process in both odd-parity and even-parity states, can be understood qualitatively. Also by comparison of the contribution from the different terms to the activation energy of the F_A - center and the ordinary F - center, the role of the impurity ion in the activation process can be qualitatively assessed.

(2) theoretical relevance

The results of the present calculation will give some indication

of how well our model and approximations can describe the properties of defects. Discrepancies with experiment will give some indication of possible modifications and improvements which should be made to the model and methods.

(3) Applications

The F_A - center occurs in photochromic materials[18] and therefore, has some relevance in design of photochromic devices. Photochromic materials are those which change color in a reversible way under illumination. The reversible photochromic process for F_A - center is

$$F_A + F_A \underset{h\nu'}{\overset{h\nu}{\rightleftharpoons}} F_A' + \text{vacancy}$$

where $h\nu$ is the energy needed to ionize the F_A - center electron to the conduction band. The electron can then be trapped by another F_A - center to form an F_A' - center, the F_A' - center consisting of two electrons trapped in the anion vacancy. The position and sharpness of the F_A' - center lines are very different from those of the F_A - center. Similarly, one of the electrons of the F_A' - center can be ionized into the conduction band and be trapped by a vacancy to form another F_A - centers, giving the original configuration. Some of the factors which determine whether a photochromic device can be based on a given electronic defect, and which could be assessed using the present model and methods are:

(1) the defect energy levels relative to the conduction band;

(2) the relative magnitudes of the absorption energy for related but different defects (e.g. F_A and F_A' - center)

(3) the presence or absence of competing absorption and emission

processes.

1.6. Brief Outline of Remainder of Thesis

The basic elements of our model and methods, namely, Tosi's single-exponential form of Born-Mayer repulsion, Franck-Condon approximation, the BSG ion size correction, and the method of lattice statics will be described and discussed in chapter 2. The details of the calculation and the results will be reported and analysed in chapter 3. This will include the energy levels and distortions for both relaxed and unrelaxed states in each of the two configurations. The role of the impurity ion in the activation process is also discussed. The critical assessment is given and suggestions are made in chapter 4.

CHAPTER 2

METHODS AND MODEL

The purpose of this chapter is to provide the theoretical background for the point defect calculation. In the present calculation, the lattice is treated as discrete point charges bound by Coulomb interaction and stabilized by a repulsive force. Tosi's single exponential form of Born-Mayer repulsion has been used. The ion-size effect of the lattice is taken care of by the BSG approximation with the empirical factor $\alpha = 0.53$, which is based on a pseudopotential method. For the electronic part of this problem, a one electron Hamiltonian is used. The variational method is used for calculating the electronic wave function and energy levels. In the variational method, the ion-size correction is just an extra term in the electronic Hamiltonian. For the lattice part of this problem, the lattice distortion is calculated rigorously by the lattice static method. Furthermore, the excess-electron wave function is not only made self-consistent with the given potential but also with the lattice distortion. However, ionic polarization and electron-phonon interaction are not included. The Franck-Condon approximation is used for calculating absorption and emission energy. In the following sections, we are going to discuss

(1) the lattice energy (2) the Franck-Condon approximation (3) the ion size correction and (4) the method of lattice statics.

2.1. The Lattice Energy

In the point ion model, the ionic interaction can be written as the sum of Coulomb (c) and repulsive (R) parts,

$$W = W^{(c)} + W^{(R)} \tag{2.1}$$

Tosi[12] has developed a Born-Mayer type single exponential (SE) form for $W^{(R)}$:

$$W^{(R)} = B \exp\left(-\frac{r}{\rho}\right) \tag{2.2}$$

$W^{(R)}$ applies only to nearest neighbour interactions. The parameters B and ρ are determined from the following equations of state which included the temperature correction.

$$\frac{dW}{dV} = -p + \frac{T\beta}{K} \tag{2.3}$$

$$V\frac{d^2W}{dV^2} = \frac{1}{K} + \frac{T}{K^2}\left[\left(\frac{\partial K}{\partial T}\right)_p + \frac{\beta}{K}\left(\frac{\partial K}{\partial p}\right)_T\right] \tag{2.4}$$

where K is the isothermal compressibility and β is the volume coefficient of thermal expansion. The determined value of β and ρ have been given in ref. (12) table VII 2nd column. The SE form is known to give reasonable results for vacancy migration[13].

2.2. Franck-Condon Principle

The following discussion of the Franck-Condon principle will be restricted to the static lattice model which we have used in the present

calculation.

There are two electronic bound states involved for each electronic transition considered in this work. For each of the electronic states, there is a different set of equilibrium lattice distortion parameters $(\underline{\mu},\underline{\xi})$, because of the different charge distributions of the excess-electron interacting with the lattice. In order to describe the Franck-Condon principle for the transition of the electron from one state to the other, we are going to introduce the so-called "configuration coordinate" diagram. The configuration coordinate can be understood by reference to figure 6, where the defect system's energies are plotted as a function of a single coordinate, different values of which correspond to different lattice configurations. The lower curve of Fig. 6 is the energy curve corresponding to the electronic state a, or ground state. The upper curve is the energy curve for the electronic state b, or first excited state. The optical absorption and emission processes for the color center can be visualized from this configuration diagram, as follows. When F_A - center is in the ground state A, it will be excited to the first excited state B after absorbing a photon. Thereafter, the lattices has to readjust to the new charge density of the electron, and so it relaxes to C by giving up energy as phonons. The emission process occurs from state C. Again, the system relaxes from state D to state A by giving up the corresponding energy as phonons.

The configuration coordinates of the state A and B are the same, namely Rg in Fig. 6. Similarly, state C and state D have the same configuration coordinate R_{ex}. This is the essence of the Franck-Condon principle, which assumes that in the most probable transitions, the ionic coordinates do not change, or "vertical transitions" occur in the configur-

Figure 6

Configuration coordinate diagram for an F_A - center. A → B is the absorption process and C → D is the emission process, in Franck - Condon approximation. E is the total defect system's energy and R is the "configuration coordinate".

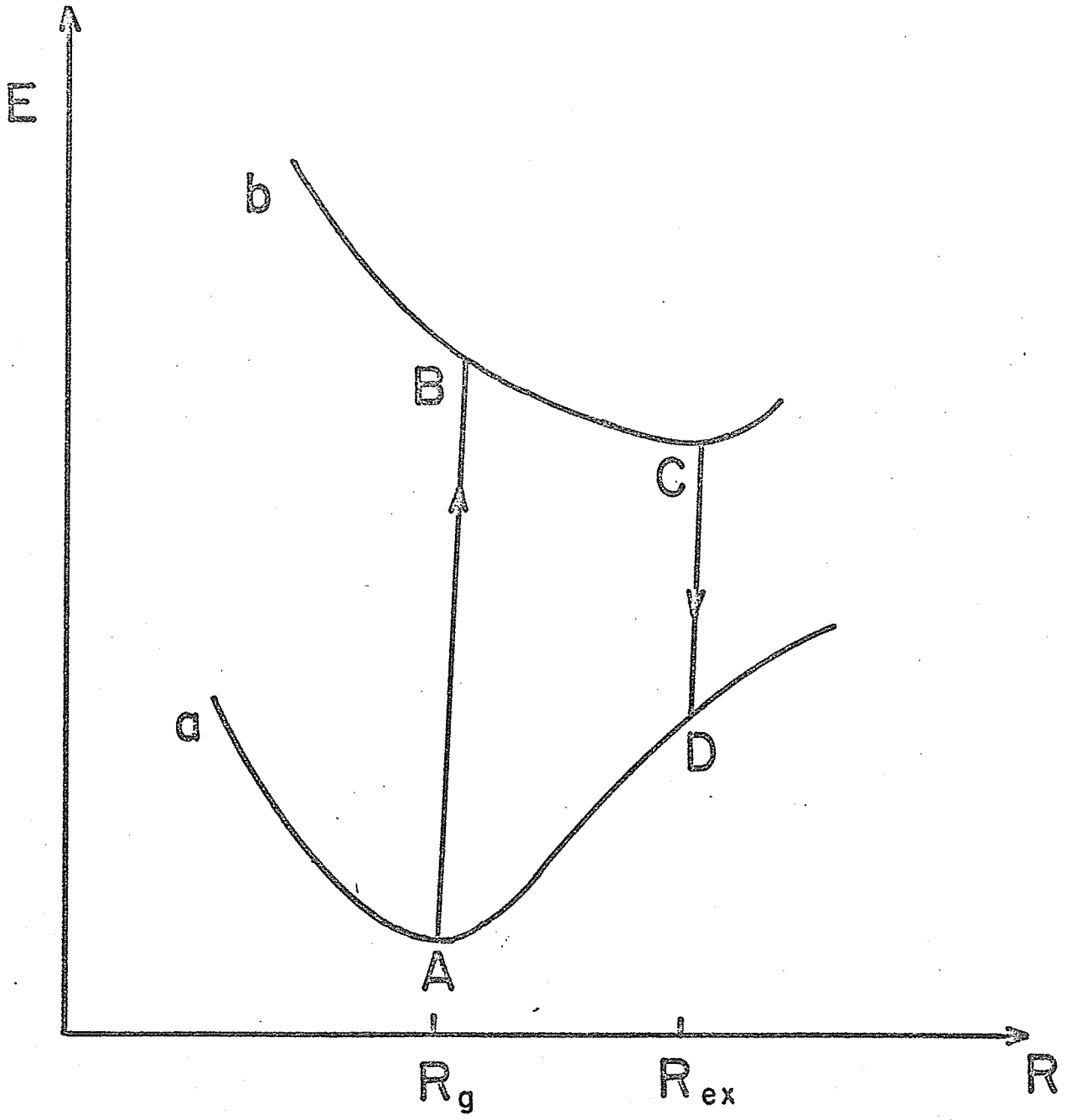
E
b
B
C
A
a
D
A
R_g
R_{ex}
R

ation diagram. In short, in terms of the configuration coordinates, the Franck-Condon principle describes the absorption energy and emission energy as the magnitude of $A \to B$ and $C \to D$, as in Fig. 6, while the Stokes shift is described as the difference of the magnitudes $A \to B$ and $C \to D$.

The limits of validity of the Franck-Condon principle are not obvious. It depends on details of the phonon distribution and on the electron phonon interaction both of which are ignored in our treatment[10),(11)].

2.3. Ion-size Correction

The following discussion on the ion-size correction is based on ref. (21).

Consider the Schrödinger equation

$$H\psi = E\psi \tag{2.5}$$

where H = one electron Hamiltonian $= T + V$

T = kinetic energy operator

V = the potential energy due to all the ions, and the eigenfunction ψ of the excess-electron must be orthogonal to the core states $|c\rangle$ of the ions. Now, let us define $|\phi\rangle$ by

$$|\psi\rangle = |\phi\rangle - \sum_c |c\rangle\langle c|\phi\rangle$$

$$= \left(1 - \sum_c |c\rangle\langle c|\right)|\phi\rangle \tag{2.6}$$

where $|\phi\rangle$ is a smooth wave function which is not orthogonal to the core state. Write

$$P = \sum_c |c\rangle\langle c| \tag{2.7}$$

which is known as the projection operator, projecting onto the core states. Then, equation (2.6) becomes

$$| \psi > = (1 - P) | \phi > \tag{2.8}$$

In the pseudopotential method, instead of solving the eigenvalue equation (2.5) for ψ, one considers another eigenvalue problem

$$(H + V_R) \phi = \tilde{E} \phi \tag{2.9}$$

which is solved for ϕ, called the pseudo-wave function. Let us write

$$V_R = P O_p \tag{2.10}$$

where O_p is an arbitrary operator. There are two different forms of V_R which are of interest in color center calculations, namely:

(1) Cohen and Heine[19] pseudopotential (V_p^{CH})

(2) Phillips and Kleinman[20] pseudopotential (V_p^{PK})

For V_p^{CH} operating with $(1 - p)$ from the left on equation (2.9) gives:

$$(1 - P) (H + V_R) \phi = (1 - P) \tilde{E} \phi \tag{2.11}$$

Making use of equation (2.10), $P^2 = P$ and $[H, P] = 0$, equation (2.11) becomes:

$$H(1 - P) \phi = \tilde{E} (1 - P) \phi \tag{2.12}$$

Therefore $(1 - P)\phi$ is a eigenfunction of H and we denote the eigenvalue $\tilde{E} = E$. Then, equation (2.9) can be written as

$$(T + V + PO_p) \phi = E \phi$$

or

$$(T + V_p) \phi = E \phi \tag{2.13}$$

where

$$V_p = (V + PO_p) \tag{2.14}$$

is called the pseudopotential.

Since O_p is arbitrary, thus far, we fix O_p by requiring smoothness of the wave function. This corresponding to minimizing the kinetic energy or maximizing $\bar{V}$, with respect to the variations of ϕ, i.e.

$$\delta \bar{V} = 0 \tag{2.15}$$

where

$$\bar{V} = \frac{< \phi \mid V + V_R \mid \phi >}{< \phi \mid \phi >} \tag{2.16}$$

We evaluate equation (2.15) by the Lagrangian multiplier method

$$\delta \left(< \phi \mid V + V_R \mid \phi > - \lambda < \phi \mid \phi >\right) = 0$$

where λ is the Lagrangian multiplier. Thus

$$< \delta \phi \mid V + V_R \mid \phi > + < \phi \mid V + V_R \mid \delta \phi >$$

$$- \lambda < \delta \phi \mid \phi > - \lambda < \phi \mid \delta \phi > = 0$$

Consider $< \phi \mid$ and $\mid \phi >$ separately. Then

$$< \delta \phi \mid V + V_R \mid \phi > - \lambda < \delta \phi \mid \phi > = 0 \tag{2.17}$$

Since this must be true for arbitrary $< \delta \phi \mid$,

$$(V + V_R) \mid \phi > - \lambda \mid \phi > = 0$$

whence;

$$\lambda = \frac{\langle \phi \,|V + V_R|\, \phi \rangle}{\langle \phi \mid \phi \rangle} = \overline{V} \tag{2.18}$$

Thus equation (2.17) becomes

$$\langle \delta \phi \mid V + V_R \mid \phi \rangle - \overline{V} \langle \delta \phi \mid \phi \rangle = 0 \tag{2.19}$$

If we substitue $| \phi' \rangle = | \phi \rangle + \sum_c \alpha_c | c \rangle$ for $| \phi \rangle$ in equation (2.8), where α_c are arbitrary constants, then we have:

$$(1 - p) | \phi \rangle = (1 - p)(| \phi' \rangle - \sum_c \alpha_c | c \rangle)$$

$$= | \phi' \rangle - \sum_c \alpha_c | c \rangle - P |\phi' \rangle + \sum_c P \alpha_c | c \rangle$$

$$= | \phi' \rangle - \sum_c \alpha_c | c \rangle - P | \phi' \rangle + \sum_c \alpha_c | c \rangle$$

$$= | \phi' \rangle - P | \phi' \rangle$$

$$= (1 - p) | \phi' \rangle \tag{2.20}$$

Thus, the result in equation (2.8) will not change if we replace ϕ by ϕ'. Thus, take $|\delta \phi \rangle = \sum_\alpha \alpha_c | c \rangle$ and substitute into equation (2.19)

$$\sum_c \alpha_c \langle c \mid V + V_R \mid \phi \rangle - \overline{V} \sum_c \alpha_c \langle c \mid \phi \rangle = 0$$

$$\sum_c \alpha_c \left[\langle c \mid V + V_R \mid \phi \rangle - \overline{V} \langle c \mid \phi \rangle \right] = 0$$

Then since the α_c's are arbitrary,

$$\langle c \mid V + V_R \mid \phi \rangle - \overline{V} \langle c \mid \phi \rangle = 0 \tag{2.21}$$

But

$$V_R | \phi \rangle = P O_p | \phi \rangle$$

$$= \Sigma_{c'} | c' \rangle \langle c' | O_p | \phi \rangle \tag{2.22}$$

And

$$< c \mid V_R \mid \phi > = \sum_{c'} < c \mid c' > < c' \mid O_p \mid \phi >$$

$$= < c \mid O_p \mid \phi > \qquad (2.23)$$

Substituting equation (2.23) into equation (2.21), we get

$$< c \mid V \mid \phi > + < c \mid O_p \mid \phi > - \overline{V} < c \mid \phi > = 0$$

then

$$< c \mid O_p \mid \phi > = < c \mid (\overline{V} - V) \mid \phi > \qquad (2.24)$$

Then equation (2.22) becomes

$$V_R \mid \phi > = \sum_{c} \mid c > < c \mid (\overline{V} - V) \mid \phi >$$

$$= P \ (\overline{V} - V) \mid \phi > \qquad (2.25)$$

Therefore, the optimum pseudopotential in this case is

$$V_P^{CH} = V + P \ (\overline{V} - V) \qquad (2.26)$$

For the Philips and Kleinmean pseudopotential V_p^{PK}, one substitutes equation (2.8) into equation (2.5). Then:

$$H(1 - p) \mid \phi > = E \ (1 - p) \mid \phi >$$

$$[H + P(E - H)] \mid \phi > = E \mid \phi > \qquad (2.27)$$

Identifying equation (2.27) with equation (2.9), we get

$$V_R^{PK} = P \ (E - H) \qquad (2.28)$$

Thus

$$V_p^{PK} = V + P\ (E - H) \tag{2.29}$$

There is also some arbitrariness of the wave function ϕ for the Philips and Kleinman pseudopotential. However, Bartram and Gash[21] believe that if the pseudo-wave function ϕ is appropriate for Cohen and Heine pseudopotential, then, it will be appropriate for Philips and Kleinman pseudopotential too.

The most important different feature between V_p^{PK} and V_p^{CH} is that V_p^{PK} is Hermitian but V_p^{CH} is not. We must notice that the variation principle cannot in general be used to solve the eigenvalue problem for non-Hermitian Hamiltonian.

BSG[8] employed the Cohen and Heine pseudopotential (equation (2.26)) in calculating the F - center absorption energy. They rewrote equation (2.26) in a form such that they could compare their results with the point-ion lattice calculation, and introduced the ion-size correction term for color centers, as follows:

$$V_p^{CH} = V_{pI} + (V - V_{pI}) + p\ (\overline{V} - V) \tag{2.30}$$

where V_{pI} is the potential energy operator when all the lattice ions are approximated as point charges. Neglecting the overlap of ion cores on different sites, we have:

$$P_\gamma = \sum_\gamma p_\gamma \tag{2.31}$$

where γ labels the ion at site γ. Similarly, V and V_{pI} can be expressed as

$$V_\gamma = \sum_\gamma V_\gamma \tag{2.32}$$

$$V_{pI} = \sum_{\gamma} V_{pI_\gamma} \tag{2.33}$$

The summation $\sum_{\gamma}$ is over all the ion sites. The equation (2.30) becomes:

$$V_p^{CH} = V_{pI} + \sum_{\gamma} [(1 - P_\gamma)(V_\gamma - V_{pI_\gamma}) - P_\gamma V_{pI_\gamma} + P_\gamma [\bar{V} - U_\gamma]$$

where U_γ is the potential energy of an excess-electron at lattice site γ due to all the other ions in the crystal, which can be written as

$$U_\gamma \equiv \sum_{\gamma' \neq \gamma} V_{\gamma'} \approx \sum_{\gamma' \neq \gamma} V_{pI_{\gamma'}} \tag{2.35}$$

Since the core orbitals are assumed to be highly localized within ion core γ.

At this stage, one has to note that $(T + V_p^{CH})$ is not Hermitian and therefore the variational principle cannot be assumed to give an upper bound of the eigenvalues. BSG[8] avoid this by assuming that the variation of the wave function inside the ion core can be neglected, since the pseudo-wave function given by V_p^{CH} must be the "smoothest". Thus, the solution of equation (2.9) is

$$\tilde{E} \leq \langle \phi \mid T + V_{pI} \mid \phi \rangle + \sum_{\gamma} \mid \phi (\vec{r}_\gamma) \mid^2 \{A_\gamma + (\bar{V} - U_\gamma) B_\gamma\} \tag{2.36}$$

where

$$A_\gamma = \int (1 - p_\gamma) (V_\gamma - V_{pI_\gamma}) \, d\tau - \int p_\gamma V_{pI_\gamma} \, d\tau \tag{2.37}$$

and

$$B_\gamma = \int P_\gamma \, d\tau \tag{2.38}$$

The numerical values of A_γ and B_γ have been computed for a number of

ions by BSG (see ref. 8, table I). Then, the form of the ion-size correction is

$$V_{IS} = \sum_{\gamma} [A_{\gamma} + B_{\gamma} (\bar{V} - U_{\gamma})] \delta (\vec{r} - \vec{r}_{\gamma}), \tag{2.39}$$

which can be used in a variational calculation.

BSG have used this approximation in calculating F - center absorption energies. Their calculated results indicated that in order to get agreement with experiment, one has to use (αA_{γ}) instead of A_{γ}, with $\alpha = 0.53$. After introducing the empirical factor $\alpha = 0.53$, they found the calculated F - center absorption energies of 16 of the 17 alkali halides with rocksalt structure to be in agreement with the experimental values. The theoretical origin of this factor α has been pursued by Gash[21]. He found that the main source of error came from the assumption of negligible variation of the pseudo-wave function over the ion cores. Furthermore, Gash[21] have developed an exact pseudopotential calculation to take care of the ion-size effect. He used the Philips and Kleinman pseudopotential instead of the Cohen and Heine form because V_p^{pK} is Hermitian. Consider the pseudopotential equation

$$[H + p (E - H)] \phi = E \phi$$

The variational method can be rigorously applied here to give

$$E \leq \frac{< \phi \mid H + p(E - H) \mid \phi >}{< \phi \mid \phi >} \tag{2.40}$$

or

$$E [< \phi \mid \phi > - < \phi \mid p \mid \phi >] \leq < \phi \mid H \mid \phi > - < \phi \mid pH \mid \phi >$$

then

$$E \leq \frac{\langle \phi \mid H \mid \phi \rangle - \langle \phi \mid pH \mid \phi \rangle}{(\langle \phi \mid \phi \rangle - \langle \phi \mid p \mid \phi \rangle)} .$$

Using normalized wave functions, i.e. $\langle \phi \mid \phi \rangle = 1$, we have

$$E \leq \frac{\langle \phi \mid H \mid \phi \rangle - \langle \phi \mid pH \mid \phi \rangle}{(1 - \langle \phi \mid p \mid \phi \rangle)}$$

$$= \frac{\langle \phi \mid H \mid \phi \rangle - \sum_{\gamma} \sum_{c} \langle \phi | c_{\gamma} \rangle \langle c_{\gamma} \mid H \mid \phi \rangle}{(1 - \sum_{\gamma} \sum_{c} \langle \phi \mid c_{\gamma} \rangle \langle c_{\gamma} \mid \phi \rangle)}$$

$$= \frac{\langle \phi \mid H \mid \phi \rangle - \sum_{\gamma} \sum_{c} E_{\gamma c} \mid \langle c_{\gamma} \mid \phi \rangle \mid^2}{(1 - \sum_{\gamma} \sum_{c} \mid \langle c_{\gamma} \mid \phi \rangle \mid^2)} \qquad (2.41)$$

where $E_{\gamma c}$ is given by:

$$E_{\gamma c} = E_c + \bar{g}_{cF} + \bar{V}_{\gamma}$$

where E_c = free-ion Hartree-Fock eigenvalues for state $\mid c \rangle$

$\bar{g}_{cF}$ = Coulomb and exchange interaction between γ^{th} free-core orbital and the excess-electron

$\bar{V}_{\gamma}$ = Coulomb potential at site γ due to the rest of the ions and the anion vacancy

The upper bound of the eigenvalue can be located by a numerical method. We are not going to pursue this approach any further here, since we have used the BSG approximation with the empirical factor $\alpha = 0.53$ in the present work.

There is no doubt that the work of Gash[21] is well beyond that of BSG. The reason we used BSG in the present work is that the

information of Gash's work was not available before the present work was completed. In fact his work is not yet published.

2.4. Method of Lattice Statics

Once we introduce a point defect into a perfect lattice, the nearer ions will be displaced from their perfect lattice sites. The method we used to calculate this lattice distortion is the method of lattice statics, which was first introduced by Kanzaki[14]. In this method, the ions in the lattice are treated as discrete. The actual displacements of the ions from the perfect lattice sites can be calculated from normal coordinates which are essentially the Fourier inverses of the direct space displacements.

(A) General Formulae

In the following illustration of the method of lattice statics, we follow Vail's notation[17] closely. In this method, those ions which have harmonic displacements in the resultant distorted defect lattice configuration are treated separately from those which have non-harmonic displacements or which were not present in the perfect lattice. We distinguish these two classes of ions by denoting those ions which were present in the host lattice and whose displacements from perfect lattice sites are within the validity of the harmonic approximation as Region II. The rest will be denoted as Region I, which consists of the defect and possibly some of its surrounding ions including impurity ions. The components of the harmonic displacements of the Region II ions are taken to be elements of the column matrix $\underline{\xi}$ and the generalized coordinates of ions in the Region I are written as the column matrix $\underline{\mu}$. The number of elements of $\underline{\mu}$ will be small for a well-localized defect.

In the framework of the harmonic approximation, we imagine a perfect lattice in which Region II has been distorted into the configuration $\underline{\xi}$ which will be in equilibrium with the defect. The system's energy can then be expanded by a Taylor expansion up to second order in $\underline{\xi}$. Thus

$$E(\underline{\xi}) = U_o + \frac{1}{2}\ \underline{\xi}^T \cdot \underline{\underline{A}} \cdot \underline{\xi} \tag{2.42}$$

where $\underline{\underline{A}}$ is the force constant matrix of the perfect lattice, $\underline{\xi}^T$ is the transpose of $\underline{\xi}$ and U_o is the energy of the perfect, undistorted lattice.

Now, let us introduce an excess-electron defect. The electronic state is described by a trial wave function $\phi(\vec{r}, \underline{\lambda})$, where $\underline{\lambda}$ is the variational parameters of the wave function. Then, the extra terms associated with the excess-electron defect have to be added to the total energy. Thus:

$$E(\underline{\xi}, \underline{\mu}, \underline{\lambda}) = U_o + \frac{1}{2}\ \underline{\xi}^T \cdot \underline{\underline{A}} \cdot \underline{\xi} + E_D(\underline{\xi}, \underline{\mu}, \underline{\lambda}) \tag{2.43}$$

where

$$E_D(\underline{\xi}, \underline{\mu}, \underline{\lambda}) = V_L(\underline{\xi}, \underline{\mu}) + \overline{T}(\underline{\lambda}) + \overline{V}(\underline{\xi}, \underline{\mu}, \underline{\lambda}) \tag{2.44}$$

and

$V_L(\underline{\xi}, \underline{\mu})$ is the energy to create the lattice defect from the perfect lattice in distortion field $\underline{\xi}$;

$\overline{T}(\underline{\lambda})$ is the expectation value of the excess-electron's kinetic energy in state $\phi(\vec{r}, \underline{\lambda})$; and

$V(\underline{\xi},\underline{\mu},\underline{\lambda})$ is the electron-lattice interaction energy.

Firstly, we will minimize equation (2.43) with $\underline{\xi} = o$ to obtain the zeroth order $\underline{\mu}_o$, $\underline{\lambda}_o$

$$\left.\frac{\partial E_D}{\partial \underline{\lambda}}\right|_{\underline{\xi} = 0} = 0 \qquad \rightarrow \underline{\lambda} = \underline{\lambda}_o \tag{2.45a}$$

$$\left.\frac{\partial E_D}{\partial \underline{\mu}}\right|_{\underline{\xi} = 0} = 0 \qquad \rightarrow \underline{\mu} = \underline{\mu}_o \tag{2.45b}$$

The partial derivatives $\frac{\partial}{\partial \underline{\lambda}}$ denotes partial derivatives with respect to each of the components of $\underline{\lambda}$. Then, expanding $E_D(\underline{\xi}, \underline{\mu}, \underline{\lambda})$ to quadratic terms in $\underline{\xi}$, $\Delta \underline{\mu}$ and $\Delta \underline{\lambda}$ by the Taylor expansion, where

$$\Delta \underline{\mu} = \underline{\mu} - \underline{\mu}_o \tag{2.46a}$$

$$\Delta \underline{\lambda} = \underline{\lambda} - \underline{\lambda}_o \tag{2.46b}$$

and

$$\begin{aligned} E_D(\underline{\xi}, \underline{\mu}, \underline{\lambda}) = E_D(0, \underline{\mu}_o, \underline{\lambda}_o) &+ \left.\frac{\partial E_D}{\partial \underline{\xi}}\right|_{\substack{\underline{\mu} = \underline{\mu}_o \\ \underline{\lambda} = \underline{\lambda}_o \\ \underline{\xi} = o}} \cdot \underline{\xi} \\ &+ \left.\frac{\partial E_D}{\partial \underline{\mu}}\right|_{\substack{\underline{\mu} = \underline{\mu}_o \\ \underline{\lambda} = \underline{\lambda}_o \\ \underline{\xi} = o}} \cdot \Delta \underline{\mu} + \left.\frac{\partial E_D}{\partial \underline{\lambda}}\right|_{\substack{\underline{\mu} = \underline{\mu}_o \\ \underline{\lambda} = \underline{\lambda}_o \\ \underline{\xi} = o}} \cdot \Delta \underline{\lambda} \\ &+ \frac{1}{2} \underline{\xi} \cdot \left.\frac{\partial^2 E_D}{\partial \underline{\xi}^2}\right|_{\substack{\underline{\mu} = \underline{\mu}_o \\ \underline{\lambda} = \underline{\lambda}_o \\ \underline{\xi} = o}} \cdot \underline{\xi} + \frac{1}{2} \Delta \underline{\mu} \cdot \left.\frac{\partial^2 E_D}{\partial \underline{\mu}^2}\right|_{\substack{\underline{\mu} = \underline{\mu}_o \\ \underline{\lambda} = \underline{\lambda}_o \\ \underline{\xi} = o}} \cdot \Delta \underline{\mu} \\ &+ \frac{1}{2} \Delta \underline{\lambda} \cdot \left.\frac{\partial^2 E_D}{\partial \underline{\lambda}^2}\right|_{\substack{\underline{\mu} = \underline{\mu}_o \\ \underline{\lambda} = \underline{\lambda}_o \\ \underline{\xi} = o}} \cdot \Delta \underline{\lambda} + \underline{\xi} \cdot \left.\frac{\partial^2 E_D}{\partial \underline{\xi} \cdot \partial \underline{\lambda}}\right|_{\substack{\underline{\mu} = \underline{\mu}_o \\ \underline{\lambda} = \underline{\lambda}_o \\ \underline{\xi} = o}} \cdot \Delta \underline{\lambda} \end{aligned}$$

$$+ \underline{\xi} \cdot \frac{\partial^2 E_D}{\partial \underline{\xi}\, \partial \underline{\mu}} \Bigg|_{\substack{\underline{\mu} = \underline{\mu}_o \\ \underline{\lambda} = \underline{\lambda}_o \\ \underline{\xi} = o}} \cdot \Delta \underline{\mu} + \Delta \underline{\mu} \cdot \frac{\partial^2 E_D}{\partial \underline{\mu}\, \partial \underline{\lambda}} \Bigg|_{\substack{\underline{\mu} = \underline{\mu}_o \\ \underline{\lambda} = \underline{\lambda}_o \\ \underline{\xi} = o}} \cdot \Delta \underline{\lambda} \tag{2.47}$$

We now denote the coefficients in this expansion as follows:

$$\underline{F}_o = \frac{\partial E_D}{\partial \underline{\xi}} \Bigg|_{\substack{\underline{\mu} = \underline{\mu}_o \\ \underline{\lambda} = \underline{\lambda}_o \\ \underline{\xi} = o}} \tag{2.48}$$

$$\underline{\underline{F}}_1 = \frac{\partial^2 E_D}{\partial \underline{\xi}^2} \Bigg|_{\substack{\underline{\mu} = \underline{\mu}_o \\ \underline{\lambda} = \underline{\lambda}_o \\ \underline{\xi} = o}} \tag{2.49}$$

$$\underline{\underline{\Lambda}}_1 = \frac{\partial^2 E_D}{\partial \underline{\lambda}^2} \Bigg|_{\substack{\underline{\mu} = \underline{\mu}_o \\ \underline{\lambda} = \underline{\lambda}_o \\ \underline{\xi} = o}} \tag{2.50}$$

$$\underline{\underline{\Lambda}} = \frac{\partial^2 E_D}{\partial \underline{\xi}\, \partial \underline{\lambda}} \Bigg|_{\substack{\underline{\mu} = \underline{\mu}_o \\ \underline{\lambda} = \underline{\lambda}_o \\ \underline{\xi} = o}} \tag{2.51}$$

$$\underline{\underline{M}} = \frac{\partial^2 E_D}{\partial \underline{\xi}\, \partial \underline{\mu}} \Bigg|_{\substack{\underline{\mu} = \underline{\mu}_o \\ \underline{\lambda} = \underline{\lambda}_o \\ \underline{\xi} = o}} \tag{2.52}$$

$$\underline{\underline{M}}_1 = \frac{\partial^2 E_D}{\partial \underline{\mu}^2}\Bigg|_{\substack{\underline{\mu} = \underline{\mu}_o \\ \underline{\lambda} = \underline{\lambda}_o \\ \underline{\xi} = o}} \tag{2.53}$$

$$\underline{\underline{N}} = \frac{\partial^2 E_D}{\partial \underline{\lambda}\, \partial \underline{\mu}}\Bigg|_{\substack{\underline{\mu} = \underline{\mu}_o \\ \underline{\lambda} = \underline{\lambda}_o \\ \underline{\xi} = o}} \tag{2.54}$$

Substituting equations (2.48) to (2.54) into equation (2.47), we get

$$\begin{aligned} E_D(\underline{\xi}, \underline{\mu}, \underline{\lambda}) = {} & E_D(o, \underline{\mu}_o, \underline{\lambda}_o) + \underline{F}_o \cdot \underline{\xi} + \frac{1}{2}\, \underline{\xi} \cdot \underline{\underline{F}}_1 \cdot \underline{\xi} \\ & + \frac{1}{2}\, \Delta \underline{\mu} \cdot \underline{\underline{M}}_1 \cdot \Delta \underline{\mu} + \frac{1}{2}\, \Delta \underline{\lambda} \cdot \underline{\underline{\Lambda}}_1 \cdot \Delta \underline{\lambda} \\ & + \underline{\xi} \cdot \underline{\underline{\Lambda}} \cdot \Delta \underline{\lambda} + \underline{\xi} \cdot \underline{\underline{M}} \cdot \Delta \underline{\mu} + \Delta \underline{\mu} \cdot \underline{\underline{N}} \cdot \Delta \underline{\lambda} \end{aligned} \tag{2.55}$$

Combining this with equation (2.43), we obtain the total system's energy. We now obtain the first order small quantities by minimizing the system's energy with respect to $\underline{\xi}$, $\Delta \underline{\mu}$, $\Delta \underline{\lambda}$; that is:

$$\frac{\partial E\ (\underline{\xi}, \underline{\mu}, \underline{\lambda})}{\partial \underline{\xi}} = 0; \tag{2.56}$$

$$\frac{\partial E\ (\underline{\xi}, \underline{\mu}, \underline{\lambda})}{\partial (\Delta \underline{\mu})} = 0; \tag{2.57}$$

$$\frac{\partial E\ (\underline{\xi}, \underline{\mu}, \underline{\lambda})}{\partial (\Delta \underline{\lambda})} = 0. \tag{2.58}$$

We get the conditions;

$$\underline{\underline{A}} \cdot \underline{\xi} + \underline{F}_o + \underline{\underline{F}}_1 \cdot \underline{\xi} + \underline{\underline{\Lambda}} \cdot \Delta \underline{\lambda} + \underline{\underline{M}} \cdot \Delta \underline{\mu} = 0 \tag{2.59}$$

$$\underline{\underline{M}}_1 \cdot \Delta \underline{\mu} + \underline{\underline{N}} \cdot \Delta \underline{\lambda} + \underline{\underline{M}} \cdot \underline{\xi} = 0 \tag{2.60}$$

$$\underline{\underline{\Lambda}}_1 \cdot \Delta \underline{\lambda} + \underline{\underline{\Lambda}} \cdot \underline{\xi} + \underline{\underline{N}} \cdot \Delta \underline{\mu} = 0 \tag{2.61}$$

Decoupling equations (2.59) to (2.61), we have

$$\underline{\xi} = - \underline{\underline{A}}^{-1} (\underline{F}_o + \underline{\underline{C}} \cdot \underline{\xi}) \quad , \tag{2.62}$$

$$\Delta \underline{\lambda} = \underline{\underline{\beta}}_1 \cdot \underline{\xi} \quad , \tag{2.63}$$

$$\Delta \underline{\mu} = \underline{\underline{\beta}}_2 \cdot \underline{\xi} \quad , \tag{2.64}$$

where

$$\underline{\underline{\beta}}_1 = (\underline{\underline{N}}^{-1} \cdot \underline{\underline{\Lambda}}_1 - \underline{\underline{M}}_1^{-1} \cdot \underline{\underline{N}}^T)^{-1} \cdot (\underline{\underline{M}}_1^{-1} \cdot \underline{\underline{M}}^T - \underline{\underline{N}}^{-1} \cdot \underline{\underline{\Lambda}}^T) \tag{2.65}$$

$$\underline{\underline{\beta}}_2 = - \underline{\underline{M}}_1^{-1} \cdot (\underline{\underline{M}}^T + \underline{\underline{N}}^T \cdot \underline{\beta}_1) \tag{2.66}$$

$$\underline{\underline{C}} = (\underline{\underline{F}}_1 + \underline{\underline{\Lambda}} \cdot \underline{\beta}_1 + \underline{\underline{M}} \cdot \underline{\beta}_2) \tag{2.67}$$

In general, if $\underline{\xi}$ is known, the non-harmonic displacements $\Delta \underline{\mu}$ can be solved from equation (2.64) and the change $\Delta \underline{\lambda}$ of the trial wave function parameters due to the distortion is given in equation (2.63). The harmonic displacements $\underline{\xi}$ can be solved from equation (2.62), but it is difficult in ionic crystals due to the long-range Coulomb forces that make the direct inversion of $\underline{\underline{A}}$ particularly difficult. The solution of $\underline{\xi}$ will be discussed in the next session.

(B) Solution for $\underline{\xi}$

The equation of equilibrium has been derived (equation (2.62) in section (A). It can be solved by expanding the displacements $\underline{\xi}$ in terms

of normal coordinates; that is, the lattice equilibrium equations are solved in reciprocal space. Then the results are transformed back to configuration space by summing over the allowed wave vectors within the first Brillouin zone. We rewrite equation (2.62) as follows:

$$\underline{\xi} = - \underline{\underline{A}}^{-1} \cdot \underline{F} \tag{2.68}$$

where

$$\underline{F} = \underline{F}_o + \underline{\underline{C}} \cdot \underline{\xi} \tag{2.69}$$

and write equation (2.68) in the component form:

$$\sum_{\alpha,\ell,k'} A_{\alpha\alpha'} \begin{pmatrix} \ell & \ell' \\ k & k' \end{pmatrix} \xi_{\alpha'} \begin{pmatrix} \ell' \\ k' \end{pmatrix} = F_\alpha \begin{pmatrix} \ell \\ k \end{pmatrix} \tag{2.70}$$

where

$\xi_\alpha \begin{pmatrix} \ell \\ k \end{pmatrix}$ is the α Cartesian component of displacement of the k^{th} atom in the ℓ^{th} unit cell. Then, introduce the Fourier transform of $\xi_\alpha \begin{pmatrix} \ell \\ k \end{pmatrix}$

$$\xi_\alpha \begin{pmatrix} \ell \\ k \end{pmatrix} = \frac{1}{N} \sum_{\vec{q}} Q_\alpha \begin{pmatrix} \vec{q} \\ k \end{pmatrix} e^{-i \vec{q} \cdot \vec{x} \begin{pmatrix} \ell \\ k \end{pmatrix}} \tag{2.71}$$

where $\vec{q}$ is the vector in reciprocal space, $\vec{q}$ must be restricted in range by the periodic boundary condition such that all allowed $\vec{q}$ vectors are in the first Brillouin zone. Therefore, the number of allowed value of $\vec{q}$ vectors is equal to the number of unit cells per defect. Substituting equation (2.71) into (2.70), we have

$$\frac{1}{N} \sum_{\alpha'\ell'k'} A_{\alpha\alpha'} \begin{pmatrix} \ell & \ell' \\ k & k' \end{pmatrix} \sum_{\vec{q}'} Q_\alpha \begin{pmatrix} \vec{q}' \\ k' \end{pmatrix} e^{-i \vec{q}' \cdot \vec{x} \begin{pmatrix} \ell' \\ k' \end{pmatrix}} = F_\alpha \begin{pmatrix} \ell \\ k \end{pmatrix} \tag{2.72}$$

Operating on the left of equation (2.72) with $\sum_{\ell} e^{i\vec{q}\cdot\vec{x}\binom{\ell}{k}}$, we obtain:

$$\frac{1}{N}\sum_{\ell\ell'}\sum_{\alpha'k'\vec{q}'} A_{\alpha\alpha'}\begin{pmatrix}\ell & \ell'\\ k & k'\end{pmatrix} Q_{\alpha}\begin{pmatrix}\vec{q}'\\ k'\end{pmatrix} e^{-i\vec{q}'\cdot\left[\vec{x}\binom{\ell'}{k'}-\vec{x}\binom{\ell}{k}\right]} e^{-i(\vec{q}'-\vec{q})\cdot\vec{x}\binom{\ell}{k}}$$

$$= \sum_{\ell} F_{\alpha}\begin{pmatrix}\ell\\ k\end{pmatrix} e^{i\vec{q}\cdot\vec{x}\binom{\ell}{k}} \qquad (2.73)$$

Now $A_{\alpha\alpha'}\begin{pmatrix}\ell & \ell'\\ k & k'\end{pmatrix}$ depends only on $\ell - \ell' = \ell''$, and so does:

$$\vec{x}\binom{\ell}{k} - \vec{x}\binom{\ell'}{k'} = \vec{x}\begin{pmatrix}\ell''\\ k\ k'\end{pmatrix} \qquad (2.74)$$

Thus, equation (2.73) can be written as

$$\frac{1}{N}\sum_{\ell''}\sum_{\alpha'k'\vec{q}'} A_{\alpha\alpha'}\begin{pmatrix}\ell''\\ k\ k'\end{pmatrix} Q_{\alpha}\begin{pmatrix}\vec{q}'\\ k'\end{pmatrix} e^{i\vec{q}'\cdot\vec{x}\begin{pmatrix}\ell''\\ k\ k'\end{pmatrix}}$$

$$\times \sum_{\ell} e^{-i(\vec{q}'-\vec{q})\cdot\vec{x}\binom{\ell}{k}} = \sum_{\ell} F_{\alpha}\binom{\ell}{k} e^{i\vec{q}\cdot\vec{x}\binom{\ell}{k}} \qquad (2.75)$$

The sum

$$\frac{1}{N}\sum_{\ell} e^{-i(\vec{q}-\vec{q}')\cdot\vec{x}\binom{\ell}{k}} = \delta_{\vec{q},\vec{q}'}. \qquad (2.76)$$

This is the orthonormality of basis functions

$$\phi_{\vec{q}}\binom{\ell}{k} = \frac{1}{N^{\frac{1}{2}}} e^{-i\vec{q}\cdot\vec{x}\binom{\ell}{k}} \qquad (2.77)$$

Then equation (2.75) becomes

$$\sum_{\ell''}\sum_{\alpha'k'\vec{q}} A_{\alpha\alpha'}\begin{pmatrix}\ell''\\ k\ k'\end{pmatrix} Q_{\alpha}\begin{pmatrix}\vec{q}\\ k'\end{pmatrix} e^{i\vec{q}\cdot\vec{x}\begin{pmatrix}\ell''\\ k\ k'\end{pmatrix}}$$

$$= \sum_{\ell} F_{\alpha} \begin{Bmatrix} \ell \\ k \end{Bmatrix} e^{i \vec{q} \cdot \vec{x} \begin{Bmatrix} \ell \\ k \end{Bmatrix}} \qquad (2.78)$$

We now define

$$D_{\alpha\alpha'} \begin{Bmatrix} \vec{q} \\ k\ k' \end{Bmatrix} = \sum_{\ell''} A_{\alpha\alpha'} \begin{Bmatrix} \ell'' \\ k\ k' \end{Bmatrix} e^{i \vec{q} \cdot \vec{x} \begin{Bmatrix} \ell'' \\ k\ k' \end{Bmatrix}} \qquad (2.79)$$

and

$$G_{\alpha} \begin{Bmatrix} \vec{q} \\ k \end{Bmatrix} = \sum_{\ell} F_{\alpha} \begin{Bmatrix} \ell \\ k \end{Bmatrix} e^{i \vec{q} \cdot \vec{x} \begin{Bmatrix} \ell \\ k \end{Bmatrix}} \qquad (2.80)$$

where $D_{\alpha\alpha'} \begin{Bmatrix} \vec{q} \\ k\ k' \end{Bmatrix}$ is known as the dynamic matrix and has been calculated by Kellermann[22] for the point ion rocksalt lattice. $G_{\alpha} \begin{Bmatrix} \vec{q} \\ k \end{Bmatrix}$ is the Fourier transform of $F_{\alpha} \begin{Bmatrix} \ell \\ k \end{Bmatrix}$. Thus equation (2.78) has the matrix form:

$$\underline{\underline{D}}\,(\vec{q}) \cdot \underline{Q}(\vec{q}) = \underline{G}\,(\vec{q}) \quad . \qquad (2.81)$$

Now, we can solve $\underline{Q}\,(\vec{q})$ for a given $\vec{q}$ from equation (2.81) by using equation (2.79) and equation (2.80). The displacements of the atoms in configuration space are then given by equation (2.71).

In practice, the solution of equation (2.68) is done by the perturbative-iteration procedure, which is to start with $\underline{F} = \underline{F}_o$ in equation (2.69), as follows:

$$\underline{\xi}^{(o)} = - \underline{\underline{A}}^{-1} \cdot \underline{F}_o \qquad (2.82)$$

$$\underline{\xi}^{(1)} = - \underline{\underline{A}}^{-1} \cdot (\underline{F}_o + \underline{\underline{C}} \cdot \underline{\xi}^{(0)}] \qquad \text{etc.} \qquad (2.83)$$

This can be continued to self-consistency.

In the actual numerical calculation, one makes use of the symmetry

properties of the defect crystal lattice to simplify the calculation. Instead of doing the summation $\sum_{\ell}$ in equation (2.80), one calculates $\sum_{m}$, where m is a group of ions all of which have the same value of a given $F_\alpha(\begin{smallmatrix}\ell\\k\end{smallmatrix})$. The range of m will be small if the defect is well localized.

(B) Energy Formulae

(i) The Relaxed State

The relaxed state energy $E(\underline{\xi}, \underline{\mu}, \underline{\lambda})$ of equation (2.43) can be simplified by using the minimizing condition equations (2.59) to (2.61). From equation (2.59)

$$\underline{\underline{A}} \cdot \underline{\xi} = - \underline{F}_o - \underline{F}_1 \cdot \underline{\xi} - \underline{\underline{\Lambda}} \cdot \Delta \underline{\lambda} - \underline{\underline{M}} \cdot \Delta \underline{\mu} \tag{2.84}$$

From equation (2.60)

$$\underline{\underline{M}}_1 \cdot \Delta \underline{\mu} = - \underline{\underline{N}} \cdot \Delta \underline{\lambda} - \underline{\underline{M}} \cdot \underline{\xi} \tag{2.85}$$

From equation (2.61)

$$\underline{\underline{\Lambda}}_1 \cdot \Delta \underline{\lambda} = - \underline{\underline{\Lambda}} \cdot \underline{\xi} - \underline{\underline{N}} \cdot \Delta \underline{\mu} \tag{2.86}$$

Substituting equations (2.84) to (2.86) into equation (2.43) using equation (2.55), we get simply:

$$E(\underline{\xi}, \underline{\mu}, \underline{\lambda}) = U_o + E_D(0, \underline{\mu}_o, \underline{\lambda}_o) + \frac{1}{2} \underline{F}_o^{\mathrm{T}} \cdot \underline{\xi} \tag{2.87}$$

If we set the energy of the perfect undistorted lattice $U_o = 0$, then equation (2.87) becomes

$$E(\underline{\xi}, \underline{\mu}, \underline{\lambda}) = E_D(0, \underline{\mu}_o, \underline{\lambda}_o) + \frac{1}{2} \underline{F}_o^{\mathrm{T}} \cdot \underline{\xi} \tag{2.88}$$

which is the energy of the relaxed state.

(ii) Absorption Energy

The Franck-Condon principle is used in calculating the absorption energy. Accordingly , the absorption energy $E_{abs}(\underline{\mu}_g, \underline{\xi}_g, \underline{\lambda}_g, \underline{\lambda}_{ex}')$ is

$$E_{abs}(\underline{\mu}_g, \underline{\xi}_g, \underline{\lambda}_g, \underline{\lambda}_{ex}') = E_{ex}'(\underline{\mu}_g, \underline{\xi}_g, \underline{\lambda}_{ex}') - E_g(\underline{\mu}_g, \underline{\xi}_g, \underline{\lambda}_g) \qquad (2.89)$$

where the subscript g denotes the ground state and the subscript ex denotes the first excited state. $E_g(\underline{\mu}_g, \underline{\xi}_g, \underline{\lambda}_g)$ is the relaxed ground state energy and $E_{ex}'(\underline{\mu}_g, \underline{\xi}_g, \underline{\lambda}_{ex}')$ is the unrelaxed first excited state energy with the position of the ions $(\underline{\mu}_g, \underline{\xi}_g)$ determined by the ground state wave function and $\underline{\lambda}_{ex}'$ is the wave function parameters of the excited state, made self-consistent with $(\underline{\mu}_g, \underline{\xi}_g)$.

The unrelaxed excited state energy in the presence of the ground state distortions can be written, similar to equation (2.43), as

$$E_{ex}'(\underline{\xi}_g, \underline{\mu}_g, \underline{\lambda}_{ex}') = \frac{1}{2}\underline{\xi}_g^T \cdot \underline{\underline{A}} \cdot \underline{\xi}_g + E_D(\underline{\xi}_g, \underline{\mu}_g, \underline{\lambda}_{ex}') \qquad (2.90)$$

with $U_o = 0$. From equation (2.62), $\underline{\underline{A}} \cdot \underline{\xi}_g$ is given as

$$\underline{\underline{A}} \cdot \underline{\xi}_g = -(\underline{Fo}_g + \underline{\underline{C}}_g \cdot \underline{\xi}_g) \qquad (2.91)$$

where $\underline{Fo}_g$ and $\underline{\underline{C}}_g$ are the matrices which have been defined in equation (2.48) and (2.67), determined by the ground state wave function. Now, operating with $(\underline{\xi}_g^T \cdot)$ from the left on equation (2.91)

$$\underline{\xi}_g^T \cdot \underline{\underline{A}} \cdot \underline{\xi}_g = -\underline{Fo}_g^T \cdot \underline{\xi}_g - \underline{\xi}_g^T \cdot \underline{\underline{C}}_g \cdot \underline{\xi}_g \qquad (2.92)$$

By using equation (2.92), equation (2.90) becomes

$$E_{ex}'(\underline{\xi}_g, \underline{\mu}_g, \underline{\lambda}_{ex}') = -\frac{1}{2}\underline{Fo}_g^T \cdot \underline{\xi}_g - \frac{1}{2}\underline{\xi}_g^T \cdot \underline{\underline{C}}_g \cdot \underline{\xi}_g + E_D(\underline{\xi}_g, \underline{\mu}_g, \underline{\lambda}_{ex}') \qquad (2.93)$$

Which is the energy of the unrelaxed first excited state including the ground state distortion. Substituting equation (2.93) and (2.88) into equation (2.89), we get the formula for absorption energy.

$$E_{abs}(\underline{\xi}_g, \underline{\mu}_g, \underline{\lambda}_g, \underline{\lambda}_{ex}') = - \underline{Fo}_g{}^T \cdot \underline{\xi}_g - \frac{1}{2} \underline{\xi}_g{}^T \cdot \underline{\underline{C}}_g \cdot \underline{\xi}_g$$

$$+ E_D(\underline{\xi}_g, \underline{\mu}_g, \underline{\lambda}_{ex}') - E_D(0, \underline{\mu o}_g, \underline{\lambda o}_g) \qquad (2.94)$$

(iii) Emission Energy

According to the Franck-Condon principle , the emission energy is obtained from E_{abs}, equation (2.89) by changing the sign and interchanging the subscripts g and ex. Thus

$$E_{em}(\underline{\mu}_{ex}, \underline{\xi}_{ex}, \underline{\lambda}_{ex}, \underline{\lambda}_g')$$

$$= E_{ex}(\underline{\mu}_{ex}, \underline{\xi}_{ex}, \underline{\lambda}_{ex}) - E_g'(\underline{\mu}_{ex}, \underline{\xi}_{ex}, \underline{\lambda}_g') \qquad (2.95)$$

where $E_{ex}(\underline{\mu}_{ex}, \underline{\xi}_{ex}, \underline{\lambda}_{ex})$ is the relaxed excited state (RES) energy and $E_g'(\underline{\mu}_{ex}, \underline{\xi}_{ex}, \underline{\lambda}_g')$ is the unrelaxed ground state energy, for which the position of the ions are those of the RES. $\underline{\lambda}_g'$ is the wave function parameters corresponding to this unrelaxed ground state. Thus, we obtain the analogue of equation (2.94)

$$E_{em}(\underline{\mu}_{ex}, \underline{\xi}_{ex}, \underline{\lambda}_{ex}, \underline{\lambda}_g')$$

$$= \underline{Fo}_{ex}{}^T \cdot \underline{\xi}_{ex} + \frac{1}{2} \underline{\xi}_{ex}{}^T \cdot \underline{\underline{C}}_{ex} \cdot \underline{\xi}_{ex}$$

$$- E_D(\underline{\xi}_{ex}, \underline{\mu}_{ex}, \underline{\lambda}_g') + E_D(0, \underline{\mu o}_{ex}, \underline{\lambda o}_{ex}) \qquad (2.96)$$

where $\underline{Fo}_{ex}$ and $\underline{\underline{C}}_{ex}$ are the matrices which have been defined in equation (2.48) and (2.67) determined by the RES.

CHAPTER 3

CALCULATIONS, RESULTS AND DISCUSSION

In the present calculation, the lattice ions have been divided into two regions. Region I includes the defect and perhaps some of its surrounding ions. Region II includes the rest of the ions. The idea is that the displacements of the ions in Region I is so large that the harmonic approximation is not valid. Special care must be taken for those ions in Region I denoted by $\underline{\mu}$ in chapter 2. For those in Region II, the displacements from perfect lattice sites are small and within the range of validity of the harmonic approximation, and these displacements have been denoted $\underline{\xi}$ in chapter 2.

The calculation can be divided into two major steps namely, the zeroth order calculation and the higher order calculation. In the zeroth order calculation, we minimize the system 's energy with respect to the non-harmonic displacements $\underline{\mu}$ and wave function parameter $\underline{\lambda}$, while $\underline{\xi}$ is kept equal to zero.

$$\left.\frac{\partial E(\underline{\xi}, \underline{\mu}, \underline{\lambda})}{\partial \underline{\mu}}\right|_{\underline{\lambda} = \underline{\lambda}o} = 0 \rightarrow \underline{\mu} = \underline{\mu}o \qquad (3.1)$$

$$\left.\frac{\partial E(\underline{\xi}, \underline{\mu}, \underline{\lambda})}{\partial \underline{\lambda}}\right|_{\underline{\mu} = \underline{\mu}o} = 0 \quad \rightarrow \quad \underline{\lambda} = \underline{\lambda}o \tag{3.2}$$

Thus, we obtain a zeroth order solution, $\underline{\mu}o$ and $\underline{\lambda}o$, neglecting harmonic distortion, $\underline{\xi}$. Substituting equation (2.44) into (2.43) and putting $\underline{\mu} = \underline{\mu}o$, $\underline{\lambda} = \underline{\lambda}o$, $\underline{\xi} = 0$ and $U_o = 0$, we have the zeroth order solution for the defect system's energy:

$$E(0, \underline{\mu}o, \underline{\lambda}o) = V_L(0, \underline{\mu}o) + \langle \tilde{\phi} \,|T + V_{pI} + V_{Is}|\, \tilde{\phi} \rangle \tag{3.3}$$

where:

$\tilde{\phi}$ is the excess-electron's trial psuedo-wave function with trial parameters $\underline{\lambda} = \underline{\lambda}o$;

T is the excess-electron's kinetic energy; V_{pI} is the Coulomb interaction between the point-ion lattice and the excess-electron;

V_{Is} is the BSG ion-size correction; and $V_L(0, \underline{\mu}o)$ is the energy to create the lattice defect, including non-harmonic distortion.

In the higher order calculation, the following terms are calculated:

(1) $\Delta \underline{\mu} = (\underline{\mu} - \underline{\mu}o)$, the change of the non-harmonic displacements induced by harmonic lattice distortion, $\underline{\xi}$ (see equation (2.64)).

(2) $\Delta \underline{\lambda} = (\underline{\lambda} - \underline{\lambda}o)$, the change of the wave function parameter due to harmonic lattice distortion (see equation (2.63)). Thus, the corrected values of $\underline{\lambda}$ and $\underline{\mu}$ are obtained, namely $\underline{\lambda} = \underline{\lambda}o + \Delta \underline{\lambda}$ and $\underline{\mu} = \underline{\mu}o + \Delta \underline{\mu}$

(3) $\underline{\xi}$, the harmonic lattice distortion field of the ions in Region II, due to the electronic point defect (see section (2.4B)).

(4) $\frac{1}{2} \underline{F}o \cdot \underline{\xi}$, the change in total energy induced by harmonic relaxation of the lattice up to second order, while $\underline{F}o$ is defined in equation (2.48).

3.1. Vacancy Configuration

(A) Zeroth Order Calculation

In the vacancy configuration, the vacancy site and substitutional impurity cation constitute Region I (see Figure 2(a)). Although it is known experimentally that the Li^+ ion occupies an off-center site in $F_A(Li)$[23], there are four equivalent sites that Li^+ can occupy, so that the defect shows C_{4v} symmetry as a statistical average. It is not possible to include these off-center properties in our static model, so we consider only C_{4v} symmetry vacancy configurations, with the impurity alkali ion (Li^+ or Na^+) lying on the y-axis.

The trial pseudo-wave functions which we choose for the present calculation are Gaussian localized with low orders of Legendre polynomials. Even parity is assumed for the ground state and odd parity for the first excited state. The following trial wave functions are used in the vacancy configuration:

for vacancy ground state:

$$\phi_1 = A_1 \exp(-\alpha_1^2 r^2) \tag{3.4}$$

for F_{A1} absorption:

$$\begin{aligned}\phi_2 &= A_2\, r\, (\cos\theta_y) \exp(-\alpha_2^2 r^2) \\ &= A_2\, y \exp(-\alpha_2^2 r^2)\end{aligned} \tag{3.5}$$

for F_{A2} absorption:

$$\begin{aligned}\phi_3 &= A_3\, r\, (\cos\theta_z) \exp(-\alpha_3^2 r^2) \\ &= A_3\, z \exp(-\alpha_3^2 r^2)\end{aligned} \tag{3.6}$$

and for vacancy relaxed excited state:

$$\phi_4 = A_4 \; r(\cos\theta_y) \exp(-\alpha_4^2 r^2)$$

$$= A_4 \; y \exp(-\alpha_4^2 r^2) \qquad (3.7)$$

where $A_j (j = 1, 2, 3, 4)$ is the normalized constant, α_j $(j = 1, 2, 3, 4)$ is the wave function localization parameter, r is the radial variable with origin at the vacancy site, θy is the polar angle with the y-axis as polar axis in spherical coordinates and θ_z is the polar angle with z-axis as polar axis in spherical coordinates. The reason we used this type of pseudo-wave function is that all the matrix elements involved can be evaluated explicitly or in terms of an error function, which is a built in subroutine in the IBM 360/65 computer. Furthermore, Brown and Vail[24] have shown that the Gaussian localized wave function is qualitatively very similar to the type II and type III Gourary-Adrian wave function[7].

First we do the zeroth order calculation, so we minimized the system's energy with $\underline{\xi} = 0$, with respect to $\underline{\mu}$ and $\underline{\lambda}$, where

$$E(o, \underline{\mu}, \underline{\lambda}) = V_L(o, \underline{\mu}) + \langle \phi_1 \mid V_{pI} + V_{Is} + T \mid \phi_1 \rangle \qquad (3.8)$$

In the case of the ground state in the vacancy configuration, $\underline{\lambda} = \alpha_1$, the trial wave function's localization parameter and $\underline{\mu}$ is the non-harmonic displacement of the impurity ion along the y-axis from the perfect lattice site (010) and is denoted y_o. Here, we notice that the pseudo-wave function ϕ_1 is centered at the origin of figure (2a) but that the lattice configuration is asymmetrical due to the impurity ions. Thus, the center of the wave function should be allowed to move out from the origin. However, we fixed the center of wave function because it makes the calculation much easier to handle.

$V_L(o, \underline{\mu})$, which is the energy required to create the vacancy with an adjacent impurity cation, includes a non-harmonic distortion $\underline{\mu} = y_o$. We formulate the procedure for calculating $V_L(o, \underline{\mu})$ as follows:

(1) create the ordinary vacancy defect;

(2) remove the positive ion from (010);

(3) put in the impurity ion (Na^+ or Li^+)

at lattice site which has been displaced y_o along the y-axis from the (010) site.

We used Tosi's single exponential parameters (ref. 12 Table VII 2nd column) for the Born-Mayer repulsion.

$$W^{(R)} = B \exp\left(-\frac{r}{\rho}\right) \tag{3.9}$$

in evaluating $V_L(o, \underline{\mu})$. The perfect lattice KCℓ parameters were used in the $K^+ - Cl^-$ interaction, and perfect lattice NaCl or LiCl parameters were used for the interaction of the impurity Na^+ or Li^+ ion with Cl^- ions. As we know, the interionic spacing in KCl is quite different from that in LiCl, and the second nearest neighbor of the Li^+ ion in $F_A(Li)$ in KCl and in LiCl are also different. It is a fundamental question whether the above approximation is valid. Tosi and Doyama[25] have shown that it yields reasonable result for the activation energy for diffusion of Rb^+ in NaCl and in KCl. The Coulomb contribution to $V_L(o, \underline{\mu})$ is calculated by Evjen's[12] method with Evjen cubes of sides up to 6a, where a is the interionic spacing of the crystal.

The Coulomb potential energy of the excess-electron in the presence of the defect lattice of charged point ions, $V_{pI}(\vec{r})$, is given by

$$V_{pI}(\vec{r}) = -2 \sum_i \frac{Q_i}{|\vec{r} - \vec{r}_i|} \tag{3.10}$$

where the factor 2 is introduced because the energy is expressed in Rydbergs, if $\vec{r}$ and $\vec{r}_i$ are measured in units of the first Bohr orbit a_o, where

$$a_o = \frac{\hbar^2}{m_e e^2}$$

and m_e is the mass of the electron, and if Q_i is measured in units of the proton's charge e. The expression

$$\frac{1}{|\vec{r} - \vec{r}_i|}$$

can be expanded in terms of Legendre polynomials as:

$$\frac{1}{|\vec{r} - \vec{r}_i|} = \sum_{\ell=0}^{\infty} \frac{r_<^{\ell}}{r_>^{\ell+1}} P_\ell (\cos \gamma_i) \qquad (3.11)$$

where $r_<$ ($r_>$) is the smaller (larger) of $|\vec{r}|$ and $|\vec{r}_i|$ and γ_i is the angle between $\vec{r}$ and $\vec{r}_i$ (ref (26),p.62, Fig. 3.3). We use the addition theorem for spherical harmonics, written in the following form (ref 26, p. 69 equation (3.68)):

$$P_\ell(\cos\gamma_i) = P_\ell(\cos\theta)\, P_\ell(\cos\theta_i) + 2 \sum_{m=1}^{\ell} \frac{(\ell-m)!}{(\ell+m)!} P_\ell^m (\cos\theta)\, P_\ell^m(\cos\theta_i) \cos[m(\phi - \phi_i)] \qquad (3.12)$$

where (θ,ϕ) and (θ_i, ϕ_i) are the angular variables of $\vec{r}$ and $\vec{r}_i$ respectively in spherical polar coordinates. From equation (3.11), equation (3.10) becomes

$$V_{pI}(\vec{r}) = -2 \sum_i \sum_{\ell=0}^{\infty} Q_i \frac{r_<^{\ell}}{r_>^{\ell+1}} P_\ell(\cos\gamma_i)$$

$$= -2\left[\sum_{\substack{i \\ r_i > r \\ r_i \neq 0}} \sum_{\ell=0}^{\infty} Q_i \frac{r^{\ell}}{r_i^{\ell+1}} P_\ell(\cos\gamma_i) \right.$$

$$\left. + \sum_{\substack{i \\ r_i < r \\ r_i \neq 0}} \sum_{\ell=0}^{\infty} Q_i \frac{r_i^{\ell}}{r^{\ell+1}} P_\ell(\cos\gamma_i) + \frac{Q_o}{r} \right] \qquad (3.13)$$

where Q_o is the charge on the ion at $\vec{r}_i = 0$.

The above expression, expanding the potential energy in terms of a linear combination of spherical harmonics has been used by Gourary and Adrian[7] and by others[8],[27] in F-center calculation to evaluate $\langle \Phi \mid V_{pI} \mid \Phi \rangle$. Further simplification can be made by adding to and subtracting from equation (3.13) the term

$$2 \sum_{\substack{i \\ r_i < r \\ r_i \neq 0}} \sum_{\ell=0}^{\infty} Q_i \left(\frac{r^{\ell}}{r_i^{\ell+1}} \right) P_\ell(\cos\gamma_i)$$

Then, equation (3.13) becomes:

$$V_{pI}(\vec{r}) = -2 \sum_{\substack{i \\ r_i \neq 0}} \sum_{\ell=0}^{\infty} Q_i \left\{ \frac{r^{\ell}}{r_i^{\ell+1}} \right\} P_\ell(\cos\gamma_i)$$

$$+ 2 \sum_{\substack{i \\ r_i<r \\ r_i\neq o}} \sum_{\ell=o}^{\infty} Q_i \left[\frac{r^\ell}{r_i^{\ell+1}} - \frac{r_i^\ell}{r^{\ell+1}} \right] P_\ell(\cos\gamma_i) - 2\frac{Q_o}{r} \tag{3.14}$$

Making use of equation (3.12), equation (3.14) becomes

$$V_{pI}(r) = - 2 \sum_{\substack{i \\ r_i\neq o}} \sum_{\ell=o}^{\infty} Q_i \left(\frac{r^\ell}{r_i^{\ell+1}} \right) \{P_\ell(\cos\theta)\, P_\ell(\cos\theta_i)$$

$$+ \sum_{m=1}^{\ell} 2\frac{(\ell-m)!}{(\ell+m)!}\, P_\ell^m(\cos\theta)\, P_\ell^m(\cos\theta_i)\, \cos[m(\phi - \phi_i)]\}$$

$$+ 2 \sum_{\substack{i \\ r_i<r \\ r_i\neq 0}} \sum_{\ell=o}^{\infty} Q_i \left[\frac{r^\ell}{r_i^{\ell+1}} - \frac{r_i^\ell}{r^{\ell+1}} \right] \{P_\ell(\cos\theta)\, P_\ell(\cos\theta_i)$$

$$+ \sum_{m=1}^{\ell} 2\, \frac{(\ell-m)!}{(\ell+m)!}\, P_\ell^m(\cos\theta)\, P_\ell^m(\cos\theta_i)\, \cos[m(\phi - \phi_i)]\}$$

$$- 2\frac{Q_o}{r} \tag{3.15}$$

In the case of the F_A-center ground state, the wave function $\phi_1 = A_1 \exp(-\alpha_1^2 r^2)$ can be written as

$$\phi_1 = A_1 \exp(-\alpha_1^2 r^2)\, P_o(\cos\theta) \tag{3.16}$$

i.e. the spherically symmetric wave function contains a zeroth order Legendre polynomial, and is azimuthally symmetric. Thus only terms with

$\ell = o$ and $m = o$ in equation (3.15) make a non-zero contribution to $< \phi_1 \mid V_{pI} \mid \phi_1 >$. Furthermore, there is no ion at $\vec{r}_{\hat{i}} = 0$, and therefore $Q_o = 0$. Then, from equation (3.16),

$$< \phi_1 \mid V_{pI} \mid \phi_1 > = - 2 \sum_{\substack{\hat{i} \\ r_{\hat{i}} \neq o}} \left\{ \frac{Q_{\hat{i}}}{r_{\hat{i}}} \right\} + 2 \sum_{\substack{\hat{i} \\ r_{\hat{i}} \neq o}} \int_{r_{\hat{i}}}^{\infty} |\phi_1|^2 \, Q_{\hat{i}} \left\{ \frac{1}{r_{\hat{i}}} - \frac{1}{r} \right\} d\tau \qquad (3.17)$$

In the case of the F_A-center relaxed excited state, the wave function $\phi_4 = A_4 \, r \cos\theta_y \exp(-\alpha_4^2 \, r^2)$ correspond to $\ell = 1$ and is azimuthally symmetric. Thus only $\ell = 2$, $\ell = o$ and $m = o$ in equation (3.15) have non-zero contributions to $< \phi_4 \mid V_{pI} \mid \phi_4 >$. There is still no ion at $\vec{r}_{\hat{i}} = o$. Thus, the expectation value of V_{pI} in trial state ϕ_4 becomes:

$$< \phi_4 \mid V_{pI}(\vec{r}) \mid \phi_4 > = - 2 \sum_{\substack{i \\ r_i \neq o}} Q_i \, P_2(\cos\theta_i) \int_o^{\infty} |\phi_4|^2 \left\{ \frac{r^2}{r_{\hat{i}}^3} \right\} P_2(\cos\theta) \, d\tau$$

$$+ 2 \sum_{\substack{i \\ r_i \neq o}} Q_i \, P_2(\cos\theta_i) \int_{r_i}^{\infty} |\phi_4|^2 \left[\frac{r^2}{r_i^3} - \frac{r_i^2}{r^3} \right] P_2(\cos\theta) \, d\tau$$

$$+ 2 \sum_{\substack{i \\ r_i \neq o}} Q_i \int_{r_i}^{\infty} |\phi_4|^2 \left[\frac{1}{r_i} - \frac{1}{r} \right] d\tau - 2 \sum_{\substack{i \\ r_i \neq 0}} \frac{Q_i}{r_i} \qquad (3.18)$$

For the BSG ion-size correction we had, in equation (2.39):

$$V_{Is} = \sum_{\gamma} \left[A_\gamma + B_\gamma \, (\bar{V} - U_\gamma) \right] \delta \, (\vec{r} - \vec{r}_\gamma) \qquad (3.19)$$

where

$$\bar{V} = \langle \tilde{\phi}_1 \mid V_{pI} + V_{Is} \mid \tilde{\phi}_1 \rangle \qquad (3.20)$$

for the ground state. The procedure for the zeroth order calculation is:

(1) make an initial guess for the value of $\bar{V}$;

(2) making use of this value in equation (3.19) and using (3.17), minimize $E(o, \underline{\mu}, \underline{\lambda})$ of equation (3.8) with respect to y_o and α_1 and get $y_o = y_o^{(1)}$, $\alpha_1 = \alpha_1^{(1)}$;

(3) using $y_o = y_o^{(1)}$ and $\alpha_1 = \alpha_1^{(1)}$, calculate $\bar{V}$ by equation (3.20);

(4) repeat the cycle to a self-consistency of 0.001 rydbergs, that is until two consecutive estimates of $\bar{V}$ differ by less than 0.001 rydbergs.

The minimization program was obtained from the library of subroutines at AERE, Harwell[28]. The summation in equation (3.18) is over the ions up to the sixth nearest neighbours to the vacancy, or 85 ions in 29 groups, such that the convergence is obtained to within 0.001 Ryb. The results of the zeroth order calculation of the F_A-center relaxed ground state and relaxed excited state in the vacancy configuration are reported in Table (1) and Table (2) respectively.

(B) Second Order Calculation (relaxed state)

The next step is to do the second order calculation. Our aim is to solve equation (2.81) for $\underline{Q}(\vec{q})$. $\underline{D}(\vec{q})$ is Kellermann's dynamic matrix, which has been corrected by Dayal and Tripathi[29] for 1000 $\vec{q}$ vectors in the first Brillouin zone. A brief review of Kellermann's dynamic matrix is given in appendix A. As described in section 2.3(B), we evaluate $\underline{G}(\vec{q})$ by summing over groups of ions in equivalent positions relative to

Table 1

Zeroth order calculation of F_A-center relaxed ground state in the vacancy configuration: a is the interionic spacing of the crystal

		F_A(Na)	F_A(Li)
$V_L(0,y_o)$	(eV)	6.64	6.39
$\overline{V}_{pI}$	(eV)	-7.11	-6.95
$\overline{V}_{Is}$	(eV)	0.08	0.08
$\overline{T}$	(eV)	1.44	1.43
y_o	(a)	0.077	0.115
α_o	(1/a)	1.12	1.114
$E_g(0,y_o,\alpha_o)$	(eV)	1.05	0.95

Table 2

Zeroth order calculation of F_A-center relaxed excited state (RES) in the vacancy configuration: a is the interionic spacing of the crystal

		F_A(Na)	F_A(Li)
$V_L(0,y_o)$	(eV)	6.62	6.41
$\overline{V}_{pI}$	(eV)	-6.28	-6.11
$\overline{V}_{Is}$	(eV)	0.31	0.30
$\overline{T}$	(eV)	2.68	2.64
y_o	(a)	0.071	0.103
α_o	(1/a)	1.18	1.17
$E_{ex}(0,y_o,\alpha_o)$	(eV)	3.33	3.24

the defect, the groups being denoted by an index m, instead of summing over the individual ions. In the case of the F_A-center relaxed ground state and relaxed excited state in the vacancy configuration, we included the contribution from fifteen groups, which contain a total of 49 ions. The groupings of ions and the matrix elements of $\underline{G}(\vec{q})$ are given explicitly in Appendix B.

Therefore, the Fourier transform of $\underline{Q}(\vec{q})$ into configuration space $\underline{\xi}$, the corrected value of $\underline{\lambda}$ and $\underline{\mu}$, and the distortion energy $\frac{1}{2}\ \underline{Fo} \cdot \underline{\xi}$, are calculated and are reported in Tables (3) and (4) for the relaxed ground state and the relaxed excited state respectively in the vacancy configuration. We notice that the wave function parameter α has changed from $\alpha_o = 1.114$ (Table 1) to $\alpha_g = 1.07$ (Table 3) in the case of $F_A(Li)$, as the lattice has relaxed. It is a merit of our model and methods that the wave functions are self-consistent with lattice distortion. The relaxation energy is small in the case of the ground state but is still not negligible. The contribution from the relaxation energy is larger in the case of relaxed excited state, as expected.

In Tables (5) and (6), displacement components of some near neighbours to the vacancy for the relaxed excited and relaxed ground states respectively are given. Although no experimental work on the displacements of the near neighbours of the F_A-center have been reported, Lüty et al[30] have determined the volume expansion per F-center, which corresponds to an outward displacement of the nearest neighbours by 2-3%. The displacement of the five nearest K^+ ion to the F_A-center agrees with this result. Since the excess-electron stabilizes at the lowest energy, it apparently prefers to enlarge the vacancy instead of increase its kinetic energy. Furthermore, we found that the outward relaxation of impurity Li^+ (or

Table 3

Second order calculation of F_A-center relaxed ground state in the vacancy configuration. The total relaxed state energy $E_g(\underline{\xi}_g, y_g, \alpha_g)$ is given in equation (2.88) a is the interionic spacing of the crystal

		F_A(Na)	F_A(Li)
α_g	(1/a)	1.08	1.09
y_g	(a)	0.072	0.119
$\frac{1}{2}\,\underline{Fo}_g^{\tau} \cdot \underline{\xi}_g$	(eV)	-0.04	-0.085
$\frac{1}{2}\,\underline{\xi}_g^{\tau} \cdot \underline{\underline{C}}_g \cdot \underline{\xi}_g$	(eV)	-0.01	-0.01
$E_g(0, y_o, \alpha_o)$	(eV)	1.05	0.95
$E_g(\underline{\xi}_g, y_g, \alpha_g)$	(eV)	1.01	0.87

Table 4

Second order calculation of F_A-center relaxed excited state in the vacancy configuration. The total relaxed state energy $E_{ex}(\underline{\xi}_{ex}, y_{ex}, \alpha_{ex})$ is given in equation (2.88). a is the interionic spacing of the crystal.

		F_A(Na)	F_A(Li)
α_{ex}	(1/a)	0.96	0.93
y_{ex}	(a)	0.115	0.116
$\frac{1}{2}\,\underline{Fo}_{ex}^{T} \cdot \underline{\xi}_{ex}$	(eV)	-0.49	-0.55
$\frac{1}{2}\,\underline{\xi}_{ex}^{T} \cdot \underline{\underline{C}}_{ex} \cdot \underline{\xi}_{ex}$	(eV)	-0.15	-0.12
$E_{ex}(0, y_o, \alpha_o)$	(eV)	3.33	3.24
$E_{ex}(\underline{\xi}_{ex}, y_{ex}, \alpha_{ex})$	(eV)	2.84	2.69

Table 5

Cartesian components of displacements of the ions neighboring the F_A(Na)-center in KCl in even and odd(ground and excited)parity relaxed states in the vacancy configuration, in units of the perfect KCl nearest neighbor distance.

	F_A(Na)-Center	
ion	even parity	odd parity
(0,1,0)	0,0.072,0	0,0.115,0
(1,0,0)	0.022,0.004,0	0.1,0,0
(0,-1,0)	0.0,-0.025,0	0,-0.073,0
(1,1,0)	0.004,0.01,0	0.035,-0.025,0
(1,-1,0)	-0.001,0.001,0	0.027,-0.017,0
(1,0,1)	-0.003,0.003,-0.003	-0.023,-0.012,-0.023
(1,1,1)	0,0.005,0	-0.006,0.002,-0.006
(1,-1,1)	0,0.001,0	-0.002,-0.025,-0.002
(0,2,0)	0,-0.008,0	0,-0.033,0
(2,0,0)	0,0.002,0	0.017,-0.011,0
(0,-2,0)	0,-0.003,0	0,-0.02,0
(1,2,0)	0.01,0.009,0	0.055,-0.006,0
(2,1,0)	0.008,0.006,0	0.025,0.009,0
(1,-2,0)	0.004,-0.006,0	0.011,-0.027,0
(2,-1,0)	0.005,-0.004,0	0.028,-0.026,0
(1,0,2)	0,0.001,-0.001	-0.001,-0.005,-0.006
(2,1,1)	0.002,0.002,0.001	0.004,-0.003,0.002
(2,-1,1)	0.001,0,0	0.005,-0.009,0.002
(1,2,1)	0.004,0.008,0.004	0.001,0.001,0.001
(1,-2,1)	0.001,-0.003,0.001	0.001,-0.020,0.001
(2,2,0)	0.006,0.005,0	0.007.0.003,0
(2,-2,0)	0.002,-0.002,0	0.01,-0.016,0
(2,0,2)	-0.001,0,0	-0.004,-0.003,-0.004
(2,2,1)	0.002,0.002,0.001	0,-0.001,0.001
(2,-2,1)	0.001,-0.001,0.001	0.003,-0.008,0.002
(2,1,2)	0,0.001,0	-0.001,-0.001,-0.001
(2,-1,2)	0,0,0	0.001,-0.004,0.001
(0,3,0)	0,-0.004,0	0,-0.015,0
(0,-3,0)	0,-0.002,0	0,-0.015,0
(0,0,3)	0,0,0	0,-0.003,0.006

Table 6

Cartesian components of displacements of the ions neighboring the F_A(Li)-center in KCl in even and odd parity relaxed states in the vacancy configuration, in units of the perfect KCl nearest neighbor distance.

	F_A(Li)-center	
ion	even parity	odd parity
(0,1,0)	0,0.119,0	0,0.116,0
(1,0,0)	0.026,0.012,0	0.098,-0.031,0
(0,-1,0)	0,-0.027,0	0,-0.089,0
(1,1,0)	0.011,0.023,0	0.041,-0.028,0
(1,-1,0)	0,0.004,0	0.027,-0.017,0
(1,0,1)	-0.001,0.008,-0.001	-0.022,-0.014,-0.022
(1,1,1)	0.001,0.007,0.001	-0.006,-0.002,-0.006
(1,-1,1)	-0.001,0.003,-0.001	-0.002,-0.025,-0.002
(0,2,0)	0,-0.029,0	0,-0.062,0
(2,0,0)	0.002,0.004,0	0.018,-0.013,0
(0,-2,0)	0,-0.002,0	0,-0.024,0
(1,2,0)	0.02,0.011,0	0.009,-0.012,0
(2,1,0)	0.011,0.008,0	0.028,0.006,0
(1,-2,0)	0.004,-0.004,0	0.012,-0.029,0
(2,-1,0)	0.005,-0.002,0	0.029,-0.027,0
(1,0,2)	0.001,0.003,0	-0.001,-0.006,-0.006
(2,1,0)	0.004,0.002,0.001	0.005,-0.004,-0.003
(2,-1,1)	0.001,0.001,0	0.005,-0.000,0.002
(1,2,1)	0.007,0.011,0.007	0.002,-0.002,0.002
(1,-2,1)	0,-0.001,0	0.001,-0.002,0.001
(2,2,0)	0.011,0.007,0	0.009,0.001,0
(2,-2,0)	0.002,-0.001,0	0.010,-0.017,0
(2,0,2)	0,0.001,0	-0.003,-0.004,-0.003
(2,2,1)	0.003,0.003,0.002	0.001,-0.003,0.001
(2,-2,1)	0,0.001,0.001	0.004,-0.009,0.002
(2,1,2)	0.001,0.002,0.001	0,-0.001,0
(2,-1,2)	0,0.001,0	0.001, 0.004,0.001
(0,3,0)	0,-0.012,0	0,-0.026,0
(0,-3,0)	0,-0.001,0	0,-0.017,0
(0,0,3)	0,0.001,0.002	0,-0.004,0.007

Na^+) ion is more than that of the host K^+ cation, which is not surprising, since the impurity ion is smaller in size. The displacements of the more distant ions are small.

In Table (7), we compare our results with those of Alig[4] for the radial component of nearest neighbor displacements in the ground state of the F_A-center. Qualitatively, our displacements are somewhat larger than Alig's. The displacement of the host cation K^+ at $(0\bar{1}0)$ is approximately the same as that of the K^+ at (100), as Alig assumed, but we find that the four equivalent K^+ have a small non-zero y-component of displacement, as well.

(C) Absorption Energy

In the calculation of absorption energy, one needs only to do a zeroth order calculation. The displacements field $\underline{\xi}_g$ and non-harmonic displacements $\underline{\mu}_g$ are supplied by the relaxed ground state calculation. For the zeroth order calculation, one needs only to minimize the system's energy with respect to the unrelaxed excited state trial pseudo-wave function parameter $\underline{\lambda}_{ex}'$. The F_{A1} - F_{A2} absorption splitting corresponds to the two inequivalent orientations of the unrelaxed excited state wave function (Fig. 5).

The details of the F_{A1} and F_{A2} absorption energies are shown in Tables (8) and (9) respectively. The agreement of F_{A1} absorption with experiment is within 7%. This result is encouraging because the absorption energy is a simple test of the theoretical model. Any respectable model must give a reasonable agreement for the absorption energy.

Table (10) gives the contributions to the F_{A2} - F_{A1} absorption splitting. This table may indicate the origin of the absorption splitting and pinpoint an inadequacy in our model. The theoretically estimated F_{A2} - F_{A1}

Table 7

Comparison of the theoretically estimated radial component of nearest neighbor ions displacements in the ground state of F_A-centers in KCl, in units of the perfect KCl nearest neighbor distance, with positive direction outward from the vacancy.

	F_A(Na)			F_A(Li)		
ion	(0,10)	(0,-1,0)	(1,0,0)	(0,1,0)	(0,-1,0)	(1,0,0)
Alig[a]	+0.061	0.018	0.018	0.104	0.016	0.016
Present work	0.072	0.025	0.022+	0.119	0.027	0.026+

a. reference 4 Table II

\+ there is a non-zero y-component

Table 8

F_{A1} absorption energy with contributions as given in equation (2.94), where α_2' is the wave function parameter of the F_{A1} unrelaxed excited state made self-consistent with $(\underline{\mu}_g, \underline{\xi}_g)$. Energies in eV, α_2' in units of reciprocal interionic spacing.

	F_A(Na)	F_A(Li)
α_2'	1.16	1.14
$E_D(\underline{\xi}_g, \underline{\mu}_g, \alpha_2')$	3.03	2.63
$-E_D(0, \mu_{og}, \underline{\lambda}_{og})$	-1.05	-0.95
$-\underline{Fo}_g \cdot \underline{\xi}_g$	+0.08	+0.17
$-\frac{1}{2}\ \underline{\xi}_g \cdot \underline{\underline{C}}_g \cdot \underline{\xi}_g$	+0.01	+0.01
$E_{abs}(\underline{\mu}_g, \underline{\xi}_g, \underline{\lambda}_g, \alpha_2')$	2.07	1.86
Ex'pt	2.12	1.98

Table 9

F_{A2} absorption energy with contributions as given in equation (2.94) where α_3' is the wave function parameter of the F_{A2} unrelaxed excited state made self-consistent with $(\underline{\mu}_g, \underline{\xi}_g)$. Energies in eV, α_3' in units of reciprocal interionic spacing.

	F_A(Na)	F_A(Li)
α_3'	1.36	1.34
$E_D(\underline{\xi}_g, \underline{\mu}_g, \alpha_3')$	3.82	3.39
$-E_D(0, \underline{\mu o}_g, \underline{\lambda o}_g)$	-1.05	-0.95
$-\underline{Fo}_g \cdot \underline{\xi}_g$	+0.08	0.17
$-\frac{1}{2}\underline{\xi}_g \cdot \underline{\underline{C}}_g \cdot \underline{\xi}_g$	0.01	0.01
$E_{abs}(\underline{\mu}_g, \underline{\xi}_g \underline{\lambda}_g, \alpha_3')$	2.86	2.62
Expt	2.35	2.25

Table 10

Contribution to the $F_{A2} - F_{A1}$ absorption splitting (eV), where wave functions ϕ_2, ϕ_3 are given in equation (3.5), (3.6) for F_{A1} and F_{A2} absorption respectively, and their localization parameters α are given in tables (8) and (9)

	F_A(Na)-center			F_A(Li)-center		
	F_{A2}	F_{A1}	$F_{A2}-F_{A1}$	F_{A2}	F_{A1}	$F_{A2}-F_{A1}$
$\langle\phi\|T\|\phi\rangle$	3.55	2.60	0.95	3.44	2.50	0.94
$\langle\phi\|V_{Is}\|\phi\rangle$	1.09	0.30	0.79	1.04	0.29	0.75
$\langle\phi\|V_{pI}\|\phi\rangle$	-6.91	-5.96	-0.95	-6.52	-5.59	-0.93
$V_L(\underline{\xi}_g,\underline{\mu}_g)$	6.09	6.09	0	5.43	5.43	0
Totals, theor.	3.82	3.03	0.79	3.39	2.63	0.76
exp't	-	-	0.23	-	-	0.27

absorption splittings are a factor of about three times larger than the experimental results. In Table (10), we note that the contribution of electron kinetic energy $\bar{T}$, point ion potential energy $\bar{V}_{pI}$, and BSG ion-size correction $\bar{V}_{Is}$ to the splitting are equally important. In fact, the contribution of the electron kinetic energy and the point-ion potential energy almost cancel. Therefore, the net contribution comes from the ion-size correction. One may concluded that BSG ion-size correction is over-estimated. In Alig's calculation, he also came to the conclusion that the splitting was largely due to ion-size correction. Actually, he discarded the empirical factor $\alpha = 0.53$ in the ion-size correction, and his result was then only a factor of about two times too large. Neglect of other features that may contribute to the discrepancy; for example, the electronic polarization, the off-axis properties of Li^+, and the over-simplified form of trial pseudo-wave function, may also be important.

Table (11) shows the comparison of the previous theoretical investigations with the present calculation, for the shifts of the F_{A1} and F_{A2} absorption lines of F_A-centers relative to the F-center absorption in KCl, and the $F_{A2} - F_{A1}$ absorption splitting. Smith and the present work give a result which is about three times too large, Alig and Weber and Dick have a factor of about two times too large. Although our result is quite close to theirs, one cannot get a significant conclusion from this, since their approximation is quite different from ours. A qualitative comparison among the four theoretical investigations is given in Table (12). As far as the lattice distortion is concerned, our method is more accurate than the others.

In conclusion, the results of the $F_{A2} - F_{A1}$ absorption splitting suggests that more precise ion-size correction must be introduced.

Table 11

Shift in the absorption energies (eV) of F_A-centers relative to F-centers in KCl, and the absorption line splitting

	F_A(Na) center			F_A(Li) center		
	F_{A1}	F_{A2}	Split.	F_{A1}	F_{A2}	Split.
Smith[a]	-0.38	+0.16	0.54	-0.54	+0.24	0.78
W & D[b]	-0.34	+0.05	0.39	-0.46	+0.07	0.53
Alig[c]	-0.30	+0.06	0.36	-0.38	+0.08	0.46
Present work[d]	-0.20	+0.59	0.79	-0.43	+0.33	0.76
Exp't.[a]	-0.19	+0.04	0.23	-0.33	-0.06	0.27

a Reference 1, Table 3-2, p. 193

b Reference 3 Table 9, columns I.

c Reference 4, Table 1, columns III.

d The F-absorption energies are taken from reference 24, Table 3.

Table 12

Qualitative comparison of the methods and model in F_A-absorption study in the three previous theoretical investigations and in the present work.

	Method for ion-size correction	lattice distortion	lattice polarization	trial wave function	wave function self-consistent with the lattice potential and lattice distortion	Dynamical lattice effects
Smith	pseudopotential method	neglected	neglected	Gourary-Adrian Type I	no	no
Weber and Dick	BSG without $\alpha = 0.53$	neglected	neglected	Gourary-Adrian Type I,II,III	only with lattice potential	no
Alig	basically BSG without $\alpha = 0.53$	only nearest neighbors	nearest neighbors	Gourary-Adrian Type I,II,III and others	no	no
Present work	BSG with $\alpha = 0.53$	including farther out ions	neglected	Gaussian	yes	no

3.2. Saddle-Point Configuration

(A) Zeroth Order Calculation

We have investigated the following states in the saddle-point configuration of figure (2(b)): even parity relaxed state; odd parity relaxed state and unrelaxed even parity state.

Brown and Vail[24] have treated the saddle-point configuration of the F-center as the mid-point of the straight line connecting the diffusing anion and the original F-center vacancy. In the F_A-center activation process, some other, indirect path may be favourable, namely (1) motion of the saddle-point anion out of the $y' - z'$ plane (Fig. 2b); (2) displacement of the saddle-point ion along the y'-axis. An investigation of the possibility of path (1) will be described in section (3.2D), in which we seek to minimize the energy by displacing the saddle-point Cl^- ion out of the $y' - z'$ plane, along x'-axis. The results of this investigation were tentatively negative for the F_A-centers. In the following calculation we used path (2) as the favourable trajectory for the F_A-centers vacancy diffusion. With this trajectory we maintain some symmetry of the lattice configuration, namely the reflection symmetry with respect to the $x' - y'$ and $y' - z'$ planes.

In the saddle-point configuration, Region I contains saddle-point Cl^- ion, two vacant anion sites, and the two straddling positive ions, one the impurity Na^+ or Li^+ and the other a host K^+ ion. The trial pseudo-wave functions which we choose for the saddle-point configuration are similar to those which we used for the vacancy configuration. They are Gaussian localized with low order Legendre polynomials dependence, giving double-lobed charged densities, fitting into the two-well potential of the two vacant anion sites which are separated by the saddle-point ion.

The following trial wave functions are used:

For the odd parity relaxed state:

$$\phi_5 = A_5\, r' \cos\theta_z' \exp(-\alpha_5^2\, r'^2)$$

$$= A_5\, z' \exp(-\alpha_5^2\, r'^2); \qquad (3.21)$$

for the even parity unrelaxed state:

$$\phi_6 = A_6\, r'^2 \cos^2\theta_z' \exp(-\alpha_6^2\, r'^2)$$

$$= A_6\, z'^2 \exp(-\alpha_6^2\, r'^2); \qquad (3.22)$$

and for the even parity relaxed state:

$$\phi_7 = A_7\, r'^2 \cos^2\theta_z' \exp(-\alpha_7^2\, r'^2)$$

$$= A_7\, z'^2 \exp(-\alpha_7^2\, r'^2), \qquad (3.23)$$

where A_j $(j = 5, 6, 7)$ is the normalization constant and $\alpha_j (j = 5, 6, 7)$ is the wave function localization parameters, r' is the radial variable with origin at the saddle-point and θ_z' is the polar angle with z'-axis (Fig. 2(b)) as polar axis in spherical coordinates.

For the zeroth order calculation in the saddle-point configuration, we minimized the system's energy with respect to the wave function parameter α_j, the non-harmonic displacement y_1 of the impurity cation along the y'-axis from the perfect lattice site, the non-harmonic displacement y_2 of the host cation along the y'-axis from the perfect lattice site, and the displacement y_3 of the saddle-point ion along y'-axis. As in the vacancy configuration, we here keep the center of the wave function fixed at the origin also.

We formulate the procedure for calculating the energy $V_L(o, \underline{\mu})$

required to create the saddle-point defect as follows (Fig. 2(b)).

(1) remove the Cl^- ion from $(o, o, \sqrt{2}/2)$

(2) remove the Cl^- ion from $(o, o, -\sqrt{2}/2)$

(3) remove the K^+ ion from $(o, \sqrt{2}/2, o)$

(4) remove the K^+ ion from $(o, -\sqrt{2}/2, o)$

(5) put in the Cl^- ion at the saddle-point (o, y_3, o)

(6) put in the K^+ ion at $(o, -\frac{\sqrt{2}}{2} + y_2, o)$

(7) put in impurity cation at $(o, \frac{\sqrt{2}}{2} + y_1, o)$

Regarding the point ion potential V_{pI}, in the case of the odd parity relaxed state, the trial wave function which we used (equation (3.21) has $\ell=1$ or first order Legendre polynomial dependence. Since we let the saddle-point Cl^- ion move to (o, y_3, o) along y'-axis in the primed coordinates of the Fig. 2(b), there is no lattice charge at the origin. Hence, the expression for the expectation value of V_{pI} is the same as equation (3.18) for the case of relaxed excited state in the vacancy configuration. In the case of the even parity unrelaxed state, the angular dependent part of equation (3.22) can be written as:

$$\frac{1}{2} p_o + p_2 (\cos \theta_{z'}) \qquad (3.24)$$

which has $\ell=o$ and $\ell=2$ dependence. Thus, only terms in $\ell=o$, $\ell=2$ and $\ell=4$ with $m=o$ in equation (3.15) have non-zero contribution to $< \phi_6 \mid V_{pI} \mid \phi_6 >$. Again, there is no charge point ion at $\vec{r}_i = o$. Thus, the expression for V_{pI} becomes

$$V_{pI}(\vec{r}) = -2 \sum_{\substack{i \\ r_i \neq o}} \Bigg[Q_i \left\{ \frac{1}{r_i} + \frac{r^2}{r_i^3} P_2(\cos\theta)\, P_2(\cos\theta_i) + \frac{r^4}{r_i^5} P_4(\cos\theta)\, P_4(\cos\theta_i) \right\} \Bigg] + 2 \sum_{\substack{i \\ r_i < r \\ r_i \neq o}} \Bigg[Q_i \left\{ \left(\frac{1}{r_i} - \frac{1}{r} \right) + \left(\frac{r^2}{r_i^3} - \frac{r_i^2}{r^3} \right) P_2(\cos\theta)\, P_2(\cos\theta_i) + \left(\frac{r^4}{r_i^5} - \frac{r_i^4}{r^5} \right) P_4(\cos\theta)\, P_4(\cos\theta_i) \right\} \Bigg] \quad (3.25)$$

The procedure for the zeroth order calculation is the same as described in section 3.1(A) for the case of the vacancy configuration except that the calculation is done in the primed coordinate (Fig. 2(b)) here and the sum is over 232 ions in 87 groups near the saddle-point configuration.

The results of the zeroth order calculation for F_A- center relaxed odd and even parity states in the saddle-point configuration are reported in Tables (13) and (14) respectively. These results indicate that both straddling ions move outward from the saddle-point with the impurity cation moving further out than the host cation. The saddle-point ion also moves along the positive y'-axis a significant distance.

(B) Second Order Calculation (relaxed state)

For the second order calculation, we included the contributions from thirty-five groups of ions, containing 55 ions in all. The grouping of

Table 13

Zeroth order calculation of F_A-centers relaxed odd parity state in the saddle-point configuration. a is the interionic spacing of the prefect crystal.

		F_A(Na)	F_A(Li)
y_{10}	(a)	0.159	0.139
y_{20}	(a)	-0.093	-0.061
y_{30}	(a)	0.076	0.132
α_{50}	(1/a)	0.824	0.831
$V_L(0,y_{10},y_{20},y_{30})$	(eV)	6.23	5.85
$\overline{V}_{pI}$	(eV)	-4.67	-4.76
$\overline{V}_{Is}$	(eV)	0.34	0.33
$\overline{T}$	(eV)	1.31	1.33
$E(0,y_{10},y_{20},y_{30},\alpha_{50})$	(eV)	3.21	2.75

Table 14

Zeroth order calculation of F_A-centers relaxed even parity state in the saddle-point configuration. a is the inter-ionic spacing of the crystal.

		F_A(Na)	F_A(Li)
y_{10}	(a)	0.159	0.148
y_{20}	(a)	-0.098	-0.061
y_{30}	(a)	0.072	0.139
α_{70}	(1/a)	0.967	0.972
$V_L(0,y_{10},y_{20},y_{30})$	(eV)	6.22	5.82
$\overline{V}_{pI}$	(eV)	-5.28	-5.37
$\overline{V}_{Is}$	(eV)	0.23	0.22
$\overline{T}$	(eV)	1.56	1.57
$E(0,y_{10},y_{20},y_{30},\alpha_{70})$	(eV)	2.73	2.24

ions and the matrix elements of $\underline{G}(\vec{q})$ are given explicitly in Appendix B. There are two rectangular coordinated systems involved in the saddle-point configuration calculation. One is the unprimed system and the other is the primed system (defect oriented) as in Fig. 2(b). We may obtain the unprimed system by rotating the primed system by an angle of 45°. In order to use Kellermann's dynamical matrix, we have to do the calculation in the unprimed coordinates but $F_\alpha(\vec{r}^{\,\ell}_k)$ are easier to calculate in the primed system.

Since the relationship of the two coordinates system is

$$\begin{pmatrix} \xi_x' \\ \xi_y' \\ \xi_z' \end{pmatrix} = \begin{pmatrix} 1 & 0 & 0 \\ 0 & \frac{1}{\sqrt{2}} & -\frac{1}{\sqrt{2}} \\ 0 & \frac{1}{\sqrt{2}} & \frac{1}{\sqrt{2}} \end{pmatrix} \begin{pmatrix} \xi_x \\ \xi_y \\ \xi_z \end{pmatrix} \tag{3.26}$$

We have:

$$F_x = F_x' \tag{3.27}$$

$$F_y = \frac{1}{\sqrt{2}} (F_y' + F_z') \tag{3.28}$$

$$F_z = \frac{1}{\sqrt{2}} (F_z' - F_y') \tag{3.29}$$

Therefore, the solution of $\underline{\xi}$ in equation (2.62) is in the unprimed coordinated system. The results reported in Tables (15) and (16), the displacement components of the ions neighboring the $F_A(Na)$ and $F_A(Li)$ center in KCl in even and odd parity relaxed states in the saddle-point configuration respectively, are in the primed coordinates system. Tables (15) and (16) cover all the ions shown in Fig. 2(b), plus the ions in the

Table 15

Cartesian components of displacements of the ions neighboring the F_A(Na)-center in KCl in even and odd parity relaxed states in the saddle-point configuration in units of the perfect KCl nearest neighbor distance.

	F_A(Na) Center	
ion	odd parity	even parity
$(0,\frac{1}{2}\sqrt{2},0)$	0,0.160,0	0,0.161,0
$(0,\frac{-1}{2}\sqrt{2},0)$	0,-0.094,0	0,-0.101,0
(0,0,0)	0,0.076,0	0,0.072,0
$(1,0,\frac{1}{2}\sqrt{2})$	0.017,0.006,-0.053	0.021,0.007,-0.032
$(1,\frac{1}{2}\sqrt{2},0)$	0.050,0.056,0	0.044,0.050,0
$(1,\frac{-1}{2}\sqrt{2},0)$	0.026,-0.032,0	0.021,-0.025,0
$(0,\frac{1}{2}\sqrt{2},\sqrt{2})$	0,0.056,0.020	0,0.035,0.030
$(0,\frac{-1}{2}\sqrt{2},-\sqrt{2})$	0,-0.041,-0.031	0,-0.019,-0.039
$(0,\sqrt{2},\frac{1}{2}\sqrt{2})$	0,0.040,-0.013	0,0.028,-0.011
$(0,-\sqrt{2},\frac{-1}{2}\sqrt{2})$	0,-0.007,0.008	0,0.005,0.008
$(0,3\sqrt{2}/2,0)$	0,0.055,0	0,0.048,0
$(0,-3\sqrt{2}/2,0)$	0,-0.027,0	0,-0.021,0
$(0,0,3\sqrt{2}/2)$	0,0.005,-0.025	0,0.004,0.002

Table 16

Cartesina components of displacements of the ions neighboring the F_A(Li)-center in KCl in even and odd parity relaxed states in the saddle-point configuration in units of the perfect KCl nearest neighbor distance.

ion	F_A(Li) Center odd parity	even parity
$(0,\frac{1}{2}\sqrt{2},0)$	0,0.142,0	0,0.151,0
$(0,\frac{-1}{2}\sqrt{2},0)$	0,-0.068,0	0,-0.069,0
(0,0,0)	0,0.134,0	0,0.140,0
$(1,0,\frac{1}{2}\sqrt{2})$	0.035,0.004,-0.041	0.040,0.005,-0.019
$(1,\frac{1}{2}\sqrt{2},0)$	0.063,0.040,0	0.063,0.033,0
$(1,\frac{-1}{2}\sqrt{2},0)$	0.021,-0.019,0	0.015,-0.009,0
$(0,\frac{1}{2}\sqrt{2},\sqrt{2})$	0,0.058,0.023	0,0.038,0.034
$(0,\frac{-1}{2}\sqrt{2},-\sqrt{2})$	0,-0.038,-0.042	0,-0.017,-0.052
$(0,\sqrt{2},\frac{1}{2}\sqrt{2})$	0,0.023,-0.022	0,0.012,-0.024
$(0,-\sqrt{2},\frac{-1}{2}\sqrt{2})$	0,0.013,0.010	0,0.029,0.011
$(0,3\frac{\sqrt{2}}{2},0)$	0,0.041,0	0,0.037,0
$(0,-3\frac{\sqrt{2}}{2},0)$	0,-0.011,0	0,-0.002,0
$(0,0,3\cdot\frac{\sqrt{2}}{2})$	0,0.005,-0.019	0,0.006,0.009

two nearest planes parallel to the $y' - z'$ plane which are immediately adjacent to the Region I. The most important displacements are those of the straddling positive ions and of the saddle-point ions. The impurity ion Li^+ or Na^+ at $(0, \sqrt{2}/2, 0)$ site moves along positive y'-axis a distance about 0.15 time the perfect lattice spacing, and the saddle-point ion follows it about the same amount for the $F_A(Li)$-center, and about half that distance for the $F_A(Na)$-center. On the other hand, the host K^+ ion at $(0, -\sqrt{2}/2, 0)$, i.e. on the other side of the saddle-point move outward by about 0.07 and 0.09 nearest neighbor distances in $F_A(Li)$ and $F_A(Na)$ respectively.

The results for the relaxed odd and even parity states are given in Tables (17) and (18). The second-order corrected wave function has its localization parameter changed by 0.04 and 0.06 for odd and even parity respectively, in units of reciprocal nearest neighbor spacing. This shows how the wave function of the F_A-center in the saddle-point configuration responds to the lattice distortion. The relaxation energy is larger in the case of the odd parity state than for the even parity state, as one might expected, for both $F_A(Na)$ and $F_A(Li)$-centers. The splitting between the odd parity state and even parity relaxed state is 0.37 eV and 0.32 eV for $F_A(Li)$ and $F_A(Na)$ respectively. This separation is not enough to allow for the emission process for $F_A(Li)$-center in the saddle-point configuration, which is 0.46 eV. Therefore, we do not expect our estimated emission energy to agree with the experiment, except possibly in the order of magnitude. The calculation to be reported in the next section shows that our model and approximation fails to describe the emission process at all. Further discussion of this point will be deferred to section (3.2c). Regarding the odd parity relaxed state in the saddle-

Table 17

Second order calculation of F_A-centers relaxed odd parity state in the saddle-point configuration. The total relaxed state energy $E(\underline{\xi},y_1,y_2,y_3,\alpha_5)$ is given in equation (2.88) a is the interionic spacing of the crystal.

		F_A(Na)	F_A(Li)
α_5	(1/a)	+0.81	0.79
y_1	(a)	0.160	0.142
y_2	(a)	-0.094	-0.068
y_3	(a)	0.076	0.135
$\frac{1}{2}\,\underline{F_o}^T \cdot \underline{\xi}$	(eV)	-0.45	-0.48
$E(0,y_{10},y_{20},y_{30},\alpha_{50})$	(eV)	3.21	2.75
$\frac{1}{2}\,\underline{\xi}^T \cdot \underline{\underline{C}} \cdot \underline{\xi}$	(eV)	0.04	0.06
$E(\underline{\xi},y_1,y_2,y_3,\alpha_5)$	(eV)	2.76	2.27

Table 18

Second order calculation of F_A-centers relaxed even parity state in the saddle-point configuration. The total relaxed state energy $E(\underline{\xi},y_1,y_2,y_3,\alpha_7)$ is given in equation (2.88). a is the interionic spacing of the crystal.

		F_A(Na)	F_A(Li)
α_7	(1/a)	0.93	0.91
y_1	(a)	0.161	0.151
y_2	(a)	-0.101	0.069
y_3	(a)	0.072	0.140
$\frac{1}{2}\,\underline{F_0}^T \cdot \underline{\xi}$	(eV)	-0.29	-0.34
$E(0,y_{10},y_{20},y_{30},\alpha_{70})$	(eV)	2.73	2.24
$\frac{1}{2}\,\underline{\xi}^T \cdot \underline{\underline{C}} \cdot \underline{\xi}$	(eV)	0.02	0.02
$E(\underline{\xi},y_1,y_2,y_3,\alpha_7)$	(eV)	2.44	1.90

point configuration, it is 0.42 eV lower than in the vacancy configuration for the F_A(Li)-center. This means that the relaxed excited state is stabilized in the saddle-point configuration, in agreement with the experiment[1]. For the F_A(Na)-center, the relaxed excited state in the saddle-point configuration lies lower than in the vacancy configuration by 0.08 eV. This means that the relaxed excited state is also stabilized in the saddle-point configuration for this center, which contradicts the experimental result, where it is found to be stabilized in the vacancy configuration by 0.09 eV. This result then indicates that our model and approximations are not generally accurate to better than a few tenths of an eV, when dealing with the relaxed excited state.

(C) Emission Energy

It has been found experimentally that the emission process occurs in the saddle-point configuration for the F_A(Li)-center. Similar to the absorption energy, section 3.1(c), we calculated the unrelaxed even parity state in the presence of the distortion field of the odd parity state, minimizing the energy with respect to the even parity wave function parameter only. The result of the calculation is shown in Table (19), where the superscripts (e), (o) refer to even and odd parity. The square bracket in Table (19) means that a negative (unphysical) result is obtained; i.e. our even parity unrelaxed state lies higher than the odd parity relaxed excited state in the saddle-point configuration. In order to understand the origin of this discrepancy, we re-examined our even-parity wave function ϕ_6 in the saddle-point configuration. We observe that ϕ_6, with only one variational parameter, fits its two charge-density lobes to the two-well potential in the relaxed even-parity state, but apparently

Table 19

Emission energy (eV) of $F_A(Li)$ in KCl in the saddle-point configuration with contributions as given in equation (2.96) where $\lambda^{(e)'}$ is the wave function parameters of the unrelaxed even parity state made self-consistent with $(\underline{\mu}^{(o)}, \underline{\xi}^{(o)})$. $\underline{\lambda}^{(e)'}$ in units of reciprocal interionic spacing

	ϕ_6	ϕ_6'	ϕ_6''
$\underline{\lambda}^{(e)'}$ b ; β		0.182	0.362
α	0.983	0.979	0.931
$V_L(\underline{\xi}^{(o)}, \underline{\mu}^{(o)})$	5.13	5.13	5.13
$\langle\phi_6 \mid T \mid \phi_6\rangle$	1.61	1.53	1.55
$\langle\phi_6 \mid V_{Is} \mid \phi_6\rangle$	0.17	0.18	0.17
$\langle\phi_6 \mid V_{pI} \mid \phi_6\rangle$	-4.86	-4.81	-4.87
$-E_D(\underline{\xi}^{(o)}, \underline{\mu}^{(o)}, \underline{\lambda}^{(e)'})$	-2.05	-2.03	-1.98
$E_D(0, \underline{\mu}^{(o)}, \underline{\lambda}^{(o)})$	2.75	2.75	2.75
$\underline{Fo}^{(o)T} \cdot \underline{\xi}^{(o)}$	-0.96	-0.96	-0.96
$\frac{1}{2} \underline{\xi}^{(o)T} \cdot \underline{\underline{C}}^{(o)} \cdot \underline{\xi}^{(o)}$	0.06	0.06	0.06
$E_{em}(\underline{\mu}^{(o)}, \underline{\xi}^{(o)}, \underline{\lambda}^{(o)}, \underline{\lambda}^{(e)'})$	[0.20]	[0.18]	[0.13]

cannot do so well in the unrelaxed state, where the lattice distortion field $(\underline{\xi}, \underline{\mu})$ is determined by the relaxed odd-parity state, ϕ_5. It needs more than one variational parameter to adjust simultaneously the position and sharpness of its two charge-density lobes to the two-well potential. We therefore tried two other forms of two-parameters trial wave functions in place of ϕ_6, in an attempt to describe the emission process, namely:

$$\phi_6' = A_6'(b^2 + \frac{3}{2} r'^2 \cos\theta_{z'}) \exp(-\alpha^2 r'^2) \tag{3.30}$$

$$\phi_6'' = A_7' [1 - \exp(-\beta^2 r'^2)] \cos^2\theta_{z'} \cdot \exp(-\alpha^2 r'^2) \tag{3.31}$$

The results of the calculation (last two column of Table 19) show that the above two trial wave functions, each having two variational parameters (b,α) and (β,α) respectively, are just slightly more feasible than ϕ_6, lowering the energy by 0.02 eV and 0.07 eV respectively.

Several deficiencies of the model may contribute to the failure to describe this emission process. The most likely is the lack of flexibility of the wave function. Secondly, the Condon approximation may not apply in this emission process. Thirdly, interaction of the excess-electron with phonons, and parity mixing of the wave function may occur, as in the RES of the ordinary F-center in KCl. Ionic polarization may also be important. Further discussion of these points will be deferred to Chapter 4.

(D) Investigation of the Stability of the Saddle-Point Configuration

A preliminary investigation of the stability of the saddle-point configuration has been made in the present work.

The question is whether the diffusing anion Cl^- will move out of the $y' - z'$ plane (Fig. 2(b)). The procedure we have used is to evaluate the defect's energy in zeroth order as a function of displacement x' of

the diffusing (saddle-point) ion along the x'-axis for the $F_A(Na)$, $F_A(Li)$ and ordinary F-centers, in KCl. That is, for a given value of x', we minimize the system's energy with respect to the odd-parity wave function's localization parameter and with respect to displacements along the y'-axis of the two straddling cations. There is difficulty in the numerical calculation because the energy is such that it becomes a relatively small difference between very large numbers for $x' \sim 0.01$, so that double-precision accuracy is required in the computation, and the results become unreliable for $x' \leq 0.01$, though they are reliable for $x' = 0$.

The results are plotted in Fig. 7. For the $F_A(Li)$ and $F_A(Na)$ - centers in KCl, figure 7(a) and (b) respectively, apart from the vicinity of $x' = 0.01$, there is a flat minimum around $x' = 0.1$ times the nearest neighbour spacing. The difference in energy between $x' = o$ (strict saddle-point) and the flat minimum is about 0.02 eV. Accordingly, we have carried out all the calculations in the saddle-point configuration for $x' = 0$, because this configuration still preserves the reflection symmetry with respect to the $y' - z'$ and $x' - y'$ plane for which it is analytically much easier to calculate than with $x' \neq 0$. Furthermore, we do not find that our model and approximations are generally accurate to better than a few tenths of an eV.

In the case of the F-center in KCl, Figure 7(c), apart from the vicinity $x' = 0.01$, the curve appears to be monotonic decreasing with increasing x'. We have calculated only up to $x' = 0.3a$ because the calculation become complicated beyond that due to the Born-Mayer repulsion and displacement of the two nearest Cl^- ions as well as of the two nearest cations and the wave function must be allowed to displace in the x'-direction as well, for

Figure 7

The zeroth order odd - parity energy (eV) $E^{(o)}$ as a function of the displacements of the saddle point ions along x' - axis (see fig. 2(b)). x' in units of perfect KCl nearest neighbor distance.

(a) F_A (Li) - center in KCl

(b) F_A (Na) - center in KCl

(c) F - center in KCl

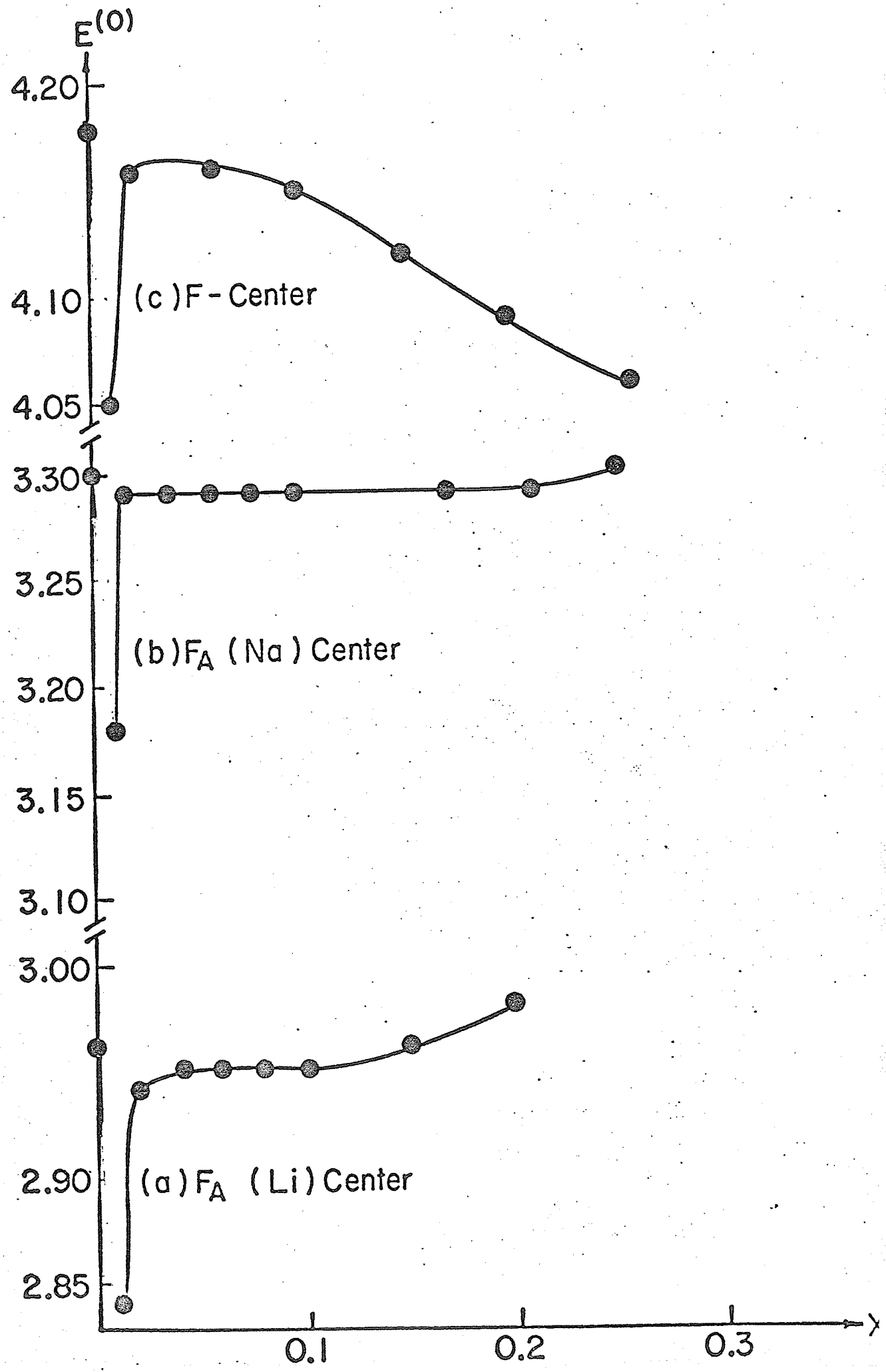
E(0)
4.20
4.10
4.05
3.30
3.25
3.20
3.15
3.10
3.00
2.90
2.85
(c) F - Center
(b) F_A (Na) Center
(a) F_A (Li) Center
0.1
0.2
0.3
λ

a highly asymmetric saddle-point.

In summary, we do not consider that the question of the saddle-point configuration is settled. However, the results of Fig. 7 suggest that for the F_A(Na) and F_A(Li)-centers in KCl, a value $x' \leq 0.1$ gives the stable configuration with energy only slightly lower than that for $x' = o$, while for the ordinary F-center, an asymmetrical saddle-point configuration seems probable.

3.3 Reorientation Activation Processes

The reorientation activation energy for both even and odd parity states of the F_A-centers are analysed in Table (20), where "d.e." is the change in total energy induced by harmonic relaxation of the lattice (to second order). The total differences in Table (20) represent the activation energies. For the even parity reorientation activation energy, the relaxed states are relatively low-lying in both the vacancy and saddle-point configurations. The agreement with the experiment is within 15%, the theoretical result being 0.18 eV too high for F_A(Na) and 0.12 eV too high for F_A(Li). We notice that the excess-electron's kinetic energy $\bar{T}$ and ion size correction rises slightly in going from vacancy to saddle-point configuration, but the point ion term rises considerably, and the lattice defect energy $V_L(0, \underline{\mu})$ drops considerably.

For the odd parity state, our calculation predicts a relatively large stabilization energy of 0.42 eV for the F_A(Li)-center, in the saddle-point configuration, in qualitative agreement with experiment. The F_A(Na)-center is found experimentally to have a small positive reorientation energy 0.09 eV, our theoretical results give a small value of opposite sign namely -0.08 eV. This discrepancy perhaps gives an indication of

Table 20

Contributions (eV) to energy differences between saddle-point (s.p.) and vacancy (vac.) configurations for even and odd parity relaxed states of the F_A center in KCl.

Center	F_A(Na)						F_A(Li)					
parity	even			odd			even			odd		
	s.p.	vac.	diff.	s.p.	vac.	diff.	s.p.	vac.	diff.	s.p.	vac.	diff.
$\langle\phi\|T\|\phi\rangle$	+1.56	+1.44	+0.12	+1.31	+2.68	-1.37	+1.57	+1.43	+0.14	+1.33	+2.64	-1.31
$\langle\phi\|V_{pI}\|\phi\rangle$	-5.28	-7.11	+1.83	-4.67	-6.28	+1.61	-5.37	-6.95	+1.58	-4.76	-6.11	+1.35
$\langle\phi\|V_{Is}\|\phi\rangle$	+0.23	+0.08	+0.15	+0.34	+0.31	+0.03	+0.22	+0.08	+0.14	+0.33	+0.30	+0.03
$V_L(0,\underline{\mu}_o)$	+6.22	+6.64	-0.42	+6.23	+6.62	-0.39	+5.82	+6.39	-0.57	+5.85	+6.41	-0.56
d.e	-0.29	-0.04	-0.25	-0.45	-0.49	+0.04	-0.34	-0.08	-0.26	-0.48	-0.55	+0.07
Totals, theor.	+2.44	+1.01	+1.43	+2.76	+2.84	-0.08	+1.90	+0.87	+1.03	+2.27	+2.69	-0.42
Experiment	-	-	+1.25	-	-	+0.09	-	-	+0.91	-	-	<0

the limit of accuracy of our model and approximation. We notice that the odd parity excess-electron's kinetic energy drops considerably in going from vacancy to saddle-point configuration, since the electron goes from localization near two positive ions adjacent to the vacancy, to localization in the rather shallow double-well potential of the saddle-point configuration, and the wave function delocalizes somewhat. The point-ion potential rises considerably and ion-size correction rises slightly and the lattice defect energy drops considerably, in going from vacancy to saddle-point configuration, as in the even parity case. Thus, the major difference between the odd parity and even parity reorientation energy are the different behaviour of the electron's kinetic energy, and the different effect of harmonic (Region II) distortion, which lowers the even parity energy, but raises the odd parity energy.

In order to understand the role of the impurity cations in the activation process, we are going to compare with the results for the ordinary F-center which has been analyzed by Brown and Vail[31]. The theoretically estimated reorientation energies of F_A(Na)-, F_A(Li)-, and ordinary F-centers in KCl are analysed in Table (21). Let us look at the even parity states first (Table 21(A)). The contribution from the harmonic distortion (d.e.) energy is almost the same for all cases. The same is true for the electron's kinetic energy and for the ion-size correction. Regarding $\bar{V}_{pI}$, it is 0.57 eV lower for F_A(Li) and 0.32 eV lower for F_A(Na) than for the F-center. For $\bar{V}_L$, it is 0.61 eV lower for F_A(Li) and 0.46 eV lower for F_A(Na) than for the F-center. Thus, we see that the impurity ion lowers the even parity activation energy of the F-center through its effects on the lattice energy and on the point-ion potential for the excess-electron about equally.

Table 21

Comparison of the contributions (eV) to the reorientation activation energies of $F_A(Na)$, $F_A(Li)$ and F-centers in KCl.

(A) Even parity

	$F_A(Li)$	$F_A(Na)$	F	$F_A(Li)$-F	$F_A(Na)$-F
$\overline{T}$	0.14	0.12	0.09	0.05	0.03
$\overline{V}_{pI}$	1.58	1.83	2.15	-0.57	-0.32
$\overline{V}_{IS}$	0.14	0.15	0.20	-0.06	-0.05
$V_L(0,\underline{\mu})$	-0.57	-0.42	0.04	-0.61	-0.46
d.e.	-0.26	-0.25	-0.25	-0.01	0

(B) Odd parity

	$F_A(Li)$	$F_A(Na)$	F	$F_A(Li)$-F	$F_A(Na)$-F
$\overline{T}$	-1.31	-1.37	-1.48	0.17	0.11
$\overline{V}_{pI}$	1.35	1.61	2.05	-0.70	-0.44
$\overline{V}_{IS}$	0.03	0.03	0.17	-0.14	-0.14
$V_L(0,\underline{\mu})$	-0.56	-0.39	0.06	-0.62	-0.45
d.e.	0.07	0.04	-0.29	0.36	0.33

In the case of the odd-parity reorientation activation energy, the impurity ion not only decreases the contribution from $\bar{V}_{pI}$ and the lattice defect energy $\bar{V}_L$ but also increases the distortion energy of the lattice (Table 21(B)). Furthermore, the increases of the electron's kinetic energy and the decreases of the ion-size correction are small but not negligible.

CHAPTER 4

CONCLUSIONS

We have applied the model and methods for point defects in general and color centers in particular to study the Type I and Type II F_A-centers in KCl, and these have been described fully in previous chapters. Several basic approximations are made in this calculation:

(1) Adiabatic approximation;

(2) Franck-Condon principle to describe the optical transitions;

(3) neglect of lattice dynamic effects;

(4) perfect lattice repulsive parameters for LiCl and NaCl have been used for Li^+ and Na^+ impurities in the KCl crystal;

(5) one parameter Gaussian localization with low order Legendre polynomial for the trial wave functions;

(6) neglect of ionic polarizability

We used a variational method to locate the energy levels and calculate the wave functinns. Lattice distortion and lattice relaxation energy have been treated rigorously by the method of lattice statics, and the change of the wave-function parameter due to distortion has been calculated self-consistently.

As we have discussed in chapter 3, our theoretical results only partially agree with experiment: the theoretical values for the absorption energy and ground state reorientation energy are in good agreement with experiment, but the model and methods fail to give the $F_A(Li)$ emission energy or the $F_A(Na)$ excited state reorientation energy. It is well-known that the RES of the F-center in NaCl type ionic crystals is very complicated. For example, the RES may be diffuse and the wave function of the excess-electron may be a 2s-2p parity mixture due to coupling with the longitudinal optical phonons[32]. Recently, Mollenauer et al[33] found experimentally that the RES of KI is diffuse but not a parity mixture. In view of this complexity, it is perhaps not surprising that the present type of treatment failed to give the emission energy in agreement with experiment[24]. Since the present model is over-simplified for the RES of F-centers we have not estimated the emission energy of the $F_A(Na)$-centers in the vacancy configuration. In the present calculation, we have resisted the temptation to make any kind of empirical adjustment to improve the agreement with experiment since it will cover the weakness of the model and methods. It is one of the objects of the present work to contribute to the understanding of how current models of ionic crystals describe the properties of defects and to suggest how the model and methods could be improved.

For the absorption process, the agreement of the F_{A1}-absorption energy with experiment indicates that our model and methods are reasonable. As far as $F_{A1} - F_{A2}$ absorption splitting is concerned, by examining the electronic structure of the splitting and comparing it with other works, we conclude that the ion-size correction needs to be improved. An improvement of the BSG ion-size correction has been given by Bartram and Gash[21] who attempt to give the exact pseudopotential solution by using

the Philips and Kleinman pseudopotential[20]. However, it seems to us that the Cohen and Heine[19] pseudopotential is the better form for the variational procedure, since it is the optimum pseudopotential with respect to wave-function smoothness. Some transformation of this pseudopotential may be possible to allow the use of the variational method with an accurate treatment of the Cohen-Heine pseudopotential. Others types of corrections for the ion-size correction have been given by Martino[34], Öpik and Wood[35], and Matthew and Green[36].

Ionic polarization can be incorporated through the shell model[37] in two ways. First, both shell and core can be assumed to respond adiabatically to the excess-electron. This has been done by Stoneham and Bartram[16]. The extension of Kellermann's dynamical matrix to include the shell model is straightforward and has been done by Woods et al[38]. On the other hand, it may be more realistic to assume that only the ionic cores follow the excess-electron adiabatically. The core-shell displacements would then be treated as elements of $\underline{\lambda}$ in the method of lattice statics. This has been done by the author (ref. (39) section (3.3)) including the polarization of only a few near neighbors in a preliminary analysis of the F-center saddle-point configuration.

The failure to describe the emission process for the F_A(Li)-center in the saddle-point configuration suggests that the electron-phonon interaction may be important. If the emission process for the F_A(Li)-center in the saddle-point configuration emits phonons simultaneously with the photon, the emission energy will approach the difference between the relaxed odd and even parity states in the saddle-point configuration. This difference is equal to 0.37 eV and the experimental emission energy is 0.46 eV. A formulation to include the lattice dynamic effects in the

lattice statics treatment of the excess-electron defect has been developed by Vail[40], but has not yet been applied. Another factor which may be responsible for the failure to describe the emission energy is the trial wave function. More than one trial wave function parameter is probably necessary for the even parity state to fit in the relaxed odd-parity lattice configuration. Furthermore, the center of the wave function should not be restricted to the origin since the defect lattice is asymmetric.

The fact that our method shows the stabilization of the F_A(Li)-center in the saddle-point configuration suggests that our treatment of the saddle-point configuration is appropriate. Our theoretical results show the F_A(Na)-center is weakly stabilized in the saddle-point configuration, contrary to experiment, and the error is of the order of 0.2 eV. This may arise largely from the use of perfect repulsive parameters in the defect configuration, but other factors may be equally important.

The calculations for the reorientation energy not only show the role of the impurity ion in the activation process but also indicates that the present model and methods can adequately describe relaxed states which are well below the conduction band.

In general, the accuracy of these calculations could be improved by allowing for lower symmetry in the relaxed states, by taking account of the off-axis property of the Li^+ ion, and by including the possibility of Jahn-Teller distortions. One may also improve the accuracy of the displacements found for the distorted lattice by increasing the number of allowed wave vectors $\vec{q}$ in the reciprocal space, that is, by increasing the number of unit cells per defect. In this way, the displacements of the ions farthest from the point defect would not be affected by the defects in the adjacent super-cells generated by the periodic boundary conditions.

In conclusion, the results of the extensive study of the electronic and ionic structure of the $F_A(Na)$ and $F_A(Li)$ - centers in optical transitions and reorientation processes lead us to suggest that the following improvements to our model and methods should be incorporated and systematically investigated, namely:

(1) a more precise ion-size correction;

(2) a more flexible wave function;

(3) introduction of ionic polarization;

(4) introduction of electron-phonon effects;

(5) consideration of parity mixing in the relaxed excited states;

(6) consideration of configurations of lower symmetry.

REFERENCES

1. F. Lüty, Physics of Color Centers, edited by W.B. Fowler (Academic, N.Y. 1968) ch. 3.
2. D. Smith, unpublished (1966) reported in Ref. 1, pp. 192-193.
3. W. Weber and B.G. Dick, Phys. stat. sol. 36, 723 (1969).
4. R.C. Alig, Phys. Rev. B2, 2108 (1970).
5. K. Kojima, N. Nishimaki and T. Kojima, J. Phys. Soc. Japan 16, 2033 (1961).
6. R.A. Evarestov, Phys. Stat. Sol. 35, K157 (1969).
7. B.S. Gourary and F.J. Adrian, Phys. Rev. 105, 1180 (1957).
8. R.H. Bartram, A.M. Stoneham and P. Gash, Phys. Rev. 176, 1014 (1968).
9. M. Born and K. Huang, Dynamical Theory of crystal Lattice (Oxford, 1954) pp. 166-173.
10. H. Fröhlich, H. Pelzer and S. Zienan, Phil. Mag., 41, 221 (1950). K. Huang and A. Rhys. Proc. Roy. Soc. (London) A204, 406 (1950).
11. S.F. Wang and C. Chu, Phys. Rev. 154, 848 (1967).
12. M.P. Tosi, Solid State Physic vol. 16, (1964) pp. 1-113.
13. M.P. Tosi, J. Res. Nat. Bur. Standards, Misc. Publ. 287, (1967). Table 2, p. 2.
14. H. Kanzaki, J. Phys. Chem. Solids 2, 24 (1957).

15. J.R. Hardy, J. Phys. Chem. Solids 15, 39, (1960).

16. A.M. Stoneham and R.H. Bartram, Phys. Rev. B2, 3403 (1970).

17. J.M. Vail, Phys. Stat. Sol. (b) 44, 443, (1971).

18. Recent reveiw articles on photochromic devices are:

(a) Z.J. Kiss, Physics today, 23, #1, p. 42 (1970).

(b) M.J. Taylor, Physics Bulletin, 21, 485, (1970).

(c) B.W. Faughnan, D.L. Staebler, and Z.J. Kiss, Applied solid state Science, 2 (Ed. R. Wolfe) p. 107 (Academic Press, 1971).

19. M. Cohen and V. Heine, Phys. Rev. 122, 1821, (1961).

20. J.C. Phillips and L. Kleinman, Phys. Rev. 116, 287, (1959).

21. P. Gash. Thesis, Univ. of Connecticut, (1970).

22. E.W. Kellermann, Phil. Trans. A 238, 513 (1940).

23. F. Rosenberger and F. Lüty, Solid State commun. 7, 983 (1969).

24. R.J. Brown and J.M. Vail, Phys. Stat. Sol. 40, 737, (1970).

25. M.P. Tosi and M. Doyama, Phys. Rev. 151, 642, (1966).

26. J.D. Jackson, Classical Electrodynamics (John Wiley and Sons, 1962).

27. R.J. Brown, Thesis, Univ. of Manitoba, (1970).

28. M.J.D. Powell, Computer Journal 7, 303, (1965).

29. B. Dayal and B.B. Tripathi, Proc. Phys. Soc. 77, 303, (1961).

30. F Lüty, S. Costa Ribeiro, S. Mascarenhas and V. Sverzut, Phys. Rev. 168, 1080, (1968).

31. R.J. Brown and J.M. Vail, Phys. Stat. Sol (b) 49, K 33 (1972).

32. W.B. Fowler, Physics of Color Centers, edited by W.B. Fowler (Academic, N.Y. 1968) Ch. 2. pp. 97-109.

33. L.F. Mollenauer and G. Baldacchini, Phys. Rev. Letters 29, 465, (1972).

34. F. Martino, Internat. J. Quantum Chem. 2, 217, (1968); 2, 233 (1968).

35. U. Öpik and R.F. Wood, Phys. Rev. 179, 772, (1969).

36. J.A.D. Matthew and B. Green, J. Phys. C4, L101 (1971).

37. B.G. Dick and A.W. Overhauser, Phys. Rev. 112, 90 (1958).

38. A.D.B. Woods, W. Cochran, and B.N. Brockhouse, Phys. Rev. 119, 980, (1960).

39. C.K. Ong, M.Sc. Thesis, Univ. of Manitoba, (1971).

40. J.M. Vail, "Formulation to Include Phonon Effects in the Lattice Statics Analysis of Electronic Defects and Polarons in Ionic Crystals", published, Phys. Rev. B (1973).

41. C. Kittel, Intro. to Solid State Physics (3rd edition, 1967), pp. 60-61.

42. A.M. Stoneham, Phys. Stat. Sol. (6), 52, 9 (1972).

APPENDICES

(A) Kellermann's Dynamical Matrix

The dynamical matrix[22] $\underline{\underline{D}}$ is a 6 x 6 matrix with the elements:

$$\underline{\underline{D}} = \begin{vmatrix} \begin{bmatrix} 1 & 1 \\ x & x \end{bmatrix} & \begin{bmatrix} 1 & 1 \\ x & y \end{bmatrix} & \begin{bmatrix} 1 & 1 \\ x & z \end{bmatrix} & \begin{bmatrix} 1 & 2 \\ x & x \end{bmatrix} & \begin{bmatrix} 1 & 2 \\ x & y \end{bmatrix} & \begin{bmatrix} 1 & 2 \\ x & z \end{bmatrix} \\ \begin{bmatrix} 1 & 1 \\ x & y \end{bmatrix} & \begin{bmatrix} 1 & 1 \\ y & y \end{bmatrix} & \begin{bmatrix} 1 & 1 \\ y & z \end{bmatrix} & \begin{bmatrix} 1 & 2 \\ x & y \end{bmatrix} & \begin{bmatrix} 1 & 2 \\ y & y \end{bmatrix} & \begin{bmatrix} 1 & 2 \\ y & z \end{bmatrix} \\ \begin{bmatrix} 1 & 1 \\ x & z \end{bmatrix} & \begin{bmatrix} 1 & 1 \\ y & z \end{bmatrix} & \begin{bmatrix} 1 & 1 \\ z & z \end{bmatrix} & \begin{bmatrix} 1 & 2 \\ x & z \end{bmatrix} & \begin{bmatrix} 1 & 2 \\ y & z \end{bmatrix} & \begin{bmatrix} 1 & 2 \\ z & z \end{bmatrix} \\ \begin{bmatrix} 1 & 2 \\ x & x \end{bmatrix} & \begin{bmatrix} 1 & 2 \\ x & y \end{bmatrix} & \begin{bmatrix} 1 & 2 \\ x & z \end{bmatrix} & \begin{bmatrix} 2 & 2 \\ x & x \end{bmatrix} & \begin{bmatrix} 2 & 2 \\ x & y \end{bmatrix} & \begin{bmatrix} 2 & 2 \\ x & z \end{bmatrix} \\ \begin{bmatrix} 1 & 2 \\ x & y \end{bmatrix} & \begin{bmatrix} 1 & 2 \\ y & y \end{bmatrix} & \begin{bmatrix} 1 & 2 \\ y & z \end{bmatrix} & \begin{bmatrix} 2 & 2 \\ x & y \end{bmatrix} & \begin{bmatrix} 2 & 2 \\ y & y \end{bmatrix} & \begin{bmatrix} 2 & 2 \\ y & z \end{bmatrix} \\ \begin{bmatrix} 1 & 2 \\ x & z \end{bmatrix} & \begin{bmatrix} 1 & 2 \\ y & z \end{bmatrix} & \begin{bmatrix} 1 & 2 \\ z & z \end{bmatrix} & \begin{bmatrix} 2 & 2 \\ x & z \end{bmatrix} & \begin{bmatrix} 2 & 2 \\ y & z \end{bmatrix} & \begin{bmatrix} 2 & 2 \\ z & z \end{bmatrix} \end{vmatrix} \qquad \text{(A1)}$$

where

$$\begin{bmatrix} k & k' \\ \alpha & \beta \end{bmatrix} = \sum_{\ell''} A_{\alpha\beta} \begin{pmatrix} \ell'' \\ k & k' \end{pmatrix} e^{i \vec{q} \cdot \vec{x} \begin{pmatrix} \ell'' \\ k & k' \end{pmatrix}} \qquad \text{(A2)}$$

where $\underline{\underline{A}}$ is the force constant matrix. $\underline{\underline{D}}$ is symmetric and real, so it is Hermitian. The contribution from different interactions to $\underline{\underline{D}}$ are additive, so

$$\begin{bmatrix} k & k' \\ \alpha & \beta \end{bmatrix} = \begin{bmatrix} k & k' \\ \alpha & \beta \end{bmatrix}^{(c)} + \begin{bmatrix} k & k' \\ \alpha & \beta \end{bmatrix}^{(R)} \tag{A3}$$

where superscripts (c) and (R) denotes the Coulomb contribution and repulsive contribution respectively.

In the NaCl structure ionic crystal, the potential energy of the crystal can be written as

$$\phi = \phi^{(c)} + \phi^{(R)} \tag{A4}$$

and define A and B by

$$\frac{1}{a}\left[\frac{d}{dr}\phi^{(R)}\right]_{r=a} = \frac{e^2 B}{2v} \tag{A5}$$

$$\left[\frac{d^2}{dr^2}\phi^{(R)}\right]_{r=a} = \frac{e^2 A}{2v} \tag{A6}$$

where $v = 2a^3$, the volume of the unit cell. Thus we define:

$$R_{11}(\alpha,\alpha) = \begin{bmatrix} 1 & 1 \\ \alpha & \alpha \end{bmatrix}^{(R)} = A + 2B \tag{A7}$$

$$R_{12}(\alpha,\alpha) = \begin{bmatrix} 1 & 2 \\ \alpha & \alpha \end{bmatrix}^{(R)}$$

$$= -\{A \cos 2\pi q_x a + B[\cos 2\pi q_y a + \cos 2\pi q_z a]\} \tag{A8}$$

$$\begin{bmatrix} 1 & 1 \\ \alpha & \beta \end{bmatrix}^{(R)} = \begin{bmatrix} 1 & 2 \\ \alpha & \beta \end{bmatrix}^{(R)} = 0 \qquad \text{for } \alpha \neq \beta \tag{A9}$$

in units of $e^2/(2a^3)$, and for the contribution from Coulomb interaction, has been calculated by Kellermann using the Ewald method. If we write

$$C_{II}(\alpha,\beta) = -\begin{bmatrix} I & I \\ \alpha & \beta \end{bmatrix}^{(c)} \tag{A10}$$

$$C_{IJ}(\alpha,\beta) = \begin{bmatrix} I & J \\ \alpha & \beta \end{bmatrix}^{(c)} \tag{A11}$$

in units of $e^2/(2a^3)$. Then (A1) can be simplified as

$$\underline{\underline{D}} = \begin{pmatrix} C_{11} + R_{11} & C_{12} + R_{12} \\ C_{12} + R_{12} & C_{22} + R_{11} \end{pmatrix} \tag{A12}$$

Each term of (A12) represents a (3 x 3) matrix, whose rows and columns are labelled by α and β; i.e. the elements of C_{11} are $C_{11}(\alpha, \beta)$, equation (A10), etc. Notice that equations (A7) and (A8), differ in sign from equation (6.11) of Kellermann[22], which was incorrect.

Determining the number of allowed values of $\vec{q}$

The number of allowed values of $\vec{q}$ vectors means the number of unit cells within the boundaries which we take to repeat periodically throughout an infinite crystal. It can be determined by the cyclic boundary condition. If the unit cells are defined by $\vec{a}_1$, $\vec{a}_2$, $\vec{a}_3$ and the volume which is repeated periodically is $(N_1\vec{a}_1 \cdot N_2\vec{a}_2 \times N_3\vec{a}_3)$, then the cyclic boundary condition requires

$$e^{i\,2\pi\,\vec{q}\,\cdot\,N_i\vec{a}_i} = 1, \qquad i = 1, 2, 3. \tag{A13}$$

We use the reciprocal lattice to find the allowed values of the wave vectors $\vec{q}$ specified by the above equation (A13). Let $\vec{b}_1$, $\vec{b}_2$, $\vec{b}_3$ define a reciprocal lattice. Then, in the NaCl structure, if the generating vectors of the unit cell in direct space are:

$$\vec{a}_1 = r_o(0,\ 1,\ 1),$$

$$\vec{a}_2 = r_o(1,\ 0,\ 1), \tag{A14}$$

$$\vec{a}_3 = r_o(1,\ 1,\ 0).$$

Then the reciprocal vectors[41] are

$$\vec{b}_1 = \frac{1}{2r_o}(-1,\ 1,\ 1),$$

$$\vec{b}_2 = \frac{1}{2r_o}(1,\ -1,\ 1), \tag{A15}$$

$$\vec{b}_3 = \frac{1}{2r_o}(1,\ 1,\ -1).$$

Therefore, the allowed values of $\vec{q}$ which satisfy equation (A13) are given by

$$\vec{q} = \sum_{i=1}^{3} \frac{p_i \vec{b}_i}{N_i} \qquad p_i = 1,\ 2,\ \ldots\ N_i \tag{A16}$$

So, each unit cell of the reciprocal lattice contains $N_1N_2N_3 = N$ distinct value of $\vec{q}$. Kellermann[22] subdivided the range of the basic vectors of the reciprocal lattice into tenths. Therefore, the total number of $\vec{q}$'s in the first Brillouin zone is 1000. We rewrite equation (A16) as

$$\vec{q} = \sum_{i} k_i \vec{b}_i = \frac{1}{2r_o}(q_x,\ q_y,\ q_z) \tag{A17}$$

where

$$q_x = k_2 + k_3 - k_1$$

$$q_y = k_3 + k_1 - k_2 \tag{A18}$$

$$q_z = k_1 + k_2 - k_3$$

The primitive cell in $\vec{q}$ space is the truncated octahedron, which is the first Brillouin zone of the f.c.c. crystal lattice with the boundary conditions.

$$q_x \pm q_y \pm q_z = \pm 3/2$$

$$q_x = \pm 1$$

$$q_y = \pm 1 \qquad \text{(A19)}$$

$$q_z = \pm 1$$

Since the orthogonal transformations of the dynamical matrix will leave its eigenvalues invariant, we do the calculation only for those points which lie in 1/48 th of the first Brillouin zone; that is, only in the region:

$$0 \leq q_z \leq q_y \leq q_x \leq 1$$

$$q_x + q_y + q_z \leq \frac{3}{2} \qquad \text{(A20)}$$

There are 48 points in $\vec{q}$ space which satisfy the latter inequalities (A20). Each point has to be weighted appropriately according to the number of equivalent points in the whole of the zone. The total number of allowed values of $\vec{q}$ vector is then 1000.

(B) Grouping of Ions for the Second Order Calculation

As we have described in chapter 2, instead of summing over all ions in:

$$G_\alpha \begin{pmatrix} \vec{q} \\ k \end{pmatrix} = \sum_{\ell} F_\alpha \begin{pmatrix} \ell \\ k \end{pmatrix} e^{i \vec{q} \cdot \vec{x} \binom{\ell}{k}} \qquad \text{(B1)}$$

We group together those ions which have equal values of $F_\alpha \binom{\ell}{k}$. The equation (B1) can be written as

$$G_\alpha \begin{pmatrix} \vec{q} \\ k \end{pmatrix} = \sum_m \sum_{\ell'}^{(m)} F_\alpha \begin{pmatrix} \ell' \\ k \end{pmatrix} e^{i \vec{q} \cdot \vec{x} \begin{pmatrix} \ell' \\ k \end{pmatrix}} \tag{B2}$$

and $\sum_{\ell'}^{(m)}$ is a sum over all values of ℓ' which correspond to a single group of m. In this appendix, the explicit form of the matrix element of each group m,

$$G_\alpha \begin{pmatrix} \vec{q} \\ k \end{pmatrix}_m = \sum_{\ell'}^{(m)} F_\alpha \begin{pmatrix} \ell' \\ k \end{pmatrix} e^{i \vec{q} \cdot \vec{x} \begin{pmatrix} \ell' \\ k \end{pmatrix}}, \tag{B3}$$

are given for the relaxed ground state, the F_{A1} relaxed excited state in the vacancy configuration, which has the same grouping as the ground state, and the odd-and even-parity relaxed states in the saddle-point configuration. $\underline{G}(\vec{q}_k)_m$ is a 6 x 1 column matrix, whose first three elements are the x, y, z components of $\underline{G}\,(\vec{q}_k)_m$ of the anion (k = 1) and the last three elements are the x, y, z components of $\underline{G}\,(\vec{q}_k)_m$ of the cation (k = 2).

(i) F_A-Centers Ground State and F_{A1} Relaxed Excited State in the Vacancy Configuration

The following fifteen groups of ions are included in the summation of equation (B1)

group 1	(0, 1, 0)
group 2	(1,0,0) (0,0,1), (0,0,$\bar{1}$), ($\bar{1}$,0,0)
group 3	(0,$\bar{1}$,0)
group 4	(1,1,0), ($\bar{1}$,1,0), (0,1,1), (0,1,$\bar{1}$)
group 5	(1,$\bar{1}$,0), ($\bar{1}$,$\bar{1}$,0), (0,$\bar{1}$,1), (0,$\bar{1}$,$\bar{1}$)
group 6	(1,0,1), ($\bar{1}$,0,1), (1,0,$\bar{1}$), ($\bar{1}$,0,$\bar{1}$)
group 7	(1,1,1), ($\bar{1}$,1,1), (1,1,$\bar{1}$), ($\bar{1}$,1,$\bar{1}$)
group 8	(1,$\bar{1}$,1), ($\bar{1}$,$\bar{1}$,1), (1,$\bar{1}$,$\bar{1}$), ($\bar{1}$,$\bar{1}$,$\bar{1}$)

group 9 (0,2,0)

group 10 $(2,0,0)$, $(\bar{2},0,0)$, $(0,0,2)$, $(0,0,\bar{2})$

group 11 $(0,\bar{2},0)$

group 12 $(1,2,0)$, $(\bar{1},2,0)$, $(0,2,1)$, $(0,2,\bar{1})$

group 13 $(2,1,0)$, $(\bar{2},1,0)$, $(0,1,2)$, $(0,1,\bar{2})$

group 14 $(1,\bar{2},0)$, $(\bar{1},\bar{2},0)$, $(0,\bar{2},1)$, $(o,\bar{2},\bar{1})$

group 15 $(2,\bar{1},0)$, $(\bar{2},\bar{1},0)$, $(0,\bar{1},2)$, $(0,\bar{1},\bar{2})$

The explicit form of the matrix of $\underline{G}(\vec{q})$ for each group, except group 1, which is included in Region I, is shown below:

$$\underline{G}(\vec{q})_2 = 2 \begin{bmatrix} F_x(1,0,0)\ (i \sin q_x a) \\ F_y(1,0,0)\ (\cos q_x a + \cos q_z a) \\ F_x(1,0,0,)\ (i \sin q_z a) \\ 0 \\ 0 \\ 0 \end{bmatrix} \tag{B4}$$

$$\underline{G}(\vec{q})_3 = \begin{bmatrix} 0 \\ F_y(0,\bar{1},0)\ (\cos q_y a - i \sin q_y a) \\ 0 \\ 0 \\ 0 \\ 0 \end{bmatrix} \tag{B5}$$

$$\underline{G}(\vec{q})_4 = 2 \begin{bmatrix} 0 \\ 0 \\ 0 \\ F_x(1,1,0)[-\sin(q_x a)\sin(q_y a) + i\cos(q_y a)\sin(q_x a)] \\ F_y(1,1,0)[\cos(q_y a)\{\cos(q_x a) + \cos(q_z a)\} + i\sin(q_y a) \\ \qquad \{\cos(q_x a) + \cos(q_z a)\}] \\ F_x(1,1,0)[-\sin(q_y a)\sin(q_z a) + i\cos(q_z a)\sin(q_z a)] \end{bmatrix}$$

(B6)

$$\underline{G}(\vec{q})_5 = 2 \begin{bmatrix} 0 \\ 0 \\ 0 \\ F_x(1,\bar{1},0)\ [\sin(q_y a)\sin(q_x a) + i\sin(q_x a)\cos(q_y a) \\ F_y(1,\bar{1},0)\ [\cos q_y a\ (\cos q_x a + \cos q_z a) \\ \qquad - i\sin(q_y a)(\cos q_x a + \cos q_z a)] \\ F_x(1,\bar{1},0)\ [\sin(q_y a)\sin(q_z a) + i\sin(q_z a)\cos(q_y a)] \end{bmatrix}$$

(B7)

$$\underline{G}(\vec{q})_6 = 2 \begin{bmatrix} 0 \\ 0 \\ 0 \\ F_x(1,0,1)(i)[\sin(q_x + q_z)a + \sin(q_x - q_z)a] \\ F_y(1,0,1)[\cos(q_x + q_z)a + \cos(q_x - q_z)a] \\ F_z(1,0,1)(i)\ [\sin(q_x + q_z)a - \sin(q_x - q_z)a] \end{bmatrix}$$

(B8)

$$\underline{G}(\vec{q})_7 = 2 \begin{bmatrix} F_x(1,1,1)[-\sin(q_y a)\{\sin(q_x + q_z)a + \sin(q_x - q_z)a\} \\ \qquad + i\cos(q_y a)\{\sin(q_x + q_z)a + \sin(q_x - q_z)a\}] \\ F_y(1,1,1)[\cos(q_y a)\{\cos(q_x + q_z)a + \cos(q_x - q_z)a\} \\ \qquad + i\sin(q_y a)\{\cos(q_x + q_z)a + \cos(q_x - q_z)a\}] \\ F_x(1,1,1)[-\sin(q_y a)\{\sin(q_x + q_z)a - \sin(q_x - q_z)a\} \\ \qquad + i\cos(q_y a)\{\sin(q_x + q_z)a - \sin(q_x - q_z)a\}] \\ 0 \\ 0 \\ 0 \end{bmatrix}$$

(B9)

$$\underline{G}(\vec{q})_8 = 2 \begin{bmatrix} F_x(1,\bar{1},1)[(\sin q_y a + i \cos q_y a)\sin(q_x + q_z)a + \sin(q_x - q_z)a] \\ F_y(1,\bar{1},1)[(\cos q_y a - i \sin q_y a)\{\cos(q_x + q_z)a + \cos(q_x - q_z)a\}] \\ F_x(1,\bar{1},1)[(\sin q_y a + i \cos q_y a)\{\sin(q_x + q_z)a - \sin(q_x - q_z)a\}] \\ 0 \\ 0 \\ 0 \end{bmatrix} \tag{B10}$$

$$\underline{G}(\vec{q})_9 = \begin{bmatrix} 0 \\ 0 \\ 0 \\ 0 \\ F_y(0,2,0)[\cos(2q_y a) \; i \sin(2q_y a)] \\ 0 \end{bmatrix} \tag{B11}$$

$$\underline{G}(\vec{q})_{10} = 2\begin{bmatrix} 0 \\ 0 \\ 0 \\ F_x(2,0,0)\ (i)\ \sin(2\ q_x a) \\ F_y(2,0,0)\ [\cos\ 2\ q_x a + \cos\ 2q_z a] \\ F_x(2,0,0)\ (i)\ \sin\ (2q_z a) \end{bmatrix} \tag{B12}$$

$$\underline{G}(\vec{q})_{11} = \begin{bmatrix} 0 \\ 0 \\ 0 \\ 0 \\ F_y(o,\bar{2},0)\ [\cos(2q_y) - i\ \sin(2q_y a)] \\ 0 \end{bmatrix} \tag{B13}$$

$$\underline{G}(\vec{q})_{12} = 2\begin{bmatrix} F_x(1,2,0)[\{-\sin(2q_y a)\ \sin(q_x a)\} + i\ \cos(2q_y a)\ \sin(q_x a)] \\ F_y(1,2,0)[\cos(2q_y a)(\cos q_x a + \cos\ q_z a) \\ \qquad + i\ \sin(2q_y a)(\cos\ q_x a + \cos\ q_z a)] \\ F_x(1,2,0)[-\sin(2q_y a)\sin(q_z a) + i\ \cos(2q_y a)\ \sin(q_z a)] \\ 0 \\ 0 \\ 0 \end{bmatrix} \tag{B14}$$

$$\underline{G}(\vec{q})_{13} = 2\begin{bmatrix} F_x(2,1,0)[-\sin(q_y a)\sin(2q_x a) + i\cos(q_y a)\sin(2q_x a)] \\ F_y(2,1,0)[\cos(q_y a)[\cos 2q_x a + \cos 2q_z a] \\ \qquad + i\sin(q_y a)(\cos 2q_x a + \cos 2q_z a)] \\ F_x(2,1,0)[-\sin(q_y a)\sin(2q_z a) + i\cos(q_y a)\sin(2q_z a)] \\ 0 \\ 0 \\ 0 \end{bmatrix} \tag{B15}$$

$$\underline{G}(\vec{q})_{14} = 2\begin{bmatrix} F_x(1,\bar{2},0)[\{\sin(2q_y a) + i\cos(2q_y a)\}\sin q_x a] \\ F_y(1,\bar{2},0)[\{\cos(2q_y a) - i\sin(2q_y a)\}(\cos q_x a + \cos q_z a)] \\ F_x(1,\bar{2},0)[\{\sin(2q_y a) + i\cos(2q_y a)\}\sin q_z a] \\ 0 \\ 0 \\ 0 \end{bmatrix} \tag{B16}$$

$$\underline{G}(\vec{q})_{15} = 2 \begin{bmatrix} F_x(2,\bar{1},0)[(\sin q_y a + i \cos q_y a) \sin (2q_x a)] \\ F_y(2,\bar{1},0)[(\cos q_y a + i \sin q_y a) \{\cos(2q_x a) + \cos(2q_z a)\}] \\ F_x(2,\bar{1},0)[(\sin q_y a + i \cos q_y a) \sin(2q_z a)] \\ 0 \\ 0 \\ 0 \end{bmatrix} \tag{B17}$$

(ii) F_A-centers even and odd parity relaxed state in the saddle-point configuration

The following 35 groups of ions , expressed in the unprimed coordinate system (Fig. 2(b)), are included in the summation of equation (B1):-

group 1 $(0, \frac{1}{2}, -\frac{1}{2})$

group 2 $(0, -\frac{1}{2}, \frac{1}{2})$

group 3 $(0, 0, 0)$

group 4 $(1, \frac{1}{2}, \frac{1}{2}), (-1, \frac{1}{2}, \frac{1}{2})$

group 5 $(1, -\frac{1}{2}, -\frac{1}{2}), (-1, -\frac{1}{2}, -\frac{1}{2})$

group 6 $(1, \frac{1}{2}, -\frac{1}{2}), (-1, \frac{1}{2}, -\frac{1}{2})$

group 7 $(1, -\frac{1}{2}, \frac{1}{2}), (-1, -\frac{1}{2}, \frac{1}{2})$

group 8 $(0, 3/2, \frac{1}{2})$

group 9 $(0, -3/2, -\frac{1}{2})$

group 10 $(0, \frac{1}{2}, 3/2)$

group 11 $(0, -\frac{1}{2}, -3/2)$

group 12 $(0, 3/2, -\frac{1}{2})$

group 13 $(0, -3/2, \frac{1}{2})$

group 14 $(0, \frac{1}{2}, -3/2)$

group 15 $(0, -\frac{1}{2}, 3/2)$

group 16 $(1, 3/2, -\frac{1}{2})$, $(-1, 3/2, -\frac{1}{2})$

group 17 $(1, \frac{1}{2}, -3/2)$, $(-1, \frac{1}{2}, -3/2)$

group 18 $(1, -3/2, \frac{1}{2})$, $(-1, -3/2, \frac{1}{2})$

group 19 $(1, -\frac{1}{2}, 3/2)$, $(-1, -\frac{1}{2}, 3/2)$

group 20 $(1, -\frac{1}{2}, -3/2)$, $(-1, -\frac{1}{2}, -3/2)$

group 21 $(1, 3/2, \frac{1}{2})$, $(-1, 3/2, \frac{1}{2})$

group 22 $(1, \frac{1}{2}, 3/2)$, $(-1, \frac{1}{2}, 3/2)$

group 23 $(1, -3/2, -\frac{1}{2})$, $(-1, -3/2, -\frac{1}{2})$

group 24 $(0, 3/2, -3/2)$

group 25 $(0, -3/2, 3/2)$

group 26 $(0, 3/2, 3/2)$

group 27 $(0, -3/2, -3/2)$

group 28 $(2, \frac{1}{2}, \frac{1}{2})$, $(-2, \frac{1}{2}, \frac{1}{2})$

group 29 $(2, -\frac{1}{2}, \frac{1}{2})$, $(-2, -\frac{1}{2}, \frac{1}{2})$

group 30 $(2, \frac{1}{2}, -\frac{1}{2})$, $(-2, \frac{1}{2}, -\frac{1}{2})$

group 31 $(2, -\frac{1}{2}, -\frac{1}{2})$, $(-2, -\frac{1}{2}, -\frac{1}{2})$

group 32 $(1, 3/2, -3/2)$, $(-1, 3/2, -3/2)$

group 33 $(1, -3/2, 3/2)$, $(-1, -3/2, 3/2)$

group 34 $(1, 3/2, 3/2)$, $(-1, 3/2, 3/2)$

group 35 $(1, -3/2, -3/2)$, $(-1, -3/2, -3/2)$

The explicit form of the matrix of $\underline{G}(\vec{q})$ for each group, except groups 1, 2, 3, which are included in Region I, is shown below:-

$$\underline{G}(\vec{q})_4 = 2 \begin{bmatrix} F_x(1,\tfrac{1}{2},\tfrac{1}{2})\left[-\sin q_x a \left\{\sin\left(\frac{q_y a}{2}+\frac{q_z a}{2}\right) - i\cos\left(\frac{q_y a}{2}+\frac{q_z a}{2}\right)\right\}\right] \\ F_y(1,\tfrac{1}{2},\tfrac{1}{2})\left[\cos q_x a \left\{\cos\left(\frac{q_y a}{2}+\frac{q_z a}{2}\right) + i\sin\left(\frac{q_y a}{2}+\frac{q_z a}{2}\right)\right\}\right] \\ F_z(1,\tfrac{1}{2},\tfrac{1}{2})\left[\cos q_x a \left\{\cos\left(\frac{q_y a}{2}+\frac{q_z a}{2}\right) + i\sin\left(\frac{q_y a}{2}+\frac{q_z a}{2}\right)\right\}\right] \\ 0 \\ 0 \\ 0 \end{bmatrix} \quad \text{(B18)}$$

$$\underline{G}(\vec{q})_5 = 2 \begin{bmatrix} F_x(1,-\tfrac{1}{2},-\tfrac{1}{2})\left[\sin q_x a\left\{-\sin\left(\frac{-q_y a}{2}-\frac{q_z a}{2}\right) + i\cos\left(\frac{-q_y a}{2}-\frac{q_z a}{2}\right)\right\}\right] \\ F_y(1,-\tfrac{1}{2},-\tfrac{1}{2})\left[\cos q_x a\left\{\cos\left(\frac{-q_y a}{2}-\frac{q_z a}{2}\right) + i\sin\left(\frac{-q_y a}{2}-\frac{q_z a}{2}\right)\right\}\right] \\ F_z(1,-\tfrac{1}{2},-\tfrac{1}{2})\left[\cos q_x a\left\{\cos\left(\frac{-q_y a}{2}-\frac{q_z a}{2}\right) + i\sin\left(\frac{-q_y a}{2}-\frac{q_z a}{2}\right)\right\}\right] \\ 0 \\ 0 \\ 0 \end{bmatrix} \quad \text{(B19)}$$

$$\underline{G}(\vec{q})_6 = 2 \begin{bmatrix} 0 \\ 0 \\ 0 \\ F_x(1,\tfrac{1}{2},-\tfrac{1}{2})\left[\sin q_x a\left\{-\sin\left(\frac{q_y a}{2} - \frac{q_z a}{2}\right) + i\cos\left(\frac{q_y a}{2} - \frac{q_z a}{2}\right)\right\}\right] \\ F_y(1,\tfrac{1}{2},-\tfrac{1}{2})\left[\cos q_x a\left\{\cos\left(\frac{q_y a}{2} - \frac{q_z a}{2}\right) + i\sin\left(\frac{q_y a}{2} - \frac{q_z a}{2}\right)\right\}\right] \\ F_z(1,\tfrac{1}{2},-\tfrac{1}{2})\left[\cos q_x a\left\{\cos\left(\frac{q_y a}{2} - \frac{q_z a}{2}\right) + i\sin\left(\frac{q_y a}{2} - \frac{q_z a}{2}\right)\right\}\right] \end{bmatrix}$$

(B20)

$$\underline{G}(\vec{q})_7 = 2 \begin{bmatrix} 0 \\ 0 \\ 0 \\ F_x(1,-\tfrac{1}{2},\tfrac{1}{2})\left[\sin q_x a\left\{\sin\left(-\frac{q_y a}{2} + \frac{q_z a}{2}\right) + i\cos\left(-\frac{q_y a}{2} + \frac{q_z a}{2}\right)\right\}\right] \\ F_y(1,-\tfrac{1}{2},\tfrac{1}{2})\left[\cos q_x a\left\{\cos\left(\frac{-q_y a}{2} + \frac{q_z a}{2}\right) + i\sin\left(\frac{-q_y a}{2} + \frac{q_z a}{2}\right)\right\}\right] \\ F_z(1,-\tfrac{1}{2},\tfrac{1}{2})\left[\cos q_x a\left\{\cos\left(\frac{-q_y a}{2} + \frac{q_z a}{2}\right) + i\sin\left(\frac{-q_y a}{2} + \frac{q_z a}{2}\right)\right\}\right] \end{bmatrix}$$

(B21)

$$\underline{G}(\vec{q})_8 = \begin{bmatrix} 0 \\ F_y(0,3/2,\tfrac{1}{2})\left[\cos\left(\frac{3q_x a}{2} + \frac{q_z a}{2}\right) + i \sin\left(\frac{3q_x a}{2} + \frac{q_z a}{2}\right)\right] \\ F_x(0,3/2,\tfrac{1}{2})\left[\cos\left(\frac{3q_x a}{2} + \frac{q_z a}{2}\right) + i \sin\left(\frac{3q_x a}{2} + \frac{q_z a}{2}\right)\right] \\ 0 \\ 0 \\ 0 \end{bmatrix}$$

(B22)

$$\underline{G}(\vec{q})_9 = \begin{bmatrix} 0 \\ F_y(0,-3/2,-\tfrac{1}{2})\left[\cos\left(\frac{3q_y a}{2} + \frac{q_z a}{2}\right) - i \sin\left(\frac{3q_y a}{2} + \frac{q_z a}{2}\right)\right] \\ F_z(0,-3/2,-\tfrac{1}{2})\left[\cos\left(\frac{3q_y a}{2} + \frac{q_z a}{2}\right) - i \sin\left(\frac{3q_y a}{2} + \frac{q_z a}{2}\right)\right] \\ 0 \\ 0 \\ 0 \end{bmatrix}$$

(B23)

$$\underline{G}(\vec{q})_{10} = \begin{bmatrix} 0 \\ F_y(0,\tfrac{1}{2},3/2)\left[\cos\left(\frac{q_y a}{2} + \frac{3q_z a}{2}\right) + i \sin\left(\frac{q_y a}{2} + \frac{3q_z a}{2}\right)\right] \\ F_z(0,\tfrac{1}{2},3/2)\left[\cos\left(\frac{q_y a}{2} + \frac{3q_z a}{2}\right) + i \sin\left(\frac{q_y a}{2} + \frac{3q_z a}{2}\right)\right] \\ 0 \\ 0 \\ 0 \end{bmatrix}$$

(B24)

$$\underline{G}(\vec{q})_{11} = \begin{bmatrix} 0 \\ F_y(0,-\tfrac{1}{2},-3/2)\left[\cos\left(\frac{q_y a}{2} + \frac{3q_z a}{2}\right) - i \sin\left(\frac{q_y a}{2} + \frac{3q_z a}{2}\right)\right] \\ F_z(0,-\tfrac{1}{2},-3/2)\left[\cos\left(\frac{q_y a}{2} + \frac{3q_z a}{2}\right) - i \sin\left(\frac{q_y a}{2} + \frac{3q_z a}{2}\right)\right] \\ 0 \\ 0 \\ 0 \end{bmatrix}$$

(B25)

$$\underline{G}(\vec{q})_{12} = \begin{bmatrix} 0 \\ 0 \\ 0 \\ 0 \\ F_y(0,3/2,-\tfrac{1}{2})\left[\cos\left(\frac{3q_y a}{2} - \frac{q_z a}{2}\right) + i \sin\left(\frac{3q_y a}{2} - \frac{q_z a}{2}\right)\right] \\ F_x(0,3/2,-\tfrac{1}{2})\left[\cos\left(\frac{3q_y a}{2} - \frac{q_z a}{2}\right) + i \sin\left(\frac{3q_y a}{2} - \frac{q_z a}{2}\right)\right] \end{bmatrix} \qquad \text{(B26)}$$

$$\underline{G}(\vec{q})_{13} = \begin{bmatrix} 0 \\ 0 \\ 0 \\ 0 \\ F_y(0,-3/2,\tfrac{1}{2})\left[\cos\left(\frac{-3q_y a}{2} + \frac{q_z a}{2}\right) + i \sin\left(\frac{-3q_y a}{2} + \frac{q_z a}{2}\right)\right] \\ F_z(0,-3/2,\tfrac{1}{2})\left[\cos\left(\frac{-3q_y a}{2} + \frac{q_z a}{2}\right) + i \sin\left(\frac{-3q_y a}{2} + \frac{q_z a}{2}\right)\right] \end{bmatrix} \qquad \text{(B27)}$$

$$\underline{G}(\vec{q})_{14} = \begin{bmatrix} 0 \\ 0 \\ 0 \\ 0 \\ F_y(0,\frac{1}{2},-\frac{3}{2})\left[\cos\left(\frac{q_y a}{2} - \frac{3q_z a}{2}\right) + i\sin\left(\frac{q_y a}{2} - \frac{3q_z a}{2}\right)\right] \\ F_z(0,\frac{1}{2},-\frac{3}{2})\left[\cos\left(\frac{q_y a}{2} - \frac{3q_z a}{2}\right) + i\sin\left(\frac{q_y a}{2} - \frac{3q_z a}{2}\right)\right] \end{bmatrix} \quad \text{(B28)}$$

$$\underline{G}(\vec{q})_{15} = \begin{bmatrix} 0 \\ 0 \\ 0 \\ 0 \\ F_y(0,\frac{-1}{2},\frac{3}{2})\left[\cos\left(\frac{-q_y a}{2} + \frac{3q_z a}{2}\right) + i\sin\left(\frac{-q_y a}{2} + \frac{3q_z a}{2}\right)\right] \\ F_z(0,\frac{-1}{2},\frac{3}{2})\left[\cos\left(\frac{-q_y a}{2} + \frac{3q_z a}{2}\right) + i\sin\left(\frac{-q_y a}{2} + \frac{3q_z a}{2}\right)\right] \end{bmatrix} \quad \text{(B29)}$$

$$G(\vec{q})_{16} = \begin{bmatrix} F_x(1,\frac{3}{2},\frac{-1}{2})[\sin q_x a\{-\sin(\frac{3q_y a}{2} - \frac{q_z a}{2}) + i\cos(\frac{3q_y a}{2} - \frac{q_z a}{2})\}] \\ F_y(1,\frac{3}{2},\frac{-1}{2})[\cos q_x a\{\cos(\frac{3q_y a}{2} - \frac{q_z a}{2}) + i\sin(\frac{3q_y a}{2} - \frac{q_z a}{2})\}] \\ F_z(1,\frac{3}{2},\frac{-1}{2})[\cos q_x a\{\cos(\frac{3q_y a}{2} - \frac{q_z a}{2}) + i\sin(\frac{3q_y a}{2} - \frac{q_z a}{2})\}] \\ 0 \\ 0 \\ 0 \end{bmatrix} \quad \text{(B30)}$$

$$\underline{G}(\vec{q})_{17} = 2\begin{bmatrix} F_x(1,\frac{1}{2},\frac{-3}{2})[\sin q_x a\{-\sin(\frac{q_y a}{2} - \frac{3q_z a}{2}) + i\cos(\frac{q_y a}{2} - \frac{3q_z a}{2})\}] \\ F_y(1,\frac{1}{2},\frac{-3}{2})[\cos q_x a\{\cos(\frac{q_y a}{2} - \frac{3q_z a}{2}) + i\sin(\frac{q_y a}{2} - \frac{3q_z a}{2})\}] \\ F_z(1,\frac{1}{2},\frac{-3}{2})[\cos q_x a\{\cos(\frac{q_y a}{2} - \frac{3q_z a}{2}) + i\sin(\frac{q_y a}{2} - \frac{3q_z a}{2})\}] \\ 0 \\ 0 \\ 0 \end{bmatrix} \quad \text{(B31)}$$

$$\underline{G}(\vec{q})_{18} = 2\begin{bmatrix} F_x(1,\frac{-3}{2},\frac{1}{2})[\sin q_x a\{-\sin(\frac{-3q_y a}{2}+\frac{q_z a}{2}) + i\cos(\frac{-3q_y a}{2}+\frac{q_z a}{2})\}] \\ F_y(1,\frac{-3}{2},\frac{1}{2})[\cos q_x a\{\cos(\frac{-3q_y a}{2}+\frac{q_z a}{2}) + i\sin(\frac{-3q_y a}{2}+\frac{q_z a}{2})\}] \\ F_z(1,\frac{-3}{2},\frac{1}{2})[\cos q_x a\{\cos(\frac{-3q_y a}{2}+\frac{q_z a}{2}) + i\sin(\frac{-3q_y a}{2}+\frac{q_z a}{2})\}] \\ 0 \\ 0 \\ 0 \end{bmatrix}$$

(B32)

$$\underline{G}(\vec{q})_{19} = 2\begin{bmatrix} F_x(1,\frac{-1}{2},\frac{3}{2})[\sin q_x a\{-\sin(\frac{-q_y a}{2}+\frac{3q_z a}{2}) + i\cos(\frac{-q_y a}{2}+\frac{3q_z a}{2})\}] \\ F_y(1,\frac{-1}{2},\frac{3}{2})[\cos q_x a\{\cos(\frac{-q_y a}{2}+\frac{3q_z a}{2}) + i\sin(\frac{-q_y a}{2}+\frac{3q_z a}{2})\}] \\ F_z(1,\frac{-1}{2},\frac{3}{2})[\cos q_x a\{\cos(\frac{-q_y a}{2}+\frac{3q_z a}{2}) + i\sin(\frac{-q_y a}{2}+\frac{3q_z a}{2})\}] \\ 0 \\ 0 \\ 0 \end{bmatrix}$$

(B33)

$$\underline{G}(\vec{q})_{20} = 2 \begin{bmatrix} 0 \\ 0 \\ 0 \\ F_x(1,\frac{-1}{2},\frac{-3}{2})[\sin q_x a\{-\sin(\frac{-q_y a}{2} - \frac{3q_z a}{2}) + i\cos(\frac{-q_y a}{2} - \frac{3q_z a}{2})\}] \\ F_y(1,\frac{-1}{2},\frac{-3}{2})[\cos q_x a\{\cos(\frac{-q_y a}{2} - \frac{3q_z a}{2}) + i\sin(\frac{-q_y a}{2} - \frac{3q_z a}{2})\}] \\ F_z(1,\frac{-1}{2},\frac{-3}{2})[\cos q_x a\{\cos(\frac{-q_y a}{2} - \frac{3q_z a}{2}) + i\sin(\frac{-q_y a}{2} - \frac{3q_z a}{2})\}] \end{bmatrix}$$

(B34)

$$\underline{G}(\vec{q})_{21} = 2 \begin{bmatrix} 0 \\ 0 \\ 0 \\ F_x(1,\frac{3}{2},\frac{1}{2})[\sin q_x a\{-\sin(\frac{3q_y a}{2} + \frac{q_z a}{2}) + i\cos(\frac{3q_y a}{2} + \frac{q_z a}{2})\}] \\ F_y(1,\frac{3}{2},\frac{1}{2})[\cos q_x a\{\cos(\frac{3q_y a}{2} + \frac{q_z a}{2}) + i\sin(\frac{3q_y a}{2} + \frac{q_z a}{2})\}] \\ F_z(1,\frac{3}{2},\frac{1}{2})[\cos q_x a\{\cos(\frac{3q_y a}{2} + \frac{q_z a}{2}) + i\sin(\frac{3q_y a}{2} + \frac{q_z a}{2})\}] \end{bmatrix}$$

(B35)

$$\underline{G}(\vec{q})_{22} = 2\begin{bmatrix} 0 \\ 0 \\ 0 \\ F_x(1,\frac{1}{2},\frac{3}{2})[\sin q_x a\{-\sin(\frac{q_y a}{2}+\frac{3q_z a}{2}) + i\cos(\frac{q_y a}{2}+\frac{3q_z a}{2})\}] \\ F_y(1,\frac{1}{2},\frac{3}{2})[\cos q_x a\{\cos(\frac{q_y a}{2}+\frac{3q_z a}{2}) + i\sin(\frac{q_y a}{2}+\frac{3q_z a}{2})\}] \\ F_z(1,\frac{1}{2},\frac{3}{2})[\cos q_x a\{\cos(\frac{q_y a}{2}+\frac{3q_z a}{2}) + i\sin(\frac{q_y a}{2}+\frac{3q_z a}{2})\}] \end{bmatrix}$$

(B36)

$$\underline{G}(\vec{q})_{23} = 2\begin{bmatrix} 0 \\ 0 \\ 0 \\ F_x(1,\frac{-3}{2},\frac{-1}{2})[\sin q_x a\{-\sin(\frac{-3q_y a}{2}-\frac{q_z a}{2}) + i\cos(\frac{-3q_y a}{2}-\frac{q_z a}{2})\}] \\ F_y(1,\frac{-3}{2},\frac{-1}{2})[\cos q_x a\{\cos(\frac{-3q_y a}{2}-\frac{q_z a}{2}) + i\sin(\frac{-3q_y a}{2}-\frac{q_z a}{2})\}] \\ F_z(1,\frac{-3}{2},\frac{-1}{2})[\cos q_x a\{\cos(\frac{-3q_y a}{2}-\frac{q_z a}{2}) + i\sin(\frac{-3q_y a}{2}-\frac{q_z a}{2})\}] \end{bmatrix}$$

(B37)

$$\underline{G}(\vec{q})_{24} = \begin{bmatrix} 0 \\ F_y(0,\frac{3}{2},\frac{-3}{2})\left[\cos\left(\frac{3q_y a}{2} - \frac{3q_z a}{2}\right) + i\sin\left(\frac{3q_y a}{2} - \frac{3q_z a}{2}\right)\right] \\ F_z(0,\frac{3}{2},\frac{-3}{2})\left[\cos\left(\frac{3q_y a}{2} - \frac{3q_z a}{2}\right) + i\sin\left(\frac{3q_y a}{2} - \frac{3q_z a}{2}\right)\right] \\ 0 \\ 0 \\ 0 \end{bmatrix} \tag{B38}$$

$$\underline{G}(\vec{q})_{25} = \begin{bmatrix} 0 \\ F_y(0,\frac{-3}{2},\frac{3}{2})\left[\cos\left(\frac{-3q_y a}{2} + \frac{3q_z a}{2}\right) + i\sin\left(\frac{-3q_y a}{2} + \frac{3q_z a}{2}\right)\right] \\ F_z(0,\frac{-3}{2},\frac{3}{2})\left[\cos\left(\frac{-3q_y a}{2} + \frac{3q_z a}{2}\right) + i\sin\left(\frac{-3q_y a}{2} + \frac{3q_z a}{2}\right)\right] \\ 0 \\ 0 \\ 0 \end{bmatrix} \tag{B39}$$

$$\underline{G}(\vec{q})_{26} = \begin{bmatrix} 0 \\ 0 \\ 0 \\ 0 \\ F_y(0,\frac{3}{2},\frac{3}{2})\left[\cos\left(\frac{3}{2}q_y a + \frac{3}{2}q_z a\right) + i\sin\left(\frac{3q_y a}{2} + \frac{3}{2}q_y a\right)\right] \\ F_z(0,\frac{3}{2},\frac{3}{2})\left[\cos\left(\frac{3}{2}q_y a + \frac{3}{2}q_z a\right) + i\sin\left(\frac{3q_y a}{2} + \frac{3}{2}q_z a\right)\right] \end{bmatrix} \tag{B40}$$

$$\underline{G}(\vec{q})_{27} = \begin{bmatrix} 0 \\ 0 \\ 0 \\ 0 \\ F_y(0,\frac{-3}{2},\frac{-3}{2})\left[\cos\left(\frac{-3q_y a}{2} - \frac{3q_z a}{2}\right) + i\sin\left(\frac{-3q_y a}{2} - \frac{3q_z a}{2}\right)\right] \\ F_z(0,\frac{-3}{2},\frac{-3}{2})\left[\cos\left(\frac{-3q_y a}{2} - \frac{3q_z a}{2}\right) + i\sin\left(\frac{-3q_y a}{2} - \frac{3q_z a}{2}\right)\right] \end{bmatrix} \tag{B41}$$

$$\underline{G}(\vec{q})_{28} = 2\begin{bmatrix} 0 \\ 0 \\ 0 \\ F_x(2,\frac{1}{2},\frac{1}{2})[\sin 2q_x a\{-\sin(\frac{q_y a}{2}+\frac{q_z a}{2}) + i\cos(\frac{q_y a}{2}+\frac{q_z a}{2})\}] \\ F_y(2,\frac{1}{2},\frac{1}{2})[\cos 2q_x a\{\cos(\frac{q_y a}{2}+\frac{q_z a}{2}) + i\sin(\frac{q_y a}{2}+\frac{q_z a}{2})\}] \\ F_z(2,\frac{1}{2},\frac{1}{2})[\cos 2q_x a\{\cos(\frac{q_y a}{2}+\frac{q_z a}{2}) + i\sin(\frac{q_y a}{2}+\frac{q_z a}{2})\}] \end{bmatrix} \quad \text{(B42)}$$

$$\underline{G}(\vec{q})_{29} = 2\begin{bmatrix} F_x(2,\frac{-1}{2},\frac{1}{2})[\sin 2q_x a\{-\sin(\frac{-q_y a}{2}+\frac{q_z a}{2}) + i\cos(\frac{-q_y a}{2}+\frac{q_z a}{2})\}] \\ F_y(2,\frac{-1}{2},\frac{1}{2})[\cos 2q_x a\{\cos(\frac{-q_y a}{2}+\frac{q_z a}{2}) + i\sin(\frac{-q_y a}{2}+\frac{q_z a}{2})\}] \\ F_z(2,\frac{-1}{2},\frac{1}{2})[\cos 2q_x a\{\cos(\frac{-q_y a}{2}+\frac{q_z a}{2}) + i\sin(\frac{-q_y a}{2}+\frac{q_z a}{2})\}] \\ 0 \\ 0 \\ 0 \end{bmatrix} \quad \text{(B43)}$$

$$\underline{G}(\vec{q})_{30} = 2 \begin{bmatrix} F_x(2,\frac{1}{2},\frac{-1}{2})[\sin 2q_x a\{-\sin(\frac{q_y a}{2} - \frac{q_z a}{2}) + i\cos(\frac{q_y a}{2} - \frac{q_z a}{2})\}] \\ F_y(2,\frac{1}{2},\frac{-1}{2})[\cos 2q_x a\{\cos(\frac{q_y a}{2} - \frac{q_z a}{2}) + i\cos(\frac{q_y a}{2} - \frac{q_z a}{2})\}] \\ F_z(2,\frac{1}{2},\frac{-1}{2})[\cos 2q_x a\{\cos(\frac{q_y a}{2} - \frac{q_z a}{2}) + i\cos(\frac{q_y a}{2} - \frac{q_z a}{2})\}] \\ 0 \\ 0 \\ 0 \end{bmatrix}$$

(B44)

$$\underline{G}(\vec{q})_{31} = 2 \begin{bmatrix} 0 \\ 0 \\ 0 \\ F_x(2,\frac{-1}{2},\frac{-1}{2})[\sin 2q_x a\{-\sin(\frac{-q_y a}{2} - \frac{q_z a}{2}) + i\cos(\frac{-q_y a}{2} - \frac{q_z a}{2})\}] \\ F_y(2,\frac{-1}{2},\frac{-1}{2})[\cos 2q_x a\{\cos(\frac{q_y a}{2} - \frac{q_z a}{2}) + i\cos(\frac{q_y a}{2} - \frac{q_z a}{2})\}] \\ F_z(2,\frac{-1}{2},\frac{-1}{2})[\cos 2q_x a\{\cos(\frac{q_y a}{2} - \frac{q_z a}{2}) + i\cos(\frac{q_y a}{2} - \frac{q_z a}{2})\}] \end{bmatrix}$$

(B45)

$$\underline{G}(\vec{q})_{32} = 2 \begin{bmatrix} 0 \\ 0 \\ 0 \\ F_x(1,\frac{3}{2},\frac{-3}{2})[\sin q_x a\{-\sin(\frac{3q_y a}{2} - \frac{3q_z a}{2}) + i\cos(\frac{3q_y a}{2} - \frac{3q_z a}{2})\}] \\ F_y(1,\frac{3}{2},\frac{-3}{2})[\cos q_x a\{\cos(\frac{3q_y a}{2} - \frac{3q_z a}{2}) + i\sin(\frac{3q_y a}{2} - \frac{3q_z a}{2})\}] \\ F_z(1,\frac{3}{2},\frac{-3}{2})[\cos q_x a\{\cos(\frac{3q_y a}{2} - \frac{3q_z a}{2}) + i\sin(\frac{3q_y a}{2} - \frac{3q_z a}{2})\}] \end{bmatrix}$$

(B46)

$$\underline{G}(\vec{q})_{33} = 2 \begin{bmatrix} 0 \\ 0 \\ 0 \\ F_x(1,\frac{-3}{2},\frac{3}{2})[\sin q_x a\{-\sin(\frac{-3q_y a}{2} + \frac{3q_z a}{2}) + i\cos(\frac{-3q_y a}{2} + \frac{3q_z a}{2})\}] \\ F_y(1,\frac{-3}{2},\frac{3}{2})[\cos q_x a\{\cos(\frac{-3q_y a}{2} + \frac{3q_z a}{2}) + i\sin(\frac{-3q_y a}{2} + \frac{3q_z a}{2})\}] \\ F_z(1,\frac{-3}{2},\frac{3}{2})[\cos q_x a\{\cos(\frac{-3q_y a}{2} + \frac{3q_z a}{2}) + i\sin(\frac{-3q_y a}{2} + \frac{3q_z a}{2})\}] \end{bmatrix}$$

(B47)

$$\underline{G}(\vec{q})_{34} = 2\begin{bmatrix} F_x(1,\frac{3}{2},\frac{3}{2})[-\sin q_x a\{\sin(\frac{3q_y a}{2}+\frac{3q_z a}{2}) + i\cos(\frac{3q_y a}{2}+\frac{3q_z a}{2})\}] \\ F_y(1,\frac{3}{2},\frac{3}{2})[\cos q_x a\{\cos(\frac{3q_y a}{2}+\frac{3q_z a}{2}) + i\sin(\frac{3q_y a}{2}+\frac{3q_z a}{2})\}] \\ F_z(1,\frac{3}{2},\frac{3}{2})[\cos q_x a\{\cos(\frac{3q_y a}{2}+\frac{3q_z a}{2}) + i\sin(\frac{3q_y a}{2}+\frac{3q_z a}{2})\}] \\ 0 \\ 0 \\ 0 \end{bmatrix}$$

(B48)

$$\underline{G}(\vec{q})_{35} = 2\begin{bmatrix} F_x(1,\frac{-3}{2},\frac{-3}{2})[\sin q_x a\{-\sin(\frac{-3q_y a}{2}-\frac{-3q_z a}{2}) + i\cos(\frac{-3q_y a}{2}-\frac{3q_z a}{2})\}] \\ F_y(1,\frac{-3}{2},\frac{-3}{2})[\cos q_x a\{\cos(\frac{-3q_y a}{2}-\frac{3q_z a}{2}) + i\cos(\frac{-3q_y a}{2}-\frac{3q_z a}{2})\}] \\ F_z(1,\frac{-3}{2},\frac{-3}{2})[\cos q_x a\{\cos(\frac{-3q_y a}{2}-\frac{3q_z a}{2}) + i\cos(\frac{-3q_y a}{2}-\frac{3q_z a}{2})\}] \\ 0 \\ 0 \\ 0 \end{bmatrix}$$

(B49)

(C) Block Diagram for the Computational Work for the Relaxed State

The function of this appendix is to summarize the computational work for a relaxed state, which has been discussed in the text. (sections 3.1(A), 3.1(B), 3.2(A), 3.2(B)). Except for the minimization program which has been obtained from Harwell (p. 49), the program for $\underline{D}^{-1}(\vec{q})$ which was supplied by Dr. R.J. Brown and modified by the author for Tosi's single exponential parameters, and the built-in subroutine for the error function in the IBM 360/65 computer (p. 43), the author had to develop the rest of the programs himself. The function of the minimization program is to find a minimum of a function of several variables. The user must supply initial approximations to the values of the variables at the minimum, and a subroutine to evaluate the function for any values of the variables. The function of the $\underline{D}^{-1}(\vec{q})$ program is to calculate and invert Kellermann's dynamical matrix. In the block diagram, Figure 8, the function of Block D is to calculate the displacement coefficient, $\xi_\alpha(^{\ell}_{K})/F_\alpha(^{\ell}_{K})$. The Fourier transform processes of equation (2.80) and (2.71) are calculated here. The input for Block E is the displacement coefficients from Block D, matrix elements from Block B, and zeroth order solution of $\underline{\mu}$, $\underline{\lambda}$ from Block A. The function of Block D is to calculate $\underline{\xi}$ by the perturbative-iteration procedure as indicated by equations (2.82) - (2.83). It essentially just multiplies the displacement coefficients by $F_\alpha(^{\ell}_{K})$. First, we set $\underline{F} = \underline{Fo}$ as in eqution (2.82) and then set $\underline{F} = \underline{Fo} + \underline{\underline{C}} \cdot \underline{\xi}^{(o)}$ as in euation (2.83), where $\underline{\xi}^{(o)}$ is given by equation (2.82). The iterative procedure substitutes the updated value $\underline{\xi}^{(1)}$ into equation (2.83) for $\underline{\xi}^{(o)}$ and proceeds until convergence is obtained, i.e. until two consecutive estimates of $\underline{\xi}$ differ by less than 0.001 times the perfect lattice

Figure 8

Block Diagram for the computational work for the Relaxed State

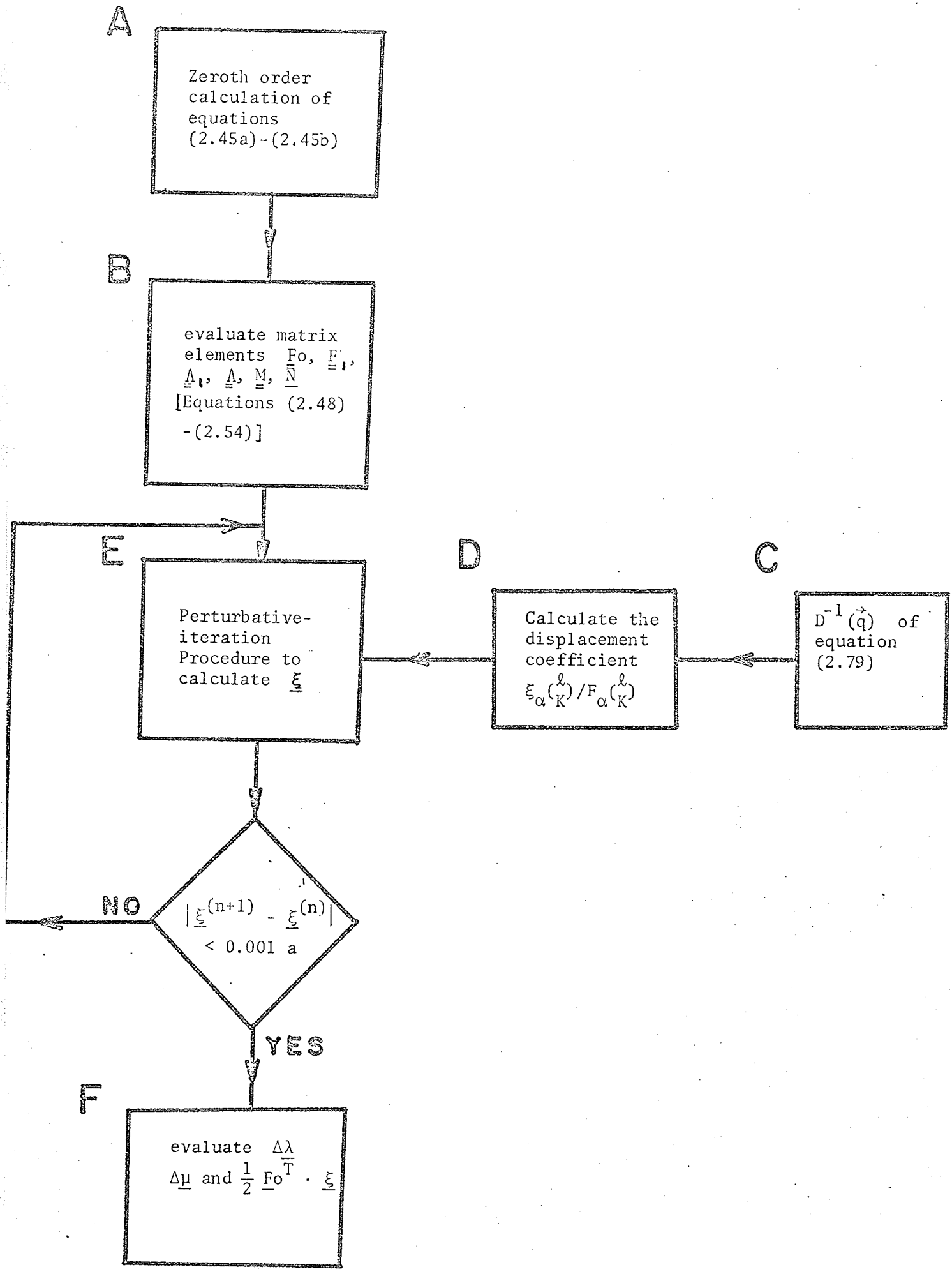
A
Zeroth order calculation of equations (2.45a)-(2.45b)
B
evaluate matrix elements Fo, F1, Λ1, Λ, M, N [Equations (2.48) -(2.54)]
E
Perturbative-iteration Procedure to calculate ξ
D
Calculate the displacement coefficient ξα(lK)/Fα(lK)
C
D-1(q) of equation (2.79)
NO
|ξ(n+1) - ξ(n)| < 0.001 a
YES
F
evaluate Δλ Δμ and 1/2 FoT · ξ

spacing. $\underline{\Delta\lambda}$ of equation (2.63), $\underline{\Delta\mu}$ of equation (2.64) and $\frac{1}{2}\ \underline{Fo}^{T} \cdot \underline{\xi}$ are evaluated in Block F.